

**EVALUATION AND DEVELOPMENT OF PLASTIC  
LAMINATED BACKING BOARD MATERIALS**

*CHARLES C. SURLAND*

*THE UNITED STATES RUBBER COMPANY*

*JANUARY 1956*

MATERIALS LABORATORY

CONTRACT No. AF 33(616)-484

SUPPLEMENTAL AGREEMENT No. S3(54-1266)

PROJECT No. 7340

TASK No. 73400

WRIGHT AIR DEVELOPMENT CENTER  
AIR RESEARCH AND DEVELOPMENT COMMAND  
UNITED STATES AIR FORCE  
WRIGHT-PATTERSON AIR FORCE BASE, OHIO

This report was prepared by the Physics Section, Divisional Development Laboratories, of the United States Rubber Company, Mishawaka, Indiana under USAF Contract No. 33(616)484 and Supplemental Agreement S3 (54-1266). This contract was initiated under Project No. 7340, "Rubber, Plastic and Composite Materials", Task No. 73400, "Structural Plastics", formerly RDO No. 619-11, "Substitutes for Critical and Strategic Materials", and was administered under the direction of the Materials Laboratory, Directorate of Research, Wright Air Development Center, with Mr. George Peterson, and the Power Plant Laboratory, Directorate of Laboratories, Wright Air Development Center, with Mr. Jack Weil acting as Project Engineers.

Dr. P. G. Roach was administrator, and Mr. W. Smith was materials and development co-ordinator for the United States Rubber Company.

Mr. D. DeWitt co-operated in the development and processing of test procedures and in editing reports and preparing photographs and drawings, and Mr. S. Piacsek assisted in the derivation of equations and analysis of the results for the United States Rubber Company.

This report covers period of work from October 1954 to September 1955

WADC TR 54-474

Different types of backing board materials were tested by internal explosion techniques to examine the feasibility of duplicating gunfire damage. Pressure deflection tests on a simulated airframe installation were made to relate mechanical properties of the backing boards to their support characteristics for both self-sealing and bladder type fuel cells.

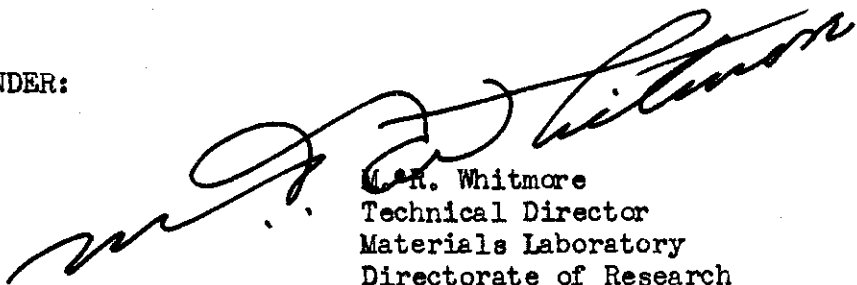
Empirical equations were developed for the deflection of backing boards under fluid pressures. The tests included encountered the maximum and minimum spans which would normally be in aircraft structures. Equations were correlated with the physical properties of the backing boards as the basis for establishing a method of specifying backing boards.

Production trials of USV CR 88 backing board were made to examine the feasibility of production by continuous methods and furnish material to the WADC.

PUBLICATION REVIEW

This report has been reviewed and is approved.

FOR THE COMMANDER:



G. R. Whitmore  
Technical Director  
Materials Laboratory  
Directorate of Research

*Contents*  
TABLE OF CONTENTS

	PAGE
Objective . . . . .	1
Introduction . . . . .	2
Discussion	
Section I Gunfire Test Jig-Internal Explosions	
Test Methods and Service Conditions . . . . .	3
Experimental Results and Analysis . . . . .	3
Summary Discussion . . . . .	13
Section II Pressure Deflection Testing	
Service Conditions . . . . .	22
Test Methods and Equipment . . . . .	23
Experimental Data . . . . .	27
Analytical Methods . . . . .	88
Sample Calculations . . . . .	90
Summary Discussion . . . . .	93
Conclusions . . . . .	105
APPENDIX I Backing Board Test Materials . . . . .	108
APPENDIX II Fuel Cell Backing Board Installation in the Airframe Industry . . . . .	109
APPENDIX III Internal Explosion and Pressure Deflection Test Jig	112
APPENDIX IV Mechanical Properties of Backing Boards . . . . .	118
APPENDIX V Cube Gunfire Tests . . . . .	126
APPENDIX VI Commercial Production of USV CR 88 Backing Board. .	129
Bibliography . . . . .	131

*Continuals*  
LIST OF ILLUSTRATIONS

Figure	Page
1. Internal Explosion Jig; Side View; (Improved) . . . . .	4
2. Cube Gunfire Test Panel USV 747-5, Type III Installation . . .	5
3. Cube Gunfire Test Panel USV 747-5, Type III Installation . . .	5
4. Cube Gunfire Test Panel USV CR 88, Type III Installation . . .	6
5. Cube Gunfire Test Panel USV CR 88, Type III Installation . . .	6
6. Internal Explosion Test, Panel 24; (30" x 40") . . . . .	8
7. Internal Explosion Test, Panels 1, 2, 3, 4, and 5 . . . . .	9
8. Internal Explosion Test, Panels 6, 7, 9, 10, 11, and 12 . . . .	10
9. Internal Explosion Test, Panel 8 . . . . .	11
10. Internal Explosion Test, Panels 13, 14, 15, 16, 17, and 18 . .	14
11. Internal Explosion Test, Panels 19, 20, 21, 22, 23, and 24 . . .	18
12. Internal Explosion Test, Panels 25, 26, 27, 28, 29, and 30 . .	19
13. Internal Explosion Test, Panels 31, 32, 33, and 34 . . . . .	20
14. Pressure Deflection Test System . . . . .	25
15. Recorder Control Unit . . . . .	26
16. Flow Chart - Pressure Deflection System . . . . .	26
17. Pressure Deflection Curves for Trial 1 . . . . .	36
18. Pressure Deflection Curves for Trial 2 . . . . .	37
19. Pressure Deflection Curves for Trial 3 . . . . .	38
20. Pressure Deflection Curves for Trial 4 . . . . .	39
21. Pressure Deflection Curves for Trial 5 . . . . .	40
22. Pressure Deflection Curves for Trial 6 . . . . .	41
23. Pressure Deflection Curves for Trial 7 . . . . .	42
24. Pressure Deflection Curves for Trial 8 . . . . .	43
25. Pressure Deflection Curves for Trial 9 . . . . .	44

*Continued*  
LIST OF ILLUSTRATIONS (Cont.)

Figure	Page
26. Pressure Deflection Curves for Trial 10 . . . . .	45
27. Pressure Deflection Curves for Trials 11, 12, 13, and 16 . . . . .	46
28. Pressure Deflection Curves for Trials 14 and 15 . . . . .	47
29. Pressure Deflection Curves for Trials 17, 19, and 20 . . . . .	48
30. Pressure Deflection Curves for Trials 18 and 21 . . . . .	49
31. Pressure Deflection Curves for Trial 22 . . . . .	50
32. Pressure Deflection Curves for Trial 23 . . . . .	51
33. Pressure Deflection Curves for Trial 24 . . . . .	52
34. Pressure Deflection Curves for Trial 25 . . . . .	53
35. Pressure Deflection Curves for Trial 26 . . . . .	54
36. Pressure Deflection Curves for Trials 27 and 29 . . . . .	55
37. Pressure Deflection Curves for Trial 28 . . . . .	56
38. Pressure Deflection Curves for Trial 30 . . . . .	57
39. Pressure Deflection Curves for Trial 31 . . . . .	58
40. Pressure Deflection Curves for Trial 32 . . . . .	59
41. Pressure Deflection Curves for Trial 33 . . . . .	60
42. Pressure Deflection Curves for Trial 34 . . . . .	61
43. Pressure Deflection Curves for Trial 35 . . . . .	62
44. Pressure Deflection Curves for Trial 36 . . . . .	63
45. Pressure Deflection Curves for Trial 37 . . . . .	64
46. Pressure Deflection Curves for Trial 38 . . . . .	65
47. Pressure Deflection Curves for Trial 39 . . . . .	66
48. Pressure Deflection Curves for Trial 40 . . . . .	67
49. Pressure Deflection Curves for Trial 41 . . . . .	68
50. Pressure Deflection Curves for Trial 42 . . . . .	69

*Continued*  
LIST OF ILLUSTRATIONS (Cont.)

Figure	Page
51. Pressure Deflection Curves for Trial 43 . . . . .	70
52. Pressure Deflection Curves for Trial 44 . . . . .	71
53. Pressure Deflection Curves for Trial 45 . . . . .	72
54. Pressure Deflection Curves for Trial 46 . . . . .	73
55. Pressure Deflection Curves for Trial 47 . . . . .	74
56. Pressure Deflection Curves for Trial 48 . . . . .	75
57. Pressure Deflection Curves for Trial 49 . . . . .	76
58. Pressure Deflection Curves for Trial 50 . . . . .	77
59. Pressure Deflection Curves for Trial 51 . . . . .	78
60. Pressure Deflection Curves for Trial 52 . . . . .	79
61. Pressure Deflection Curves for Trial 53 . . . . .	80
62. Pressure Deflection Curves for Trial 54 . . . . .	81
63. Pressure Deflection Curves for Trial 55 . . . . .	82
64. Pressure Deflection Curves for Trial 56 . . . . .	83
65. Pressure Deflection Curves for Trial 57 . . . . .	84
66. Pressure Deflection Curves for Trial 58 . . . . .	85
67. Pressure Deflection Curves for Trial 59 . . . . .	86
68. Pressure Deflection Curves for Trial 60 . . . . .	87
69. Internal Explosion Jig; Backing Board Installation . . . . .	113
70. Internal Explosion Jig; Steel Hat Sections and Support Plate . . . . .	114
71. Top and Front View of Backing Board Support Frame . . . . .	116
72. High Speed Photography Setup . . . . .	117
73. Diagram of Shock Wave Reflection . . . . .	117
74. Cube Gunfire Test; Panel USV CR 88 (Improved Construction). . . . .	127
75. Cube Gunfire Test; Panel USV CR 88 (Improved Construction). . . . .	128

*Continails*  
LIST OF TABLES

No.	Page
I Internal Explosion Data . . . . .	12
II Internal Explosion Data . . . . .	15
III Internal Explosion Results . . . . .	21
IV Pressure Deflection Trials . . . . .	28
V Pressure Deflection Equations . . . . .	94
VI Identification of Backing Board Test Materials. . . . .	108
VII Elongation of Backing Board Materials . . . . .	118
VIII Mechanical Properties of Test Materials . . . . .	120



# Contracts

## OBJECTIVE

This work relates to a study of the reaction of widely different constructions of fuel cell backing boards to fluid pressure loads under conditions simulating those existing in aircraft. These fluid loads were applied explosively and by relatively slow pressurization.

A principle part of the work was the development and construction of test devices, to produce fluid pressure loadings on simulated backing board installations, by means of which measured and calculated strength values could be compared under the action of simulated fuel heads over 30 feet. In addition, further development of a device for simulating gunfire damage to backing boards—by means of the internal explosion technique—was undertaken.

Engineering data obtained from the various test procedures was correlated with the physical properties of the materials and the dimensions of the pressure-deflection test setup to devise equations which might be used in specifying backing board materials in aircraft design. Both regular self-sealing type fuel cells and bladder type cells were used in the investigations.

*Contrails*  
INTRODUCTION

The work described in this report is correlative with Wright Air Development Center Technical Report 54-474.

The objectives of this program required the selection of backing board materials which could be expected to give the extremes of physical properties required and, in addition, be materials on which a considerable back log of experience was available. A list of backing board materials was prepared in conference with the Wright Air Development Center and these are discussed in Appendix I, page 108.

Appendix II, page 109, discusses the problems of backing board installation mentioned in conferences with engineering personnel in the airframe industry, and some aspects of these problems which influenced the design of the simulated internal explosion test and the pressure-deflection tests.

The gunfire test jig, an internal explosion device, for simulating backing board damage resulting from gunfire was designed, constructed, and evaluated. The design and construction details of this portion of the program are given in Appendix III, page 112. This jig was also used for the pressure-deflection testing.

The mechanical properties of the test materials were obtained in general by the test procedures referred to in Military Specification MIL-P-8045. The mechanical properties and elaborations on the test procedures for the backing materials used in this program are given in Appendix IV, page 118.

Appendix V, page 126, describes the cube gunfire tests.

Appendix VI, page 129, describes the method of producing USV CR 88 backing board.

The work of this report was undertaken with the understanding that simultaneous investigations of all the variables immediately apparent in any one phase, such as simulating gunfire damage to backing boards by controlled methods, was a task of a magnitude, beyond the limits imposed upon this investigation. Further, the danger of picking discrete variables for investigation while assuming constancy in the others, is well recognized.

The work was therefore undertaken essentially by systematic investigation of specific variables while holding other variables constant. The discussion of the results of the pressure-deflection testing illustrates the problems which result when a presumed constant factor is found to vary in an unknown manner.

SECTION I

GUNFIRE TEST JIG INTERNAL EXPLOSIONS

TEST METHODS AND SERVICE CONDITIONS

WADC Technical Report 54-474, Part I describes a method of testing backing boards for resistance to gunfire damage. This, in essence, involved placing a panel of test material with a simulated projectile wound against a fluid laden container, and creating rapid high fluid loads by means of an explosion in the fluid.

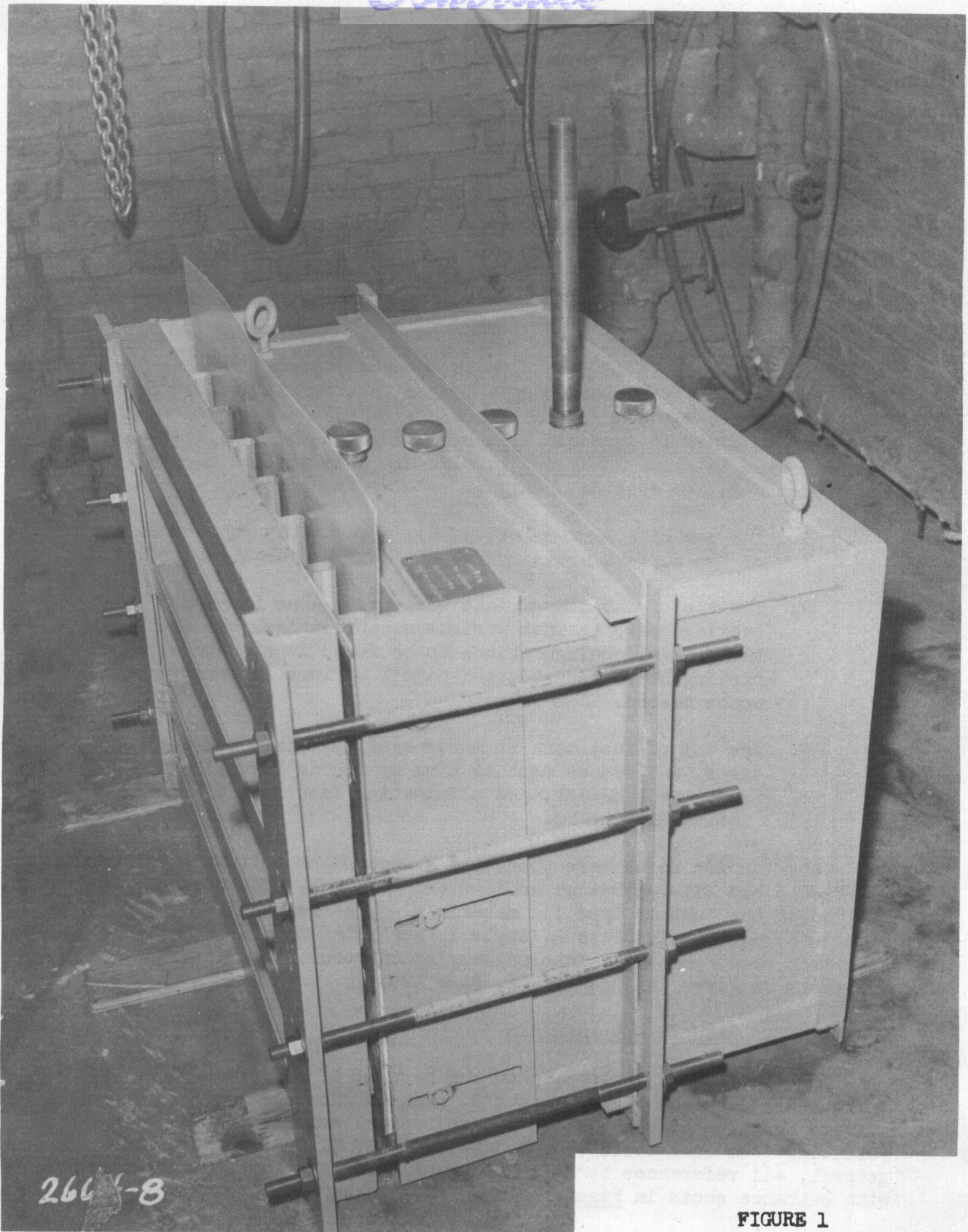
This report deals in part with the construction and evaluation of a similar type of test device using a larger test panel, mounted on a simulated aircraft structure. The construction of the internal explosion tester is outlined in Appendix III, page 112, and the finalized version of the device is shown in Figure 1, page 4. This jig has the following improvements in the original design:

1. The use of a larger test panel, more nearly representative of the surface area involved in service installations.
2. The use of a backing plate with provisions to support the backing board against various supporting members simulating the general configurations to be found in structures where backing board is used, and permit various fastening methods to be tested.
3. The use of fuel tank to more nearly simulate service conditions, and reduce testing time by making installation of the test panels easier, and eliminating fastening of the edges of the backing board.

Cube gunfire tests were conducted in accordance with the methods of MIL-P-8045 and MIL-T-5578A at ambient temperatures. The boards were installed in the cube as Type III materials. The fuel cell was a US-173 construction, Type I, Class A, Style I, per MIL-T-5578A. These tests were made to compare with internal explosion results. A description of the tests is given in Appendix VI, page 129.

EXPERIMENTAL RESULTS AND ANALYSIS

Figures 2 and 3, page 5, show the results of cube gunfire on backing boards USV 747-5 and Figures 4 and 5, page 6, show the results of cube gunfire tests on USV CR 88. These are typical examples of the damage resulting from cube tests on USV 747-5 and USV CR 88 backing boards. In general, all references to simulated gunfire damage are to be compared with entrance shots in Figures 2 thru 5, which are marked "E".



2664-8

FIGURE 1

INTERNAL EXPLOSION JIG  
SIDE VIEW (IMPROVED)

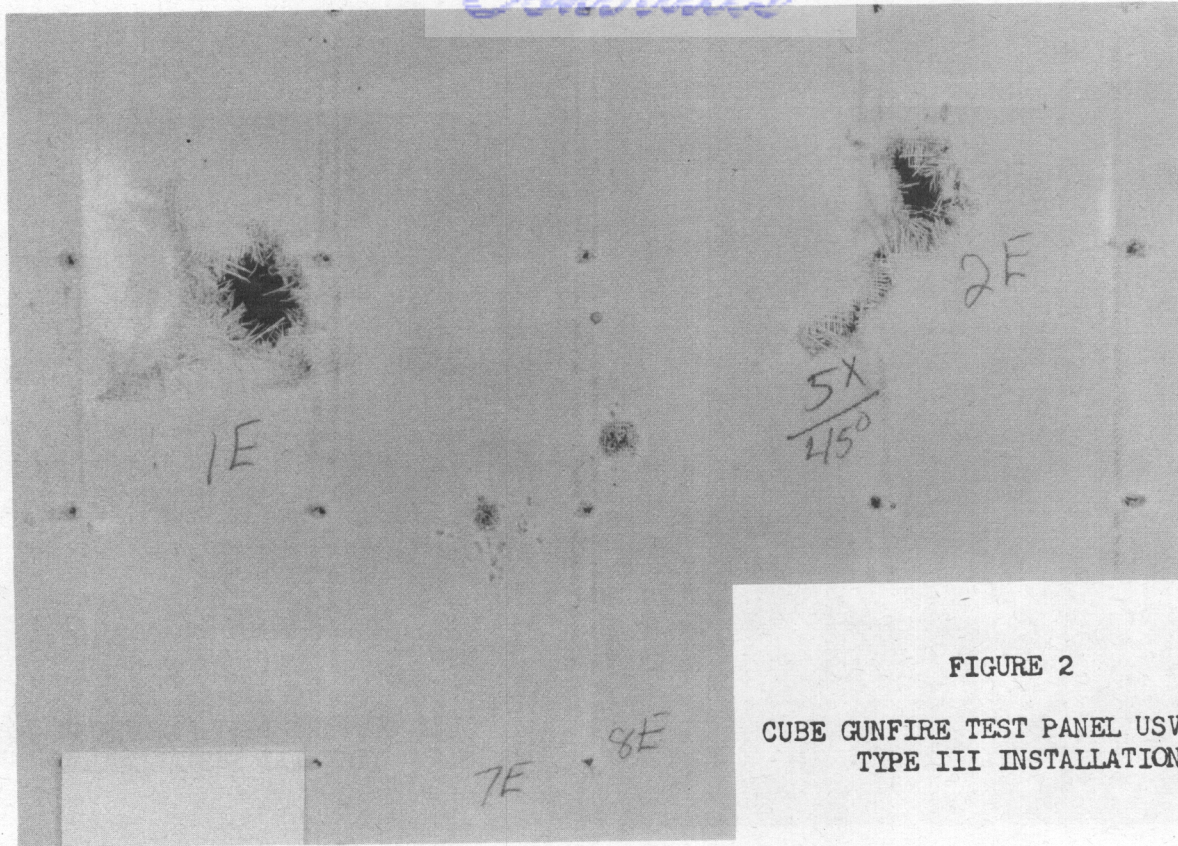


FIGURE 2  
CUBE GUNFIRE TEST PANEL USV 747-5  
TYPE III INSTALLATION

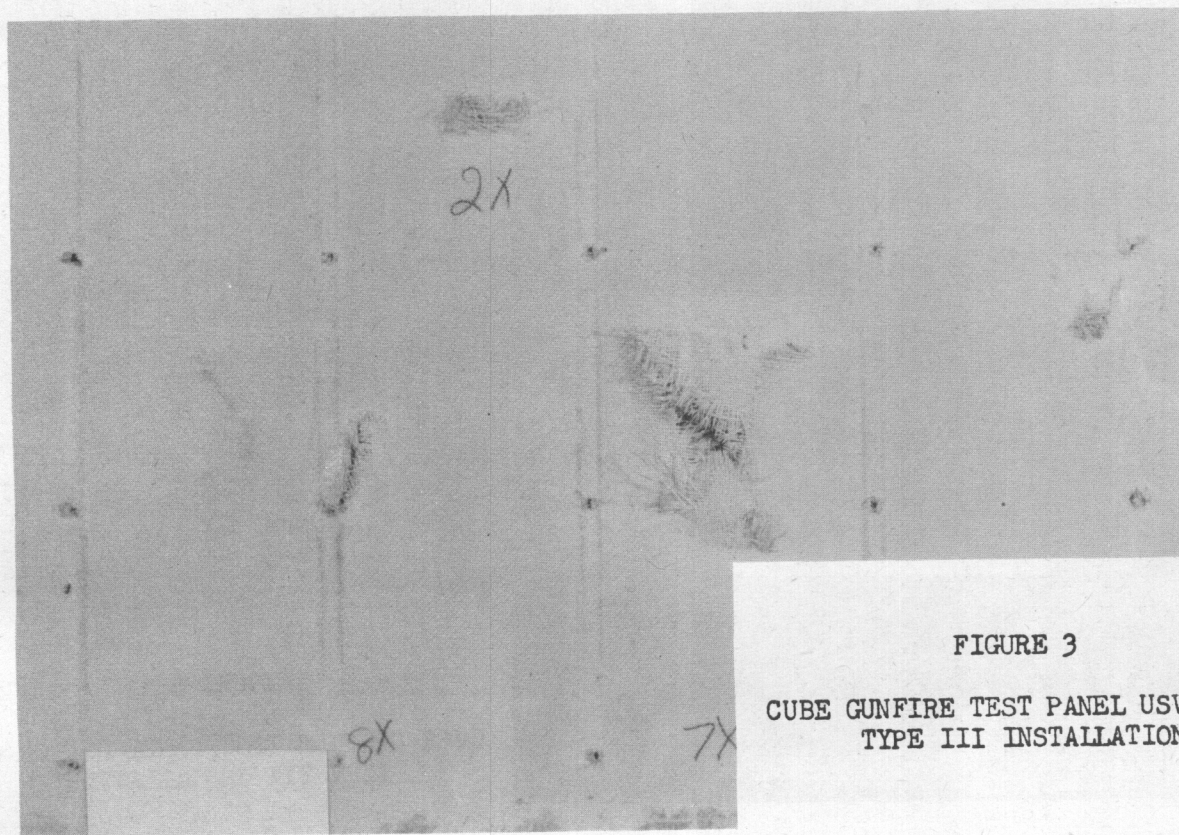


FIGURE 3  
CUBE GUNFIRE TEST PANEL USV 747-5  
TYPE III INSTALLATION

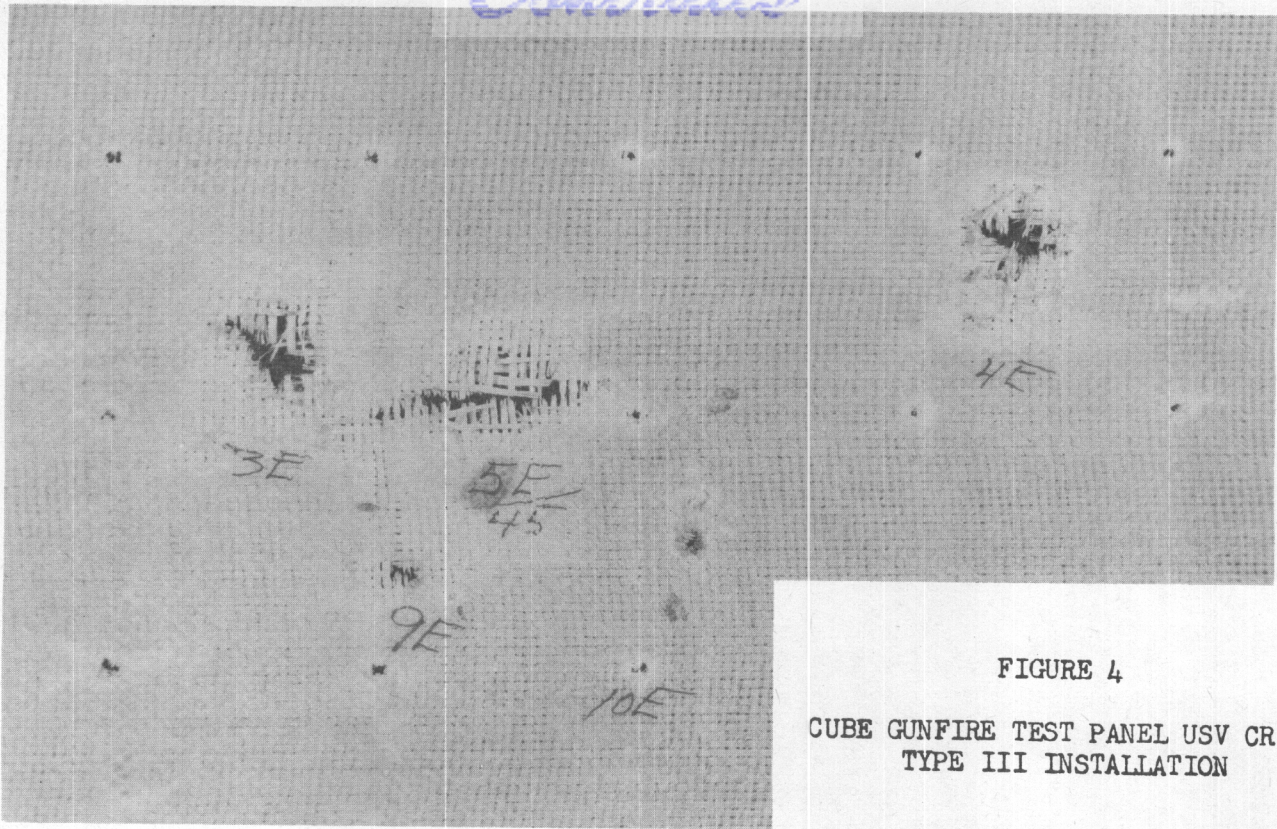


FIGURE 4  
CUBE GUNFIRE TEST PANEL USV CR 88  
TYPE III INSTALLATION

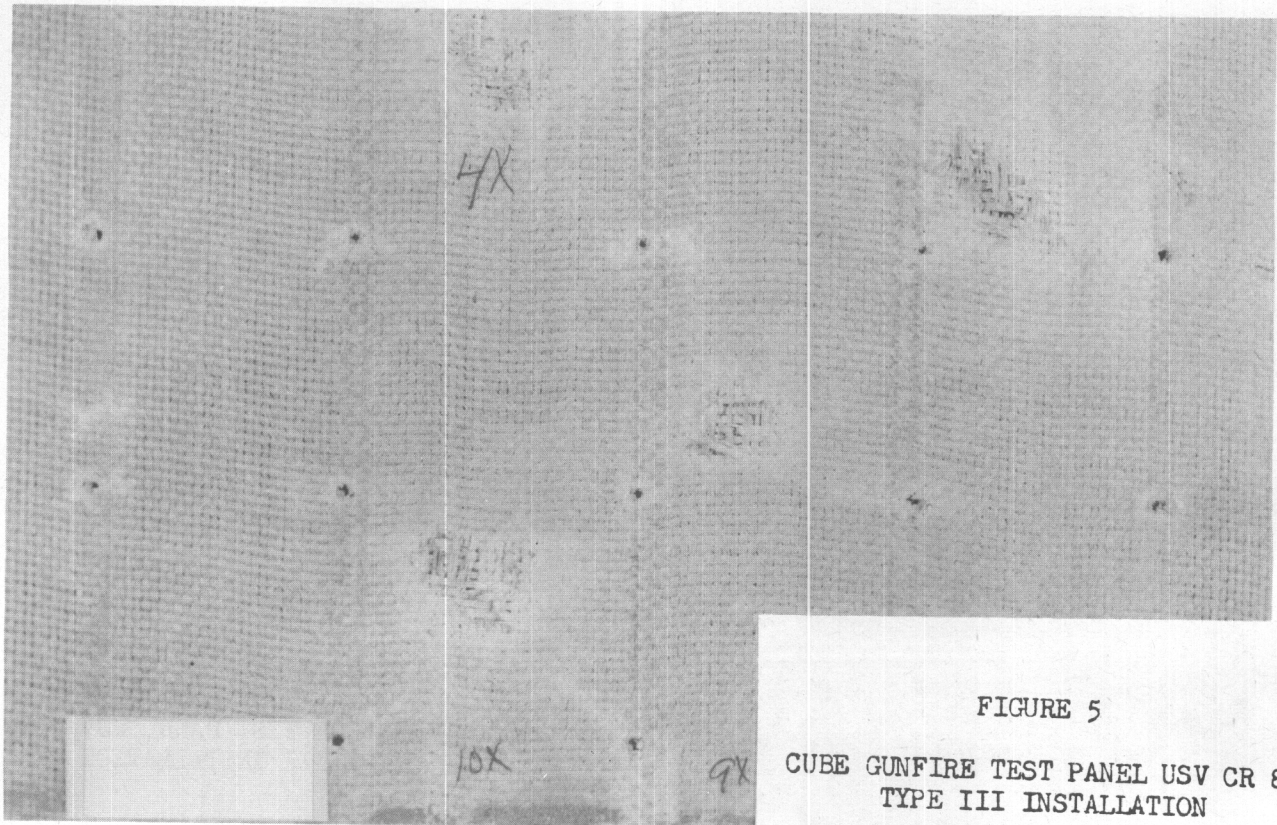


FIGURE 5  
CUBE GUNFIRE TEST PANEL USV CR 88  
TYPE III INSTALLATION

Figure 6, page 8, shows the damage caused by internal explosion testing to panel 24, see Table III, page 21. This is typical of the damage caused at the hat section supports and at the fastening points in the 30 inch x 40 inch backing board test panels tested on the internal explosion jig. All subsequent illustrations show only the 14 inch by 14 inch section of the test panels around the simulated gunfire wound. It follows that the general pressure pattern occurring in gunfire cube tests is being duplicated by the internal explosion.

The five panels shown in Figure 7, page 9, were the initial trials. The explosion was created six inches deeper in the fluid for panel 4, but the greater damage expected did not result. Table I, page 12, gives the test conditions for the first twelve internal explosion tests. In actual gunfire tests the damage has been shown to be more severe where the projectile enters lower in the fluid. It appears therefore, that the internal explosion test is not sensitive to the height of the fluid head above the explosion.

Figure 8, page 10, shows panels 6, 7, 9, 10, 11, and 12 which were run under similar conditions. The variation in the testing of these panels took place in the successive deformation of the horizontal "I" beam supports which started with panel 3 and continued to panel 9, when it seems an equilibrium was reached and no further bowing of the horizontal members occurred. The tests on panels 3 to 12 were made using the same hat sections for support, and these were progressively damaged. In these tests the simulated projectile wound was located immediately between two hat section supports. The explosions took place on a horizontal level with the wound.

Panels 10, 11, and 12 which were run after jig damage had stabilized, illustrated the repetitive action of the test. However, by referring to the results of cube gunfire tests on USV 747-5 panels, Figures 2 and 3, it is apparent that the damage caused by gunfire tests covers an area approximately two and one half inches by three and one half inches. The internal explosions results consist only of minor tears.

Figure 9, page 11, shows panel 8, which was run to determine the effect of the explosion on wounds placed above and below the standard level. These were centered between hat sections on either side of the standard position. In this test the explosion was set off in position standard to the other panels reported, which was in the front port and centered vertically and horizontally in the structure.

By examining the damage of the internal explosion on panel 8, Figure 9, it was evident that the wounds placed at positions on either side of the standard position suffer no noticeable damage. This fact combined with evidence of more severe damage to all the test boards in the area immediately in front of the explosive charge, which had been located behind a hat section, and the noticeably greater damage to this hat section, suggested that more localized damage may be produced in the wound area if the hole and hat section location were changed to bring the explosion as close as possible to the wound.

*Contrails*

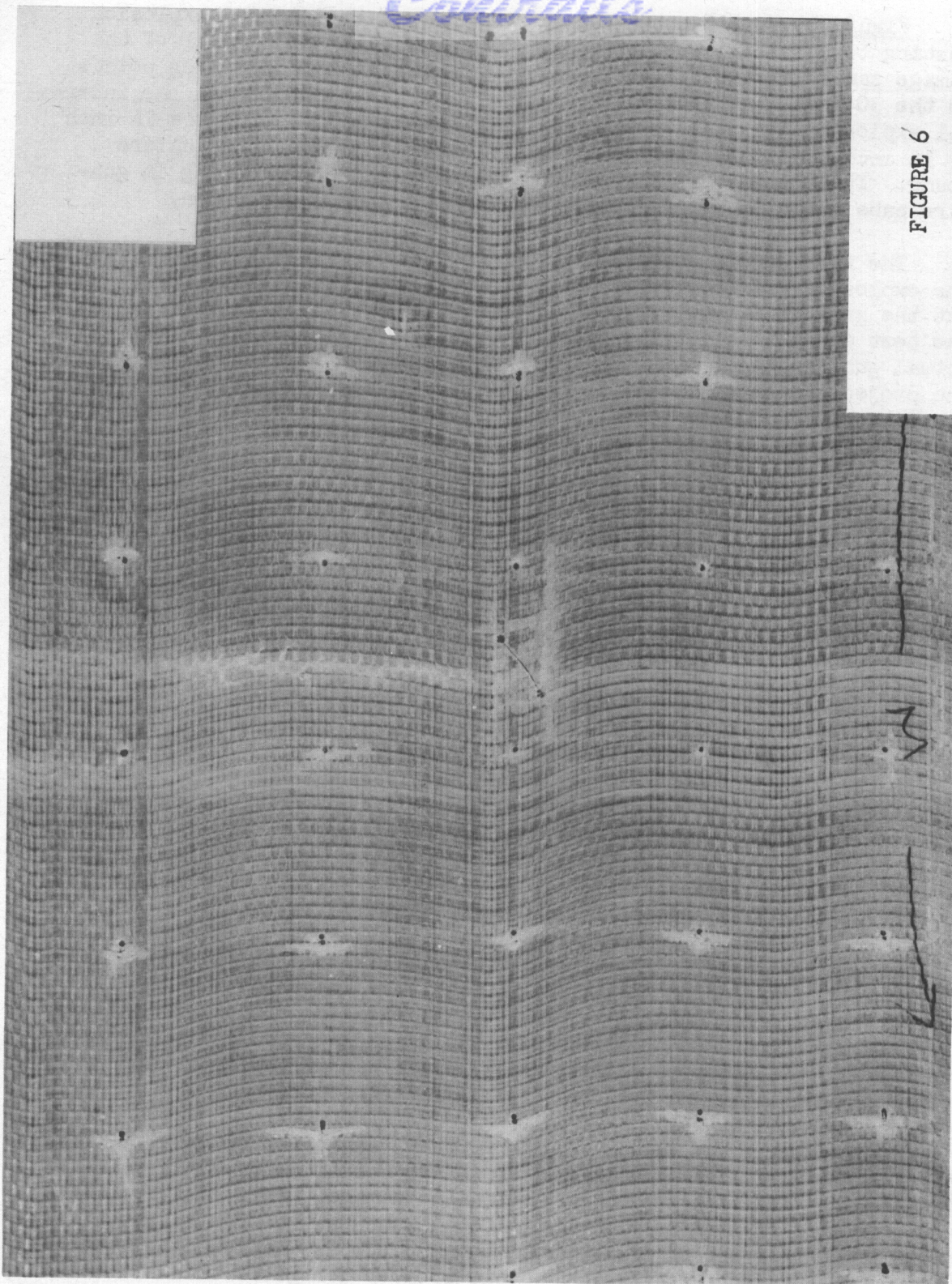


FIGURE 6

INTERNAL EXPLOSION TEST  
PANEL 24; (30" x 40")



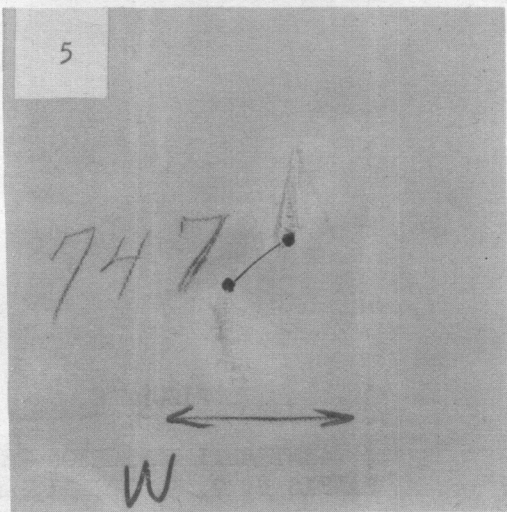
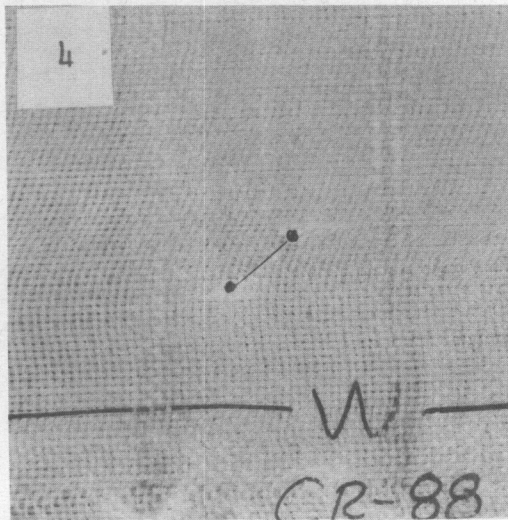
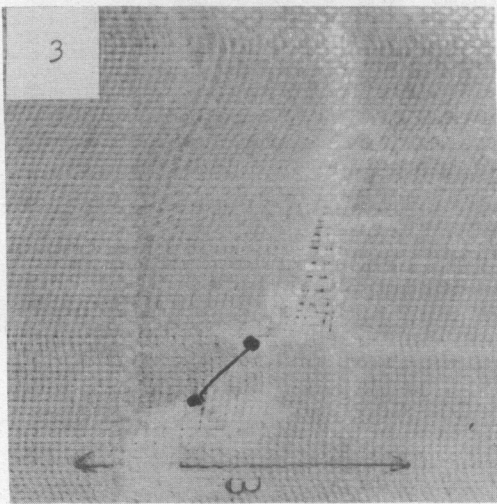
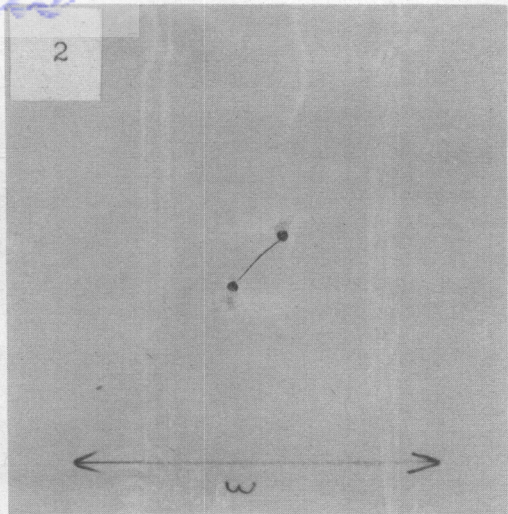
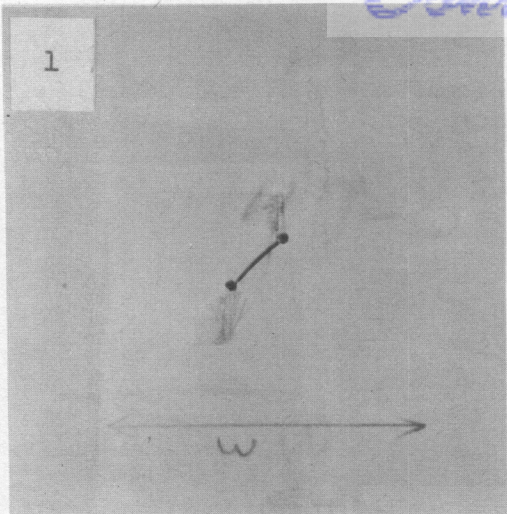


FIGURE 7  
INTERNAL EXPLOSION TEST  
PANELS 1, 2, 3, 4, and 5

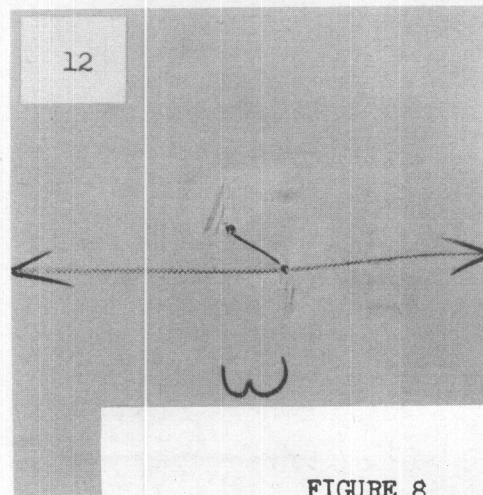
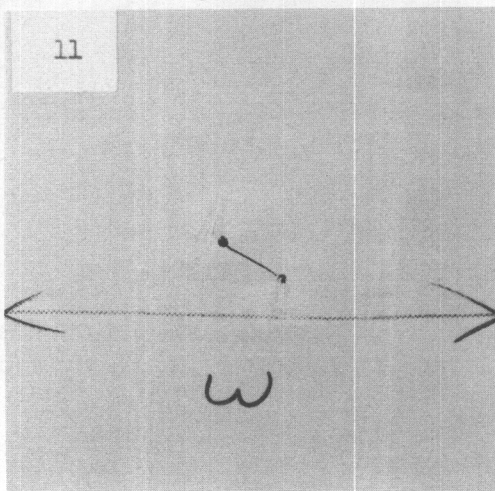
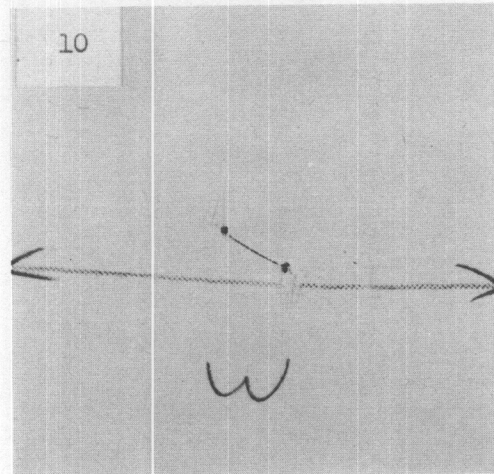
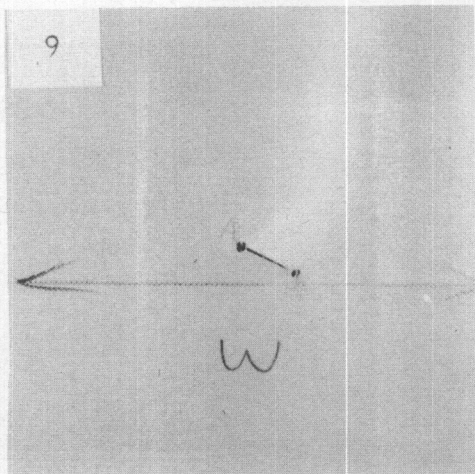
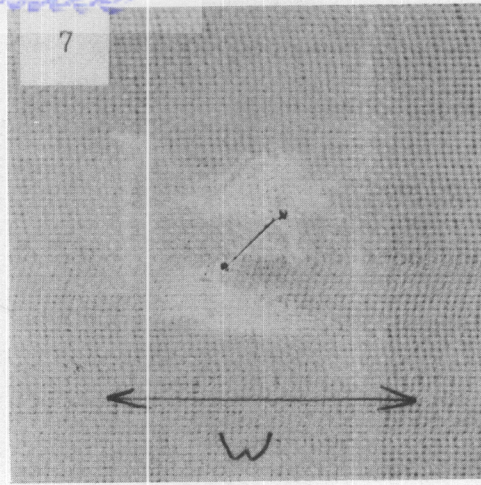
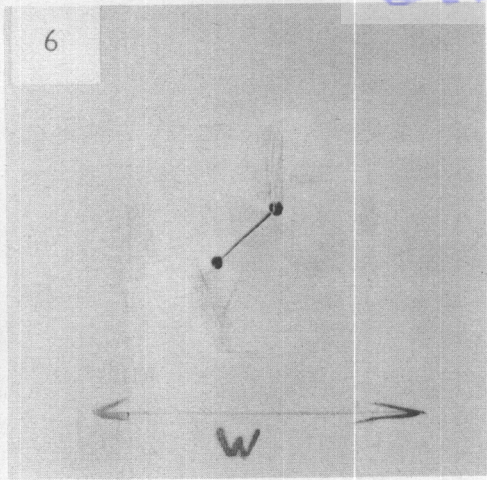


FIGURE 8

INTERNAL EXPLOSION TEST  
PANELS 6, 7, 9, 10, 11, and 12

*Contrails*

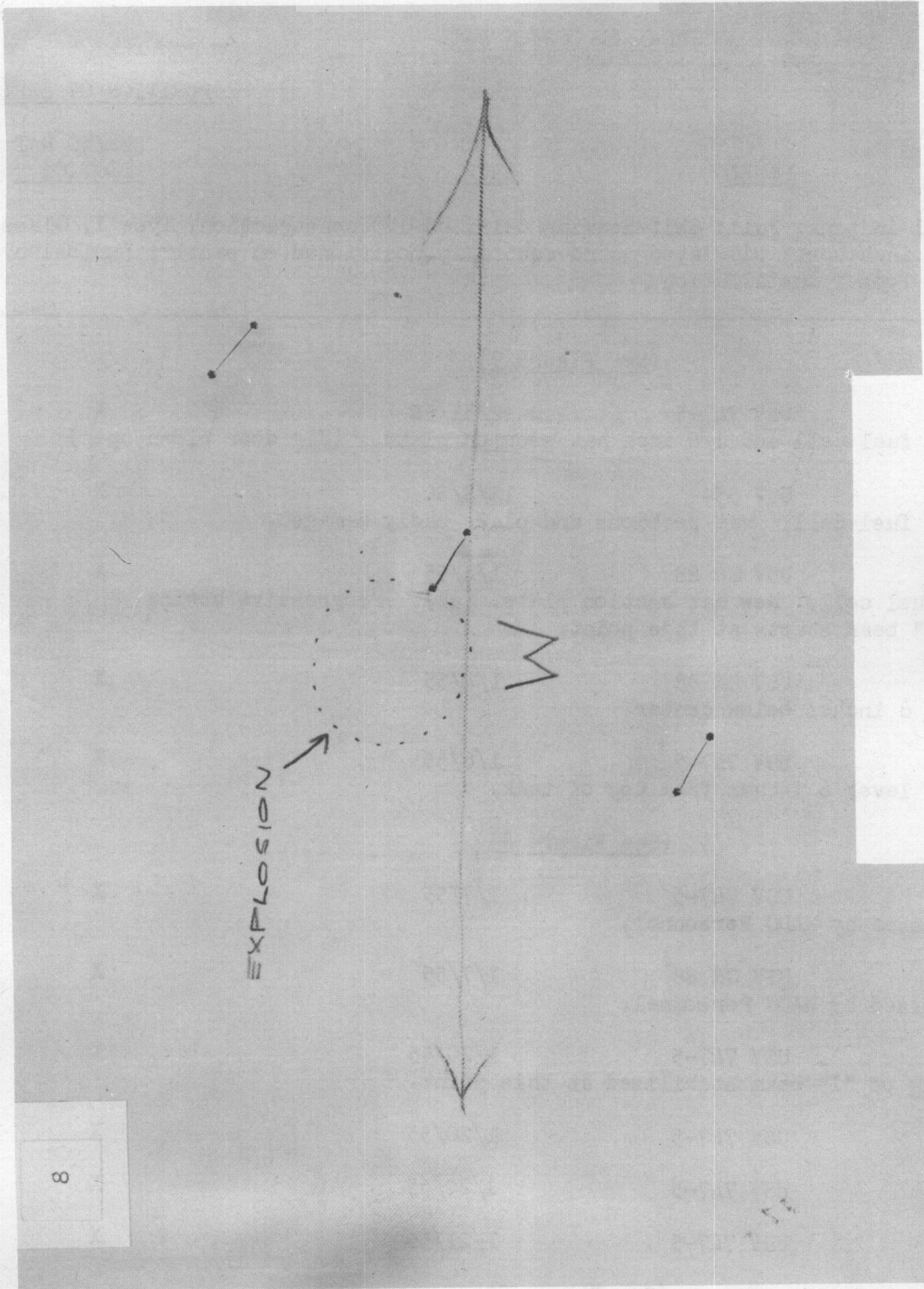


FIGURE 9  
INTERNAL EXPLOSION TEST  
PANEL 8

*Reunited*  
TABLE I

INTERNAL EXPLOSION DATA

POSITION OF EXPLOSION

<u>CODE</u>	<u>PANEL</u>	<u>DATE</u>	<u>BEHIND HAT SECTION</u>
Water level in tank: Full; Self-Sealing Cell, US-173 construction, Type I, Class A, Style I; 6 inch span; simulated wound centrally positioned on panel*; Explosion in 1st port. Type I Installation.			

(See Figure 7)

1	USV 747-5	11/31/54	X
	Large fuel cell and 1/8 inch hat section plate. (Jig door blown open)		
2	USV 55A	12/3/54	X
	Large fuel cell. Hat sections and plate badly damaged.		
3	USV CR 88	1/4/55	X
	New fuel cell. New hat section plate. ( $\frac{1}{2}$ " ). Progressive bowing of "I" beam starts at this point.		
4	USV CR 88	1/4/55	X
	Wound 6 inches below center.		
5	USV 747-5	1/6/55	X
	Water level 6 inches from top of tank.		

(See Figure 8)

6	USV 747-5	1/7/55	X
	Witnessed by WADC Personnel.		
7	USV CR 88	1/7/55	X
	Witnessed by WADC Personnel.		
9	USV 747-5	1/20/55	X
	Bowling of "I" beam stabilized at this point.		
10	USV 747-5	1/20/55	X
11	USV 747-5	1/20/55	X
12	USV 747-5	1/21/55	X

(See Figure 9)

8	USV 747-5	1/20/55	X
	Three simulated projectile wounds.		

\* See Appendix III, page 112.

# Contrails

The greater damage to test panels in the area immediately next to the explosion was noted on panel 8, Figure 8. Figure 10, page 14, shows the results of internal explosion tests on panels 13 and 14, (USV 747-5 backing board) which were made to examine the effect of placing the simulated wound as near the explosive charge as possible. These demonstrate the result of having the simulated wound directly in front of the explosive charge. More damage was created directly around the wound, although the tearing was exaggerated beyond what would be expected with this material in gunfire tests. Table II, page 15, lists the conditions for internal explosion tests on panels 13 through 18.

Panels 15 thru 18 were run to examine the variation in damage that occurs with successive changes in the structure as the test frame was damaged by the force of explosions. Panel 15 was a USV 747-5 material installed as a Type III material on the explosion jig test frame. The panel was mounted on standard cube gunfire hat sections as specified in MIL-P-8045, and the projectile wound was located midway between hat sections and directly in front of the explosive charge. Panel 15 was fired on a new test frame, with standard hat sections mounted on a new one-half inch aluminum panel. The board was fastened to the hat sections by number 6, Parker-Kaylon AN-530-6-6 sheet metal screws, spaced 6 inches on centers. It should be noted that all tests prior to panel 15 were Type I installations.

With panel 15 mounted on the new test plate, the supporting "I" beams at the jig door were bowed one-half inch from the back of the one-half inch aluminum test plate in the center of the panel. The result of the explosion test on the USV 747-5 material, panel 15, indicated that little damage occurred to the material in contrast with that of panels 13 and 14 in which the test plate was bowed by previous explosions to make contact with the supporting "I" beams, where the board was installed as a Type I material. This leads to the conclusion that wide variation of damage to test panels may be expected when the supporting members are appreciably damaged. This is further demonstrated by the more severe damage to another USV 747-5 board, panel 18, shown in Figure 10. Here the test frame used for panel 15 had bowed back to close proximity with the supporting "I" beams after explosions on panels 16 and 17. This suggests that the resiliency of the frame accounts for some absorption of energy. Panel 16 shows the relatively small damage to USV CR 88 material, when the test frame was still relatively unsupported by the "I" beams, while panel 17 shows increased delamination and excessive tearing.

## SUMMARY DISCUSSION

The results of the first 18 internal explosions indicated that the design of the explosion jig using the unstable framework and aluminum hat sections was not adequate to permit reproducible results. It was shown that the pressures created by the explosions were sufficient to change the dimensions of the supporting framework. It was evident that the overall damage to the test panels along the points of contact with the hat sections

# Contrails

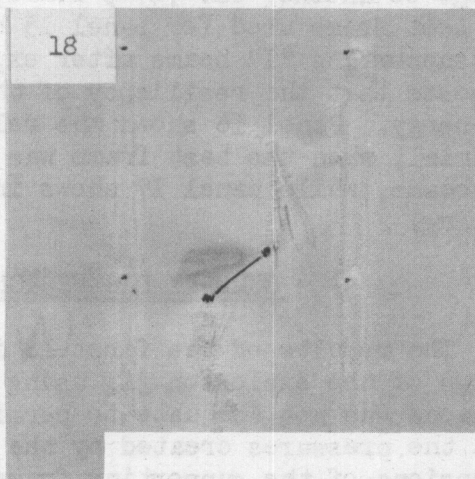
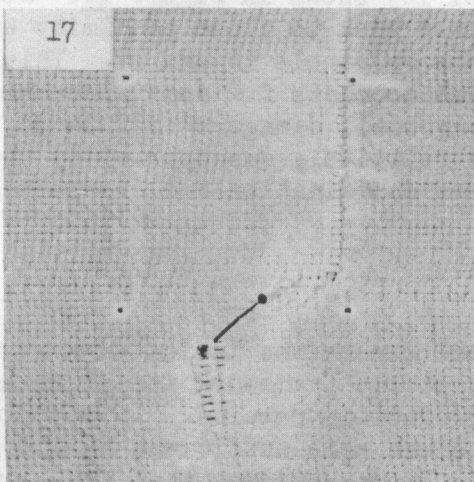
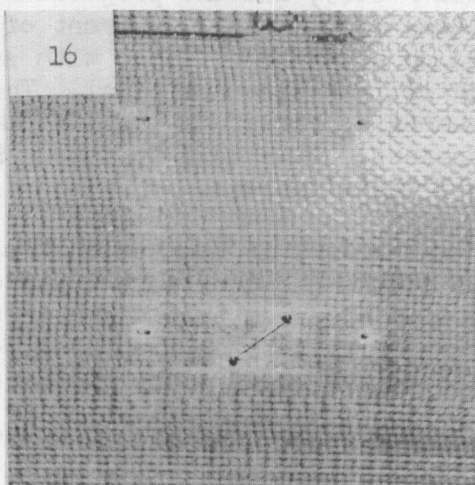
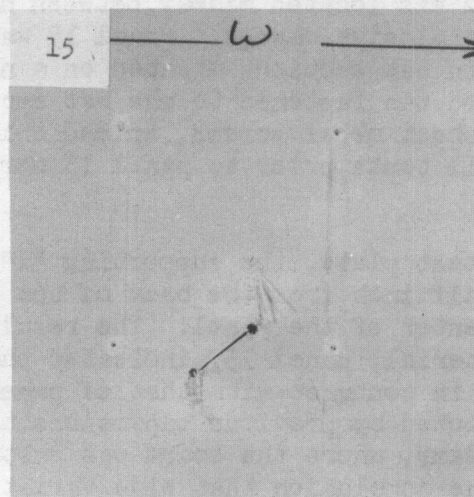
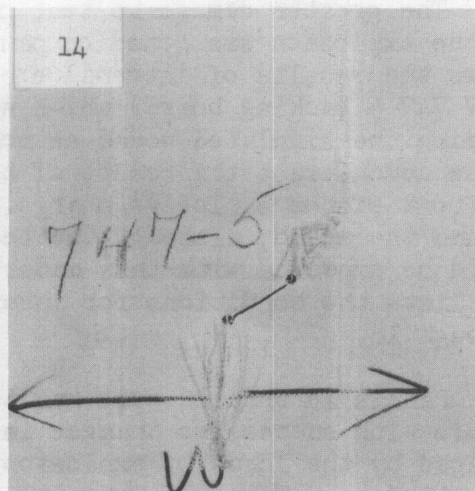
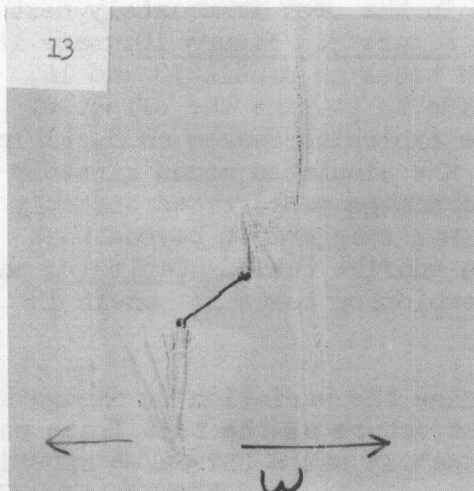


FIGURE 10

INTERNAL EXPLOSION TEST  
PANELS 13, 14, 15, 16, 17, and 18

INTERNAL EXPLOSION DATA

<u>CODE</u>	<u>PANEL</u>	<u>DATE</u>	<u>POSITION OF EXPLOSION</u>	
			<u>BEHIND HAT SECTION</u>	<u>BEHIND WOUND*</u>
Water level in tank: Full; Self-Sealing Cell, US-173 construction, Type I, Class A, Style I; 6 inch span; simulated wound centrally positioned on panel;* Explosion in 1st port. (Front Port.)				
(See Figure 10)				
13	USV 747-5	1/26/55	X	
Hat section mounting panel was unfastened and moved three inches to right to bring simulated wound nearer the explosive charge. 4 to 7 inch tears were produced with shearing along the hat sections. Type I Installation.				
14	USV 747-5	1/26/55	X	
Close duplication of damage on Panel 13 occurred. Type I Installation.				
15	USV 747-5	2/11/55		X
Type III Installation. 1 to 2 inch wounds. New test plate and hat sections. Test plate bowed after explosion.				
16	USV CR 88	2/11/55		X
Type III Installation. No tearing in panel and slight delamination. Considerable bowing in test plate. Some damage to hat sections in explosion area.				
17	USV CR 88	2/18/55		X
Type III Installation. Extensive tearing of panel and shearing at hat sections with considerable delamination in wound area. Test plate nearly in contact with previously bowed "I" beam supports on test frame.				
18	USV 747-5	2/18/55		X
Type III Installation. 2 to 3 inch tears in panel with considerable delamination in the wound area. Shearing at hat sections. Test plate nearly in contact with "I" beam supports.				

\* See Appendix III, page 112.

# Contrails

and at the fastening points, was quite similar to that experienced by the same materials in cube gunfire trials. However, the damage at the wound area of the materials was of a different general character and of either greater or lesser extent than the same materials suffered in gunfire tests.

The results of variation in the test procedure used during the first 18 explosions showed that localized damage in the wound area could best be achieved by creating the explosion directly behind the wound. The position of the concentrated affects of the explosive charge, with respect to the simulated wound, was shown in Figure 9, page 11. The position of the hat sections was changed in subsequent tests to bring the explosive charge directly behind the simulated wound in the test panel.

The preliminary tests served to show that the change of the depth of the charge in the fluid did not produce the changes in the effect of the explosion that were anticipated.

Similarly, changing the height of the water level in the fuel cell did not seem to appreciably affect the damage to the test materials. It was evident however, that the height of the water level in the tank did affect the stresses that were developed around the metal fastening plate of the fuel cell. Considerable difficulty was experienced in maintaining a leak-free seal in this area when the cell was filled with water. This difficulty was reduced when the level of the fluid was six inches from the top of the tank. This fluid level was used in all tests after the first 18.

Table III, page 21, describes the test conditions for the rest of the internal explosion trials. The results of tests on panels 19 thru 34 are shown in Figures 11, 12, and 13, on pages 18, 19, and 20. In this series of tests the solid steel hat sections and mounting plate described in Appendix III, page 112, were used as a means of maintaining stable test conditions. It should be noted that a bladder type fuel cell was used for these tests as compared with the self-sealing fuel cell previously used.

Since test panels 19 thru 34 were primarily intended to investigate the reproducibility of the test, and methods that could be used to simulate gunfire damage, the type of cell was chosen primarily on the basis that the bladder type cell exhibited better resistance to damage at the metal fastening plate. No comparison of the effects of the type of cell on the damage resulting from the testing can be made. It seems reasonable to suggest that the use of self-sealing type fuel cells would result in somewhat lower damage levels to the backing material as a result of the cushioning action of the relatively thicker construction, as compared to the thinner, more flexible bladder type materials.

The first two explosions using the conditions of Table III produced damage to USV CR 88 boards far in excess of any previous test, and very



# Contrails

different from cube gunfire tests. These are shown in Figure 11, panels 18 and 19. The similarity of the damage between the two panels was considered excellent. The greater extent of the damage compared to previous tests was attributed to the close proximity of the explosion to the simulated wound, combined with the high rigidity of the steel test members.

Panel 20 was run under the conditions above to examine the action of USV 33 backing material which is known to have unsatisfactory gunfire resistance in Type III installations. It is evident from the illustration of Figure 11, that the damage to this panel was more extreme than that of the two USV CR 88 trials. Complete shearing can be noted at the edges of the hat section supports.

In tests 22, (USV CR 88 panel) and 23 (USV 33 panel) a one-half inch sheet of cellular shock absorbing material (U.S. Ensolite) was introduced between the fuel cell wall and the test panel. A six inch diameter hole was made in the padding material centered over the simulated projectile wound. The damage to these panels under identical conditions with panels 19, 20, and 21, show the effectiveness of the padding material in concentrating damage in the wound area. The padding greatly reduced the damage along the hat section supports. This is definitely shown in comparing the USV 33 trials on panels 20 and 23.

The explosive charge was placed in the second port starting with panel 24. In this position the damage caused by the explosions was in all cases less than would be expected from actual cube gunfire testing. However, panels 24 thru 29 were run to examine the reproducibility of the method. Panels 24, 25, and 26 (USV CR 88) showed excellent similarity of damage over the entire 30 inch by 40 inch test panel. The 14 inch by 14 inch section shown in Figures 11 and 12 show the good similarity in the wound area.

Three panels of USV 33 material, panels 27, 28, and 29 of Figure 12 also showed excellent reproducibility between tests. Comparing internal explosion tests of USV CR 88 material with the USV 33 material shows greater damage to the USV 33 backing board, but not nearly in the degree that exists in cube gunfire tests.

It is concluded from these results that the test is very reproducible, and does indicate differences between materials. However, the degree of damage between test materials is considerably less on the internal explosion test, than it is on cube gunfire tests. It is known that cube gunfire tests of USV 33 materials in a Type III cube test installation would be more nearly like the front port internal explosion of panel 21, Figure 11.

Panels 30, 31, and 32, shown in Figures 12, and 13 were run on USV 747-5, Swedlow S 2N, and USV 55A backing boards respectively to provide data for comparing all the materials of the test program. Here again it was concluded that the results show differences between materials, but not in the same degree as gunfire tests.

# Contrails

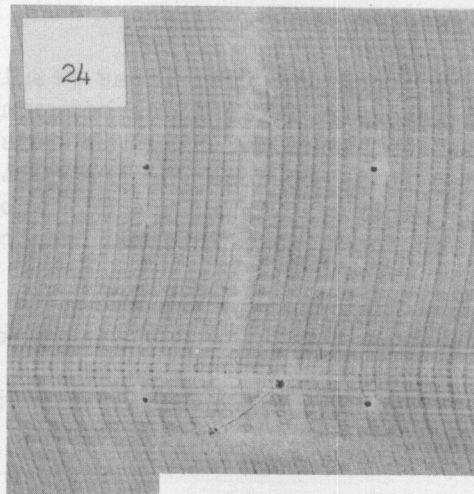
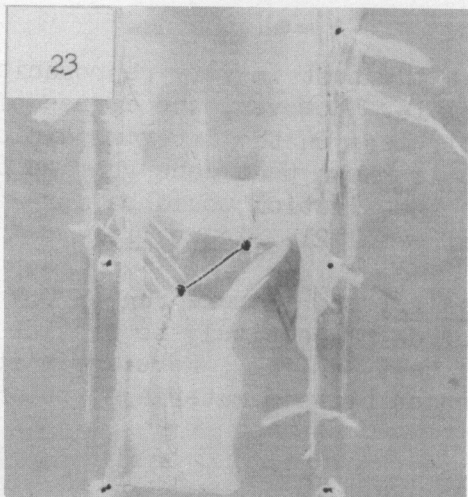
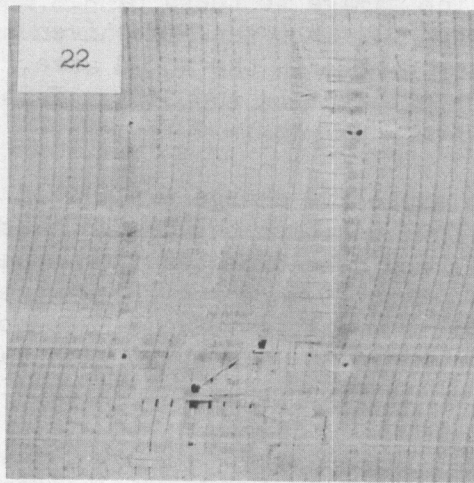
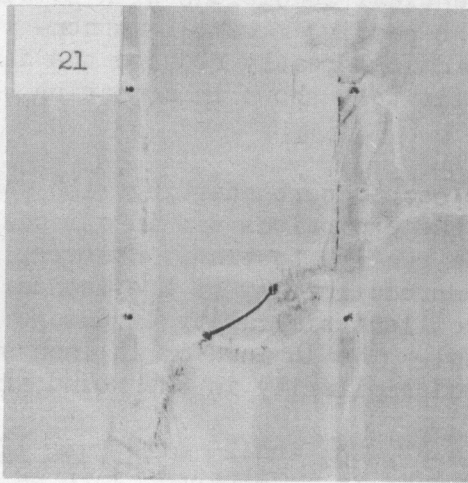
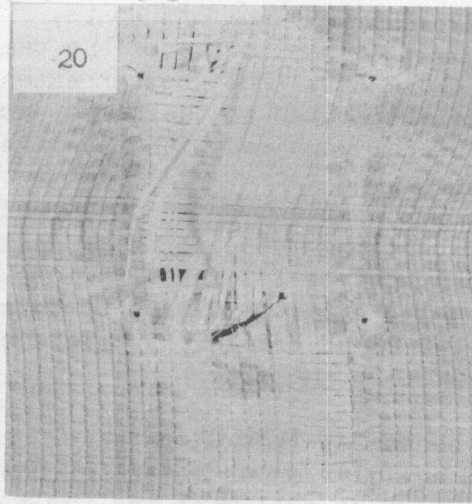
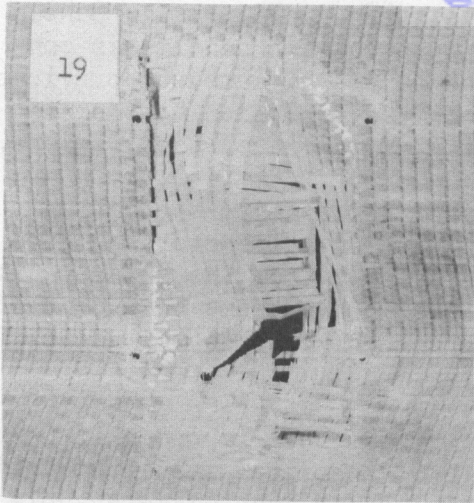


FIGURE 11

INTERNAL EXPLOSION TEST  
PANELS 19, 20, 21, 22, 23, and 24

# Contrails

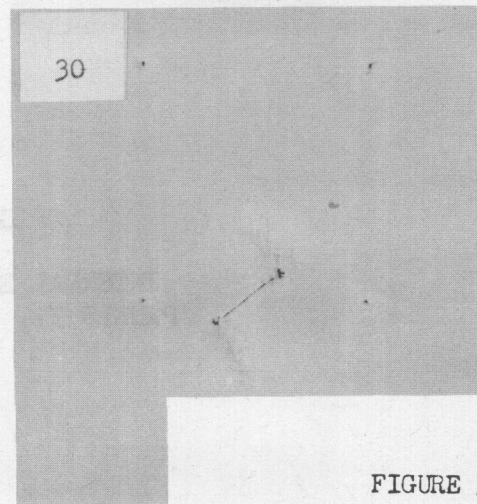
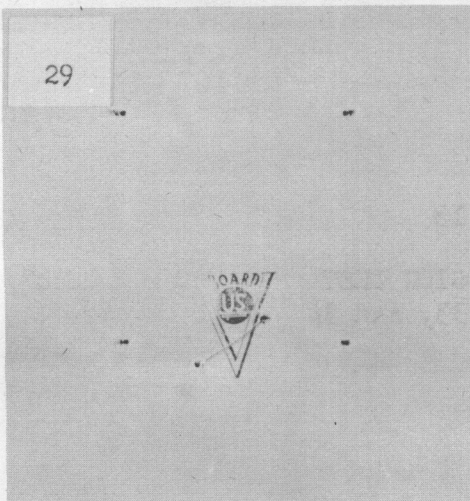
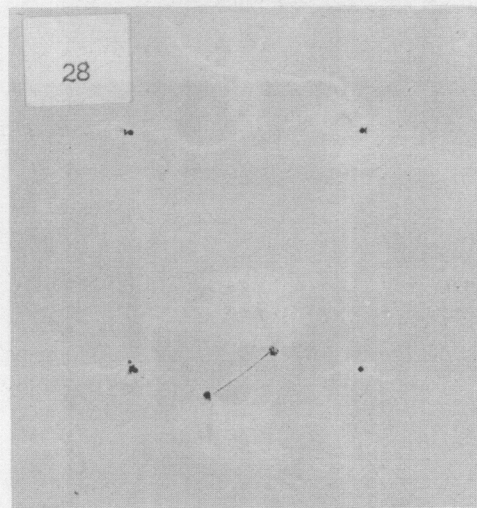
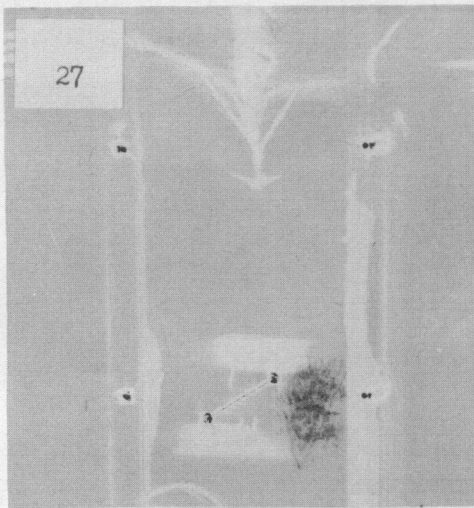
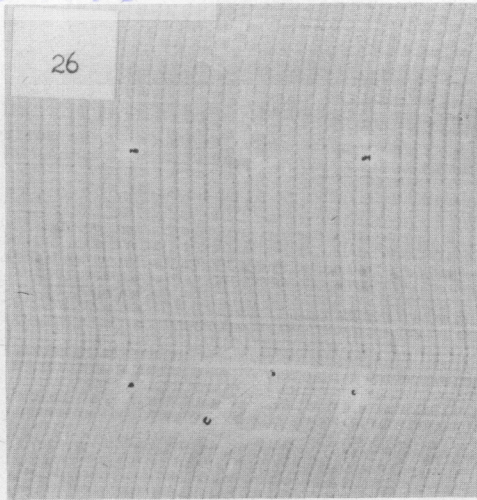
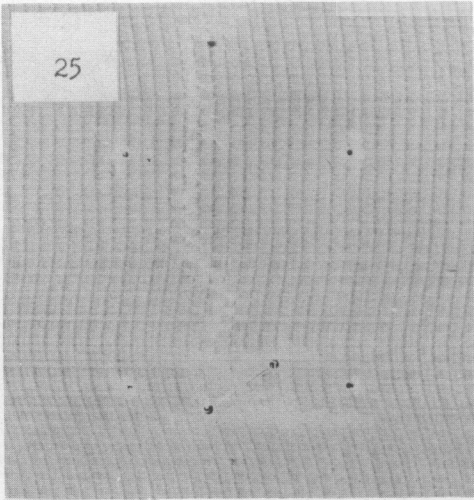


FIGURE 12

INTERNAL EXPLOSION TEST  
PANELS 25, 26, 27, 28, 29, and 30

*Contrails*

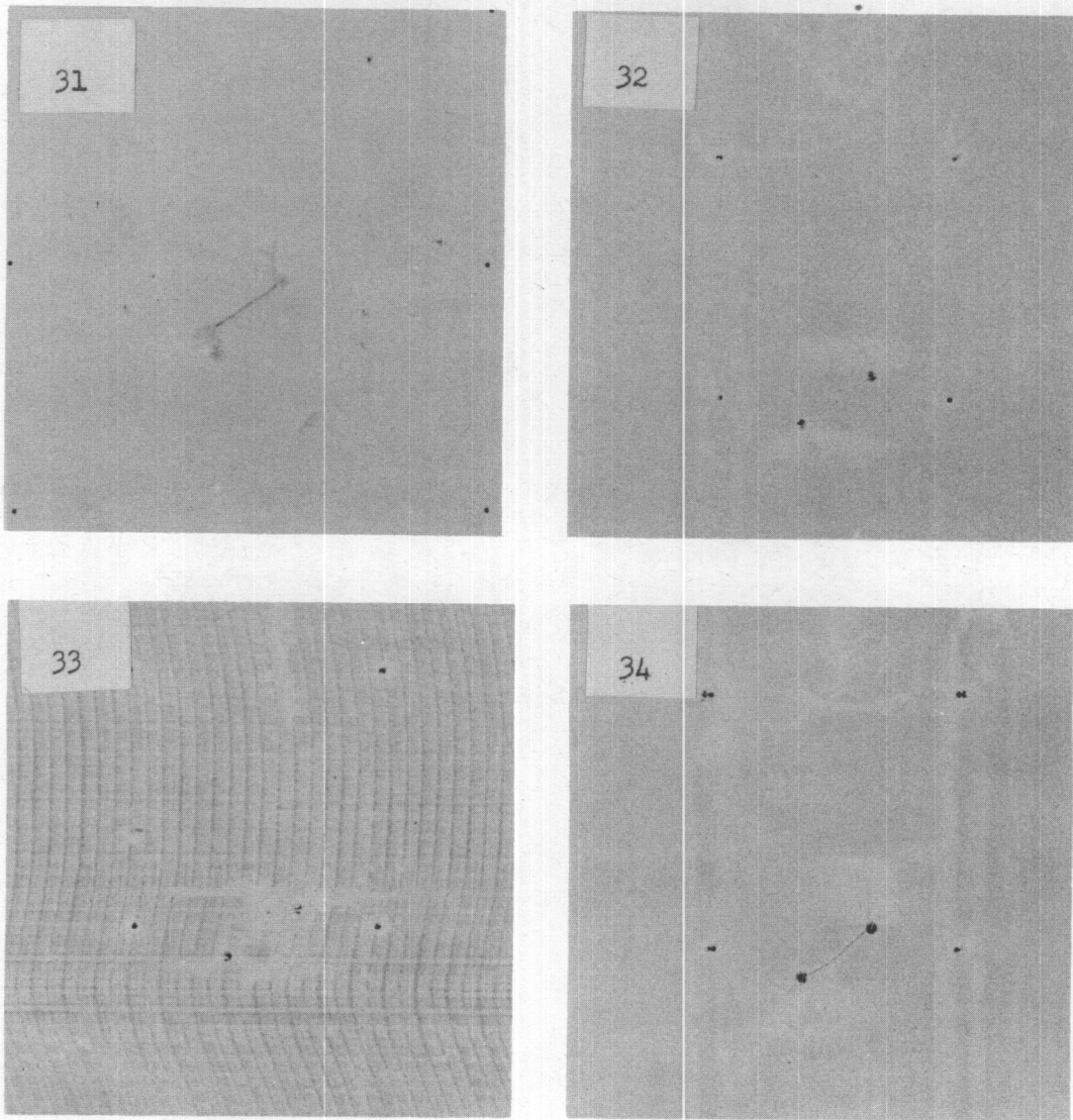


FIGURE 13  
INTERNAL EXPLOSION TEST  
PANELS 31, 32, 33, and 34

TABLE III

INTERNAL EXPLOSION RESULTS

POSITION OF EXPLOSION

CODE                      PANEL                      DATE                      (PORT)

Water level in tank: 6 inches from top; Bladder Cell, US-577 construction; 6 inch span; simulated wound centrally positioned on panel;\* Explosions placed directly behind wound area in tank. Type III Installation.

---

(See Figure 11)

19	IE-1 USV CR 88	7/25/55	1st (Front)
20	IE-2 USV CR 88	7/25/55	1st
21	IE-3 USV 33	7/26/55	1st
22	IE-4 USV CR 88	7/26/55	1st
	One-half inch sheet "Ensolute" between fuel cell and panel with hole 6 inches in diameter cut at position of wound.		
23	IE-5 USV 33	7/27/55	1st
	One-half inch sheet "Ensolute" between fuel cell and panel with hole 6 inches in diameter cut at position of wound.		
24	IE-6 USV CR 88	7/28/55	2nd

(See Figure 12)

25	IE-9 USV CR 88	7/28/55	2nd
26	IE-8 USV CR 88	7/28/55	2nd
27	IE-7 USV 33	7/28/55	2nd
28	IE-10 USV 33	7/28/55	2nd
29	IE-11 USV 33	7/29/55	2nd
30	IE-12 USV 747-5	7/29/55	2nd

(See Figure 13)

31	IE-13 S 2N	7/29/55	2nd
32	IE-14 USV 55A	7/29/55	2nd
33	IE-15 USV CR 88	8/23/55	2nd
	High Speed Photographic Analysis.		
34	IE-16 USV 33	8/23/55	2nd
	High Speed Photographic Analysis.		

\* See Appendix III, page 112.

Panel 33 (USV CR 88) and panel 34 (USV 33) were run under the conditions listed in Table III for high speed motion picture study. The sketch of Figure 72, page 117, depicts the manner in which the movies were taken. (See Appendix III.) The primary action of the explosion, is viewed through the second mirror. This shows the initial tearing and delamination. As the backing board is forced outward by the explosion, it breaks the mirror, and the remaining action is visible through the first mirror. The position of the first mirror in the line of sight of the camera is such that it reflects an image that would be seen by an observer looking downward on the test panel.

The film displays action that may be related to a peculiarity of damage that was noted on all the test panels. This can be noted particularly well on the illustration of panel 22, Figure 11, where there appear to be two distinct areas of concentrated damage. The first is in the area of the simulated wound which is on a horizontal line with the explosive charge in the fluid. The second appears six or seven inches higher on the panel directly above the simulated wound.

In analyzing the action evident in the high speed film it appears that the initial bulging of the backing material in the area of the simulated wound is followed by a more pronounced bulging above it. This suggests the possibility that a second shock wave may be formed by reflection from the walls of the test jig. Robert H. Cole, Reference 14, discusses reflection from solid members in his treatise, "Underwater Explosions". It would be beyond the scope of this work to more than suggest that phenomena described by Cole might explain the occurrence and position of a second shock front in the fluid. In any case it appears that pulsations in the test panel occur and all panels tested show what appears to be an area of concentrated damage above the initial explosion level. Figure 73, page 117, illustrates the manner in which a reflected shock wave might act, (see Appendix III.)

## SECTION II

### PRESSURE DEFLECTION TESTING

#### SERVICE CONDITIONS

One of the prime functions of backing board materials in aircraft structures is to support the fuel laden cell. The backing board serves to distribute the highly localized loads that occur at points of contact with the air frame structure over the surface of the relatively flexible fuel cell.

The work described in WADC Technical Report 54-474, Reference 15, page 131, indicated the desirability of testing backing board materials by means of a biaxial tension test. The objectives of this work involved the design, instrumentation, and evaluation of a test device for subjecting backing board materials to fluid loads. The preliminary investigation of the factors to be considered in constructing test equipment included

conferences and discussions with air frame manufacturers. The general shapes of the supporting members and the maximum and minimum spans across which the backing board would be installed was discussed in the conferences described in Appendix II, page 109. The preliminary design of the pressure deflection test equipment was then made in conference with the Materials Laboratory and Power Plant Laboratory of the Wright Air Development Center.

The general characteristics of the design first developed for internal explosion testing and pressure deflection evaluations are shown in Figure 69, page 113. The improved construction, with stable steel members described in Appendix III was obtained by eliminating deficiencies that became apparent in the internal explosion testing.

The use of the rigid steel test frame for pressure deflection testing represents the same departure from duplication of service conditions as those discussed in the internal explosion testing of Section I. The use of a rigid structure as opposed to the more flexible aluminum sections found in air frame construction was found to be justified by the results of the pressure deflection testing. It was found that small differences in fastening techniques resulted in significant variations in the response of a given material to pressurization.

Although many possibilities existed for combinations of various shapes and spacing of supporting members, and fastening procedures, a single shape of support and the fastening system used in cube gunfire testing was adopted for the pressure deflection evaluation.

#### TEST METHODS AND EQUIPMENT

A standard system of installing backing boards on the test frame was adopted. Figure 70, page 114, shows the slotted steel frame with simulated hat sections bolted at six inch center spacings. The test panels were mounted by drilling 5/32 inch holes in the panel and fastening with AN-515-8R10 screws into tapped holes in the hat section. Fasteners were placed at six inch intervals by means of a torque controlled mounting drill. Spacing for the holes was accomplished by use of a drilling template. The fasteners were spaced symmetrically along the length of the hat section.

Careful manipulation in drilling and mounting the panels was required to minimize warping and localized tensions in the test panels. In the same panels the lack of absolute flatness in the material before mounting precluded a certain unevenness in the surface of the mounted test panel.

After the panel was mounted, the test frame was swung into fastening position on the main tank, and the fasteners adjusted until the test panel was in the plane of the front edge of the test jig and the fluid filled tank in an unstressed position. Water was introduced into the tank by means of the flexible pressure hose connected from the source to the tank inlet. Other outlets on the tank were open to prevent premature

pressurizing. Deflection measurements were taken at this stage of the test to indicate the deflections caused by the static water head from the measurement position to the inlet overflow level. The 12.75 inch head of water over the position at which the deflection measurements were taken caused an initial load of 0.461 psi upon the test panel. The deflection sensing shaft contacts the panel at a distance ten inches below the top of the test frame support plate. The shaft is held in contact with the test material by light spring pressure in the deflection transducer.

Figure 14, page 25, shows the arrangement of the pressure deflection test equipment. The deflection sensing transducer is shown mounted on the test frame. Deflection was recorded by fixing the sensing arm of the Tinnius Olsen Elongation Transducer against a shaft in contact with the backing board material. Deflection of the backing board at the mid-point of the stringer span caused a lateral movement in the perpendicular sensing shaft which in turn activated the transducer arm. The shaft was held in contact with the backing board surface by spring loading, and was free to move thru a bushing support that maintained the shaft in the test position. The electrical signal from the deflection transducer was transmitted to a Model 51 Electronic Recorder manufactured by the Tinnius Olsen Testing Machine Company. This autographic recorder rotated the stress strain chart to produce the deflection axis. The recorder is shown in Figure 14, on the work table, to the left. The deflection sensing transducer, a Universal Strain Instrument, Type U-1, manufactured by the Tinnius Olsen Testing Machine Company was mounted on the test frame to sense the deflection of the test panel by contact with the center of the deflecting surface.

A pressure transducer of the SR-4, Type EMB, range 0 to 50 pounds per square inch gauge pressure was mounted on the jig and connected to the fuel cell. This transducer is manufactured by the Baldwin-Lima-Hamilton Company. The electrical signal produced by the pressure transducer was transmitted to a control unit, which subsequently presented this signal to a Brown "Elektronik" Potentiometer Type Autographic Recorder, Model 153X10P. This recorder was used to produce the pressure axis on the stress strain chart. The control unit incorporates calibrating resistors and regulation of the zero position and span width of the recorder, as shown in Figure 15, page 26.

The simultaneous operation of the two recorders produces a stress strain diagram of the test pressure against the panel deflection. Figure 16, page 26, shows a flow chart of the recording system.

The test system described above represents the general procedure used throughout the pressure deflection evaluations. Initially it was thought that regulation of the water supply used to produce the test pressures would be required. It was found however, that the rate and extent of pressurization was adequately controlled by regulating the volume flow of water into the system manually. The pressure regulation system built for this purpose was then discarded.

The feasibility of using two separate recording systems working together was first evaluated with a pneumatic-mechanical motor. The pneumatic



*Contrails*

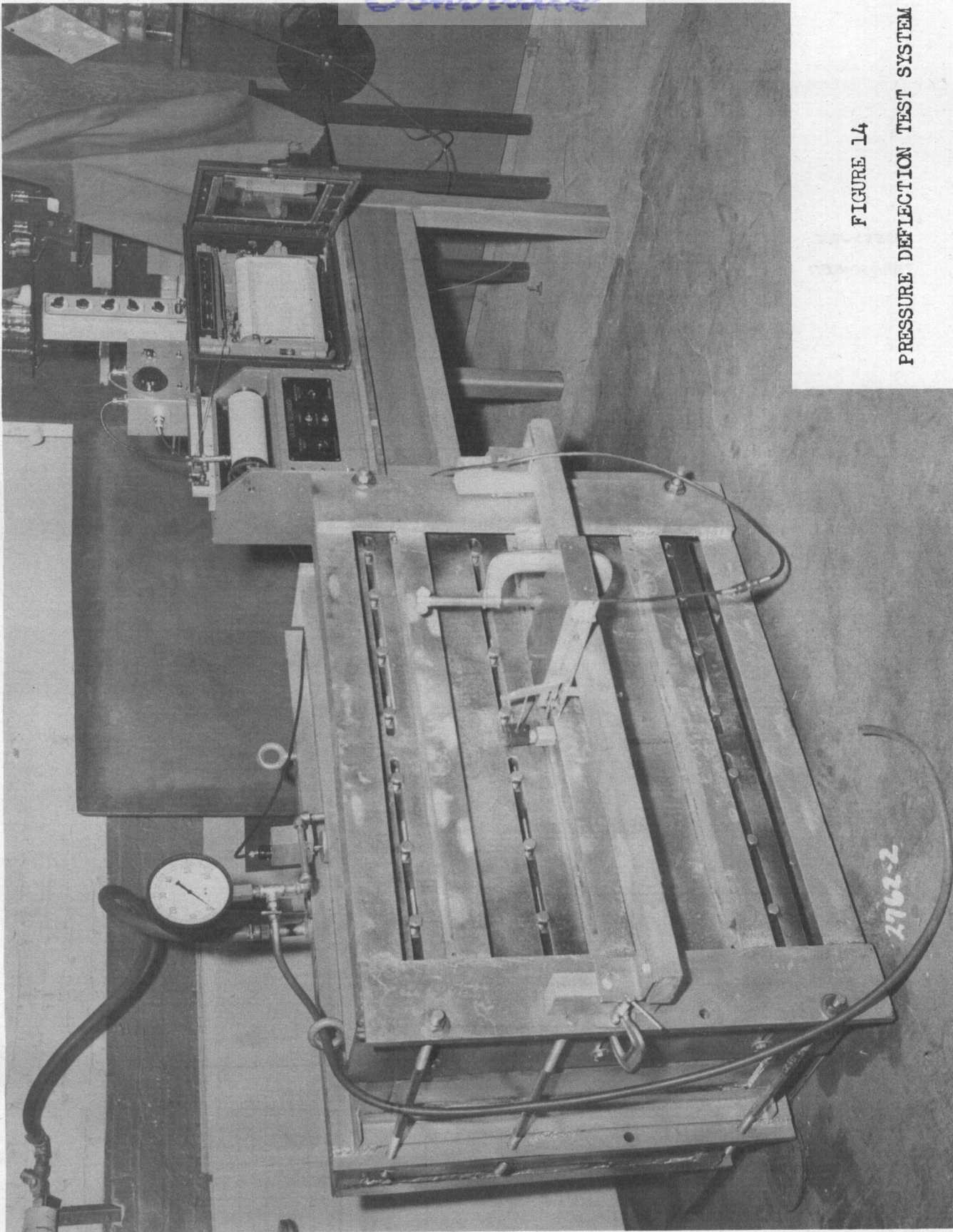


FIGURE 14

PRESSURE DEFLECTION TEST SYSTEM

RECORDER CONTROL UNIT

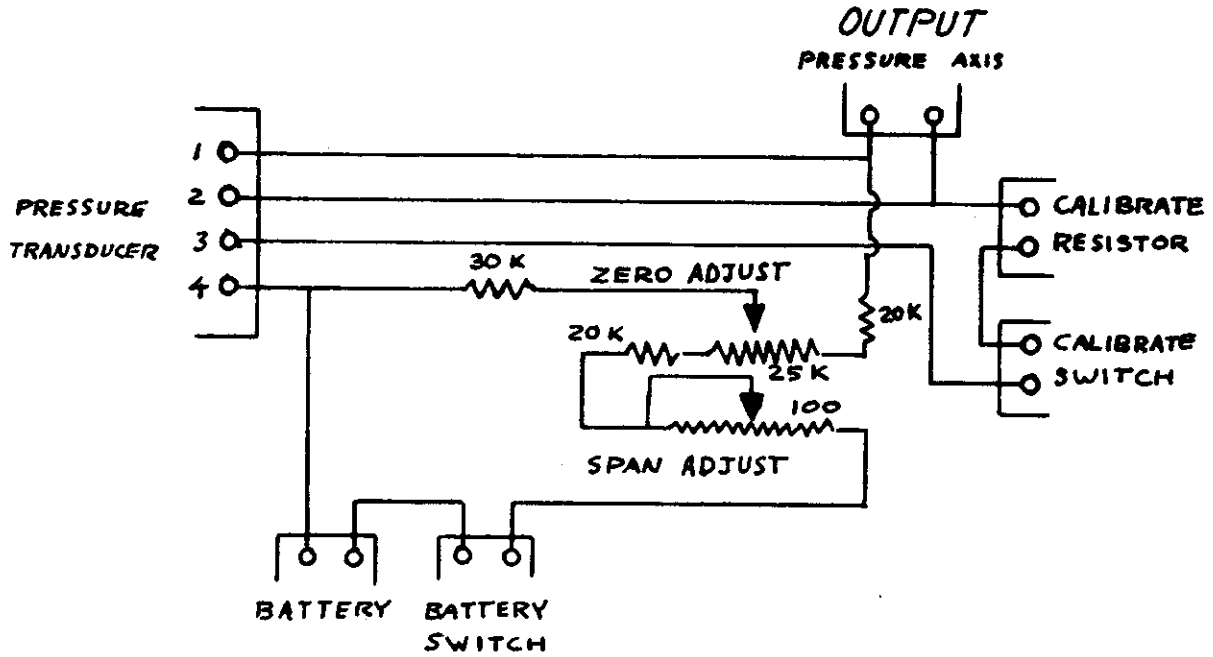
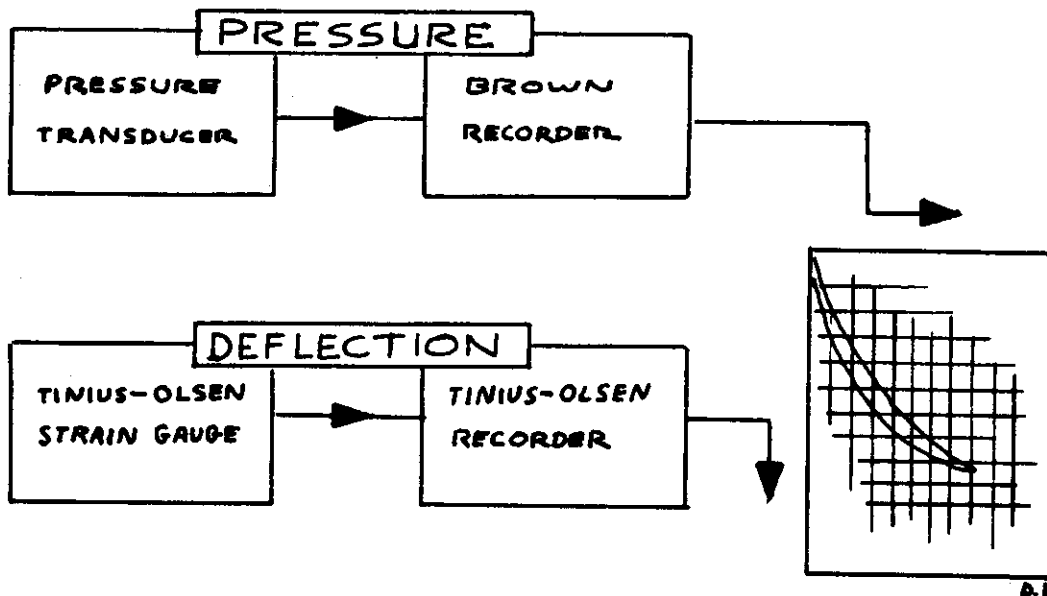


FIGURE 16

FLOW CHART  
PRESSURE DEFLECTION SYSTEM



*Continued*

motor demonstrated the usefulness of the data but its response to pressure changes was inadequate, and it was replaced by the bridge type pressure transducer regulating the electronic recorder.

In general, the test procedures were carried out with the backing board materials discussed in Appendix I, page 108. In a few instances, other materials were tested in the series, where it seemed this might supply useful information. An Introduction to Pressure Deflection Trials, page 28, explains the entries in Table IV.

#### EXPERIMENTAL DATA

Table IV, Pressure Deflection Trials, page 29, lists the conditions under which the pressure deflection tests were run for each trial. Pressure deflection data is given for the 6, 8, 10, and 12 inch hat section spacing using both bladder and self-sealing type fuel cells. Remarks regarding the results of the tests are included in this table.

The deflection readings were all taken at the center of the individual hat section spacings at a position 10 inches from the top of the test frame. All readings of deflection were taken in the hat section spacing centrally located with respect to the ends of the test frame except where noted as "left" or "right". Left or right in this case refers to the first full spacing at the extreme right or left of the test frame when facing the test jig.

The stress strain curves for each of the test panels are included as figures following Table IV, and are in the same order as the data which relates to them in the table. Since the static loading of the fluid introduced into the test cell prior to pressurization produced an initial deflection of the test panels, this deflection was graphically added to the stress strain curve where necessary.

The stress strain curves were taken at the same magnification on all the test materials. Where this produced a curve longer than the length of the recorder paper, the extended portion of the curves was brought back to the zero position and the curve continued on the same sheet. Further, several curves were represented on a single sheet by moving the zero pressure position of each succeeding curve a unit distance on the pressure axis.

Table IV gives data for the 60 pressure-deflection tests. Standard conditions were used in all tests except where otherwise designated in the notes.

Trials numbered 1 and 2, Figures 17 and 18, established a technique for testing. They also showed that considerable difference could be expected between tests made in the center hat section area and at the extremes of the test plates. This is further demonstrated in trials 3 and 4, Figures 19 and 20. These tests show the effect of the frictional forces between the hat section support and the test panels. The test panels of USV 747-5 backing board used in trials 3 and 4 were installed without fasteners in the manner of a Type I installation. The conditions were the same for the two panels except that a silicone jelly was used as a lubricant between the test panel of trial 4 and the hat sections supporting it. The greater deflection resulting from the lubrication of the supports, comparing trials 3 and 4, demonstrates the considerable effect that the edge conditions have on the system.

*Continued*  
INTRODUCTION TO TABLE IV

PRESSURE DEFLECTION TRIALS

Column one of Table IV gives the order number in which the pressure deflection tests on the materials of column three are discussed. Column two lists the PD number of the tests which numbers the order of testing.

The order in which the pressure deflection test data is presented in this report is shown in column one. The code listing of column two gives the chronological order in which the tests were performed. Column three, headed Panel, identifies the test material. The data for the pressure deflection tests is presented in the form of stress strain curves. The figure on which this data appears is listed in column four under Stress Strain Curve. It should be noted that in some instances several stress strain curves were reproduced on the same chart to consolidate the report.

The figures containing the stress strain data are exact copies of the original recordings. However, in some instances the initial deflection of the test panel resulting from the pressures created by filling the test cell with fluid were recorded separately from the pressurization cycle. In these instances the figures that are reproduced after Table IV show the initial pressure and deflection graphically added to the curve.

Column five lists the maximum pressure that was used during the test. The initial deflection that occurred as a result of filling the test cell is listed in column six.

Column six gives the permanent set for each of the test panels. This is defined as the deflection of the center of the test span that remained when the tank was depressurized following a test. This is shown as the distance between the initial deflection and the return trace on the stress strain recordings. These values can be compared only in those instances where the maximum pressures of the test were the same.

The notes of Table IV, which appear under the panel listing indicate the position of the deflection measurements and other deviations from the standard procedure. Any remarks about the performance of the panel are included here as notes.

In reading the data from the stress strain curves, it should be noted that the curves originate at zero pressure and zero deflection. One major division on the pressure or load axis represents 5 psi. Each minor division represents 0.5 psi. One major division on the deflection axis represents 0.10 inches. Each minor division represents 0.01 inches.

# Contrails

## TABLE IV

### PRESSURE DEFLECTION TRIALS

#### BLADDER CELL - 6 INCH SPAN

<u>NO.</u>	<u>CODE</u>	<u>PANEL</u>	<u>STRESS STRAIN CURVE (FIGURE)</u>	<u>MAXIMUM TEST PRESSURE (PSI)</u>	<u>INITIAL DEFLECTION (INCHES)</u>	<u>PERMANENT SET*</u>
1	PD-2	USV 747 5	17	20.46	.033 Center	
				20.46	Left	
				20.46	Right	
			Holes in panel for Type III Installation (11/64" diameter) Leakage of water around fuel cell fitting.			
2	PD-3	USV 747 5	18	20.46	.038 Right	
				20.46	Center	
				20.46	Left	
3	PD-10	USV 747 5	19	20.56	.093 Center	.105
				20.56	Left	.010
				20.56	Right	.065
			Type I Installation.			
4	PD-11	USV 747 5	20	20.66	.138 Center	.033
				20.66	Left	.016
				20.56	Right	.150
			Silicone jelly applied to hat sections to allow more freedom of motion. Type I Installation.			

\* Distance from end of initial deflection to end of return trace.

# Contrails

## TABLE IV (Cont.)

### PRESSURE DEFLECTION TRIALS

#### BLADDER CELL - 8 INCH SPAN

<u>NO.</u>	<u>CODE</u>	<u>PANEL</u>	<u>STRESS STRAIN CURVE (FIGURE)</u>	<u>MAXIMUM TEST PRESSURE (PSI)</u>	<u>INITIAL DEFLECTION (INCHES)</u>	<u>PERMANENT SET*</u>
5	PD-52	USV CR 88 Panel pulled from end fastenings.	21	30.7	.180	.270
6	PD-53	USV CR 88 Panel pulled from end fastenings.	22	31.7	.286	.273
7	PD-50	USV 33 Panel pulled from end fastenings.	23	30.6	.203	.527
8	PD-51	USV 33 Panel pulled from end fastenings.	24	32.1	.298	.267
9	PD-55	USV CR 88 2" spacing on end hat sections.	25	27.4	.193	.310
10	PD-54	USV 33 2" spacing on end hat sections.	26	29.1	.203	.305

\* Distance from end of initial deflection to end of return trace.

*Controls*  
TABLE IV (Cont.)

PRESSURE DEFLECTION TRIALS

BLADDER CELL - 6 INCH SPAN

<u>NO.</u>	<u>CODE</u>	<u>PANEL</u>	<u>STRESS STRAIN CURVE (FIGURE)</u>	<u>MAXIMUM TEST PRESSURE (PSI)</u>	<u>INITIAL DEFLECTION (INCHES)</u>	<u>PERMANENT SET*</u>
11	PD-4	USV 747 5 5/32" hole adopted for all test panels.**	27	20.46	.055	.028
12	PD-6	USV CR 88 Panel pulled from end fastenings.	27	20.46	.124	.030
13	PD-5	USV 55A Panel pulled from end fastenings.	27	20.66	.117	.098
14	PD-9	USV 33 Panel pulled from end fastenings.	28	20.56	.133	.090
15	PD-8	S 2N	28	20.66	.328	.153
16	PD-7	S 3N	27	20.66	.204	.095

SELF-SEALING CELL - 6 INCH SPAN

17	PD-14	USV 747 5 Panel pulled from end fastenings.	29	33.26	.070	.073
18	PD-17	USV CR 88 Panel pulled from end fastenings.	30	35.46	.160	.065
19	PD-16	USV 55A Panel pulled from end fastenings.	29	35.46	.100	.068
20	PD-15	USV 33 Panel pulled from end fastenings.	29	34.86	.190	.080
21	PD-18	S 2N	30	35.06	.250	.085

\* Distance from end of initial deflection to end of return trace.  
 \*\* This means all panels coded PD-4 or higher used 5/32" mounting holes.

*Contrails*  
TABLE IV (Cont.)

PRESSURE DEFLECTION TRIALS

BLADDER CELL - 8 INCH SPAN

<u>NO.</u>	<u>CODE</u>	<u>PANEL</u>	<u>STRESS STRAIN CURVE (FIGURE)</u>	<u>MAXIMUM TEST PRESSURE (PSI)</u>	<u>INITIAL DEFLECTION (INCHES)</u>	<u>PERMANENT SET*</u>
22	PD-38	USV 747 5 Panel pulled from end fastenings.	31	33.7	.100	.323
23	PD-39	USV CR 88 Panel pulled from end fastenings.	32	31.3	.355	.180
24	PD-40	USV 55A Panel pulled from end fastenings.	33	31.2	.200	.245
25	PD-41	USV 33 Panel pulled from end fastenings.	34	29.3	.217	.167
26	PD-42	S 2N Panel pulled from end fastenings.	35	26.0	.453	.290

SELF-SEALING CELL - 8 INCH SPAN

27	PD-19	USV 747 5 Water leakage from fuel cell, which started to pull out progressively from fitting at front. Panel pulled from end fastenings.	36	38.26	.083	.088
28	PD-21	USV CR 88 Panel pulled from end fastenings.	37	32.36	.297	.148
29	PD-20	USV 55A Panel pulled from end fastenings.	36	34.76	.160	.065
30	PD-23	USV 33 Panel pulled from end fastenings.	38	33.96	.205	.068
31	PD-22	S 2N Panel pulled from end fastenings.	39	34.46	.300	.327

\* Distance from end of initial deflection to end of return trace.



*Contrails*  
TABLE IV (Cont.)

PRESSURE DEFLECTION TRIALS

BLADDER CELL - 10 INCH SPAN

<u>NO.</u>	<u>CODE</u>	<u>PANEL</u>	<u>STRESS STRAIN CURVE (FIGURE)</u>	<u>MAXIMUM TEST PRESSURE (PSI)</u>	<u>INITIAL DEFLECTION (INCHES)</u>	<u>PERMANENT SET*</u>
32	PD-43	USV 747 5 Panel pulled from end fastenings.	40	29.0	.227	.410
33	PD-44	USV CR 88 Panel pulled from end fastenings.	41	28.3	.353	.464
34	PD-45	USV 55A Panel pulled from end fastenings.	42	28.5	.323	.320
35	PD-46	USV 33 Panel pulled from end fastenings.	43	27.7	.371	.511
36	PD-47	S 2N Right end of panel pulled from end fastenings.	44	25.3	.565	.385

SELF-SEALING CELL - 10 INCH SPAN

37	PD-24	USV 747 5 Some delamination; panel pulled from end fastenings.	45	31.96	.130	.187
38	PD-26	USV CR 88 Panel pulled from end fastenings.	46	34.46	.283	.269
39	PD-25	USV 55A Panel pulled from end fastenings; delamination; shear characteristics.	47	33.96	.256	.169
40	PD-27	USV 33 Delamination; panel pulled from end fastenings.	48	35.46	.430	.247
41	PD-28	S 2N Delamination; panel pulled from end fastenings.	49	33.76	.484	.425

\* Distance from end of initial deflection to end of return trace.

*Continued*  
TABLE IV (Cont.)

PRESSURE DEFLECTION TRIALS:

BLADDER CELL - 12 INCH SPAN

<u>NO.</u>	<u>CODE</u>	<u>PANEL</u>	<u>STRESS STRAIN CURVE (FIGURE)</u>	<u>MAXIMUM TEST PRESSURE (PSI)</u>	<u>INITIAL DEFLECTION (INCHES)</u>	<u>PERMANENT SET*</u>
42	PD-34	USV 747 5 Panel pulled from end fastenings.	50	35.0	.307	.604
43	PD-49	USV 747 5 Panel pulled from end fastenings.	51	12.7 Demonstrated for WADC.	.265	.560
44	PD-35	USV CR 88 Panel pulled from end fastenings.	52	33.6 Fuel cell completely filled the end positions.	.132	.743
45	PD-36	USV 55A A violent shearing action parted the left third of panel. Sensing arm was displaced and recorder shut off. Panel pulled from end fastenings.	53	13.5	.453	
46	PD-37	USV 33 Panel pulled from end fastenings. Bladder cell developed severe tear at front of fitting, causing loss of pressure.	54	26.7	.470	.617
47	PD-48	S 2N Panel pulled from end fastenings.	55	27.3	.495	.675

SELF-SEALING CELL - 12 INCH SPAN

48	PD-29	USV 747 5 Delamination; panel pulled from end fastenings.	56	33.76	.247	.525
49	PD-30	USV CR 88 Delamination; panel pulled from end fastenings.	57	32.26	.185	.515
50	PD-31	USV 55A Violent shearing action; pulled from end fastenings.	58	30.46	.363	.808
51	PD-32	USV 33 Severe delamination; pulled from end fastenings.	59	32.76	.400	.451
52	PD-33	S 2N Pulled from end fastenings.	60	30.26	.666	.469

\*Distance from end of initial deflection to end of return trace.

*Contrails*  
TABLE IV (Cont.)

PRESSURE DEFLECTION TRIALS

BLADDER CELL - 8 INCH SPAN

<u>NO.</u>	<u>CODE</u>	<u>PANEL</u>	<u>STRESS STRAIN CURVE (FIGURE)</u>	<u>MAXIMUM TEST PRESSURE (PSI)</u>	<u>INITIAL DEFLECTION (INCHES)</u>	<u>PERMANENT SET*</u>
53	PD-56	USV 747 5 Panel pulled from end fastenings.	61	32.26	.135	.168
54	PD-57	USV 747 5 Panel pulled from end fastenings.	62	33.16	.185	.140
55	PD-58	USV 747 5 Panel pulled from end fastenings.	63	31.96	.127	.172
56	PD-59	USV 747 5 Panel pulled from end fastenings.	64	34.46	.150	.177
57	PD-60	USV 747 5 Panel pulled from end fastenings.	65	33.76	.133	.196
58	PD-61	USV 747 5 Panel pulled from end fastenings.	66	35.96	.152	.228
59	PD-62	USV 747 5 Panel pulled from end fastenings.	67	37.76	.156	.218
60	PD- <del>62</del> <sup>63</sup>	USV 747 5 Panel pulled from end fastenings.	68	37.46	.153	.202

\* Distance from end of initial deflection to end of return trace.

*Centrails*

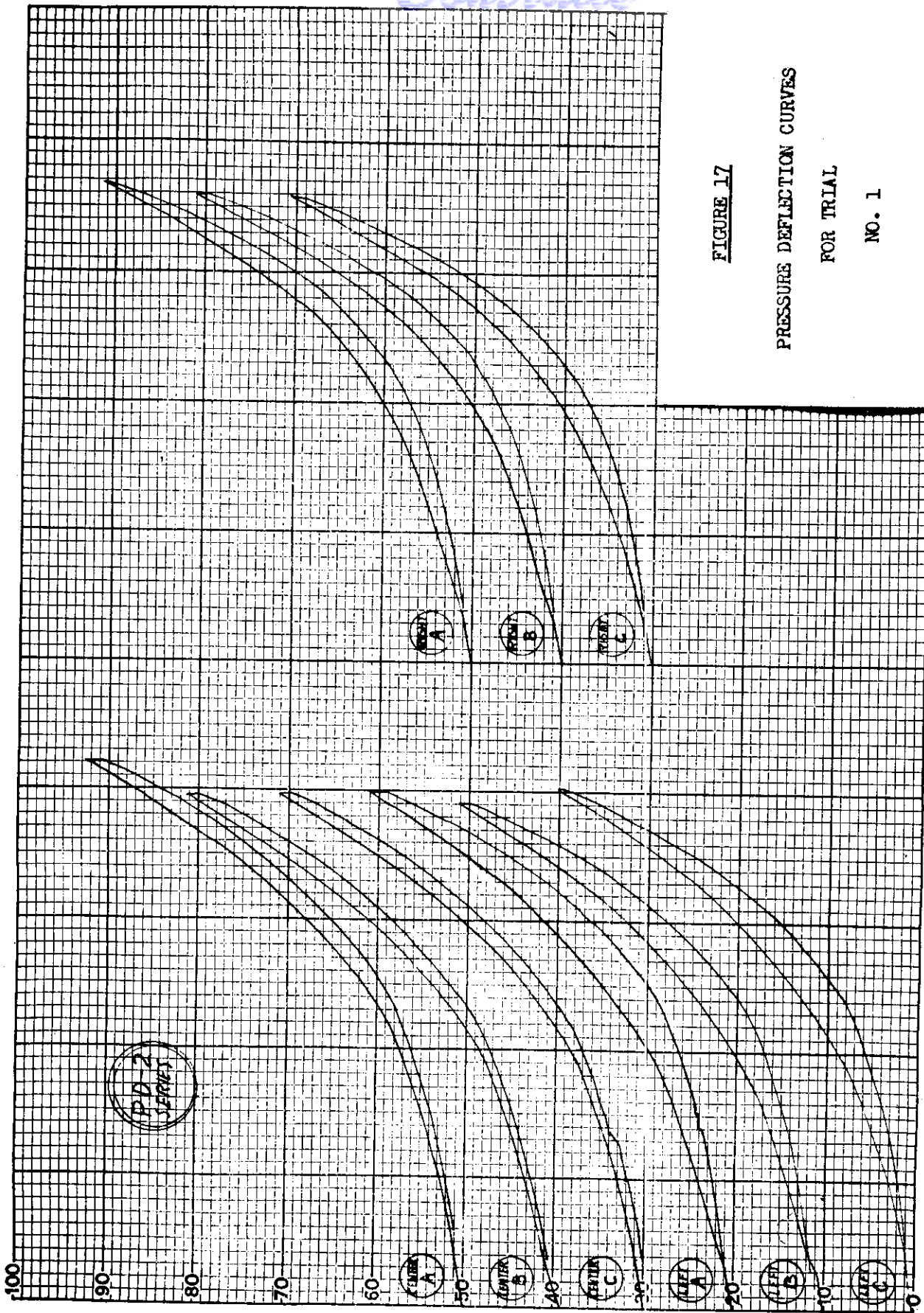


FIGURE 17

PRESSURE DEFLECTION CURVES

FOR TRIAL

NO. 1

DEFLECTION

*Centrair*

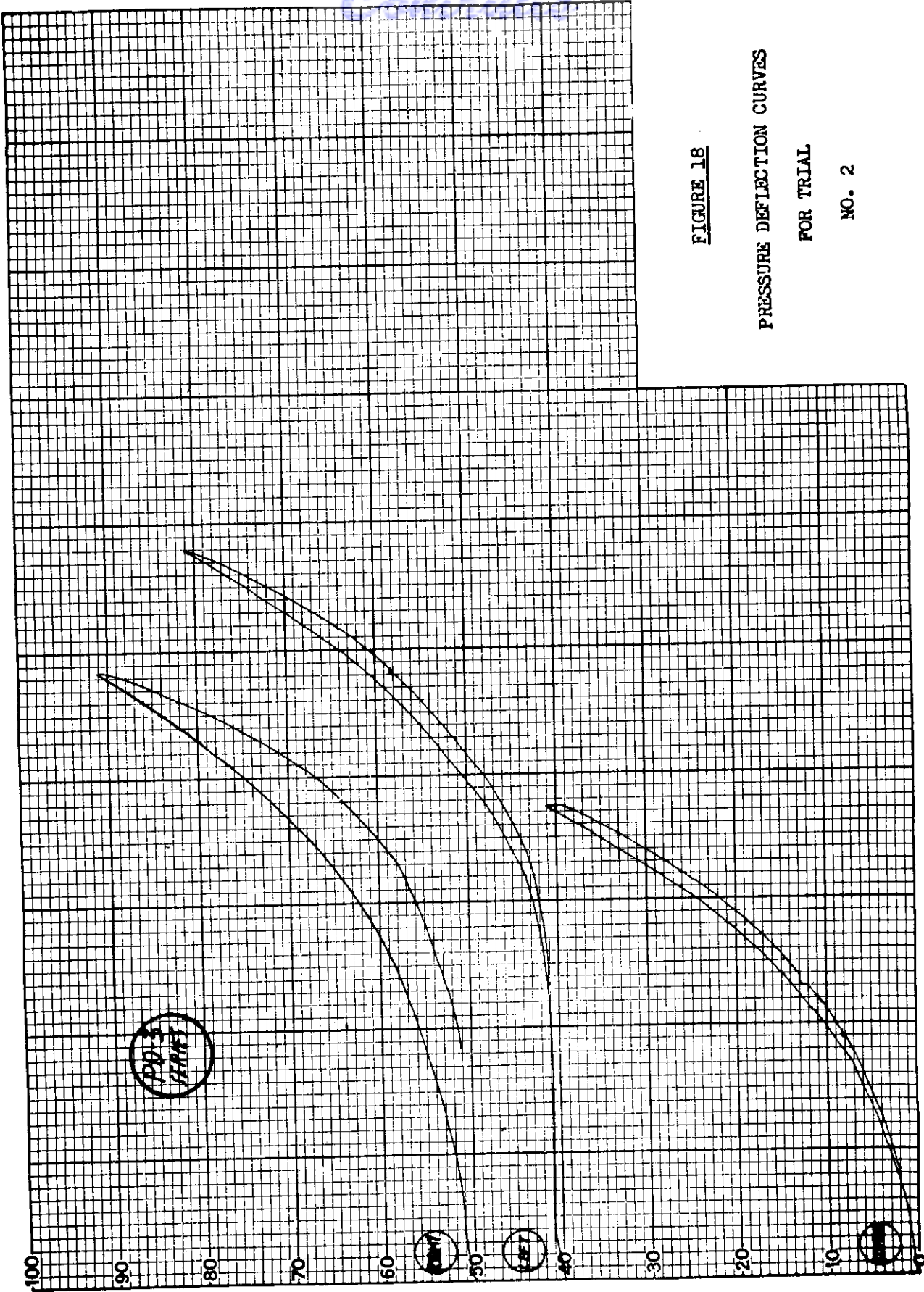


FIGURE 18

PRESSURE DEFLECTION CURVES

FOR TRIAL

NO. 2

DEFLECTION

*Centrair*

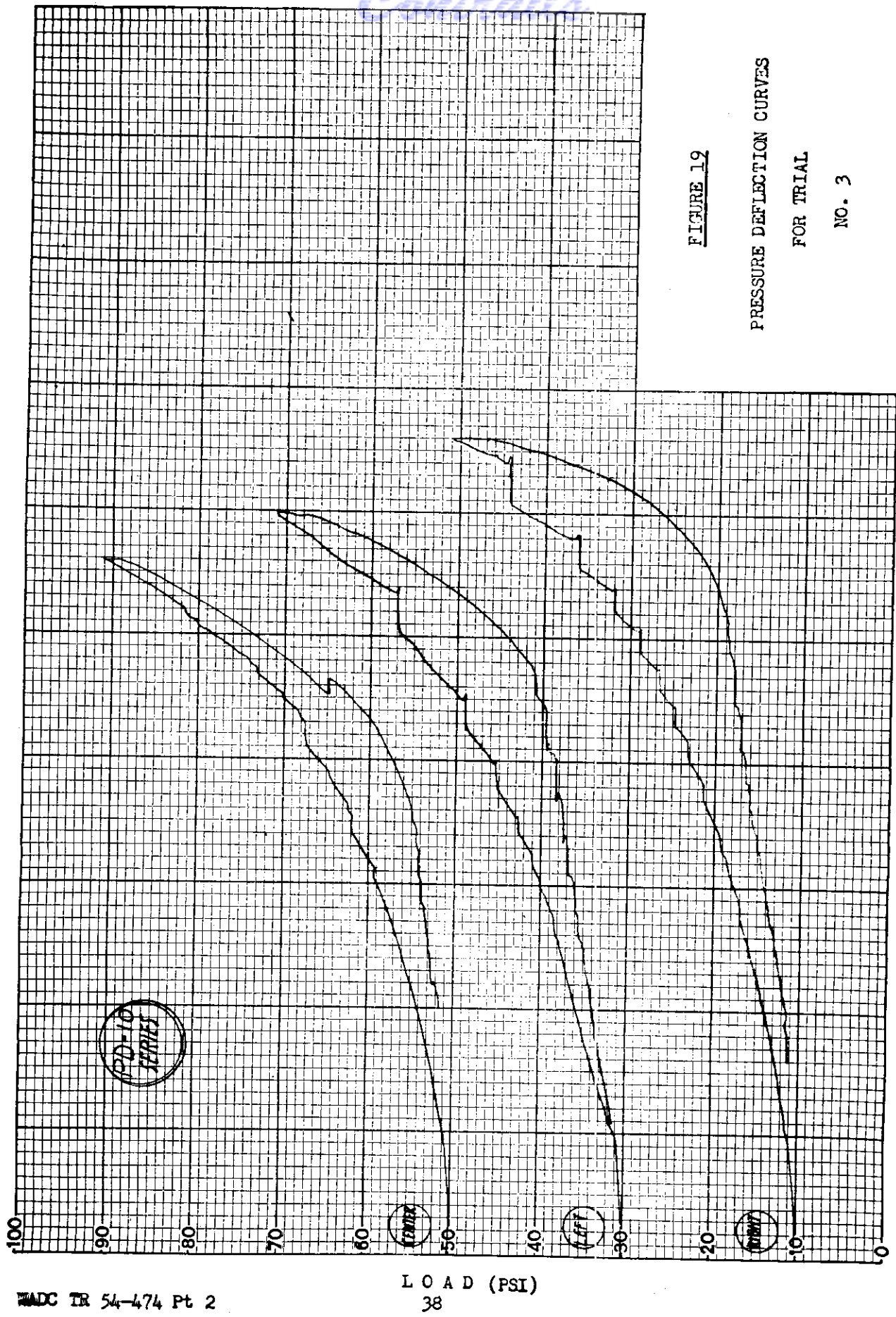


FIGURE 19

PRESSURE DEFLECTION CURVES

FOR TRIAL

NO. 3

DEFLECTION

Centraile

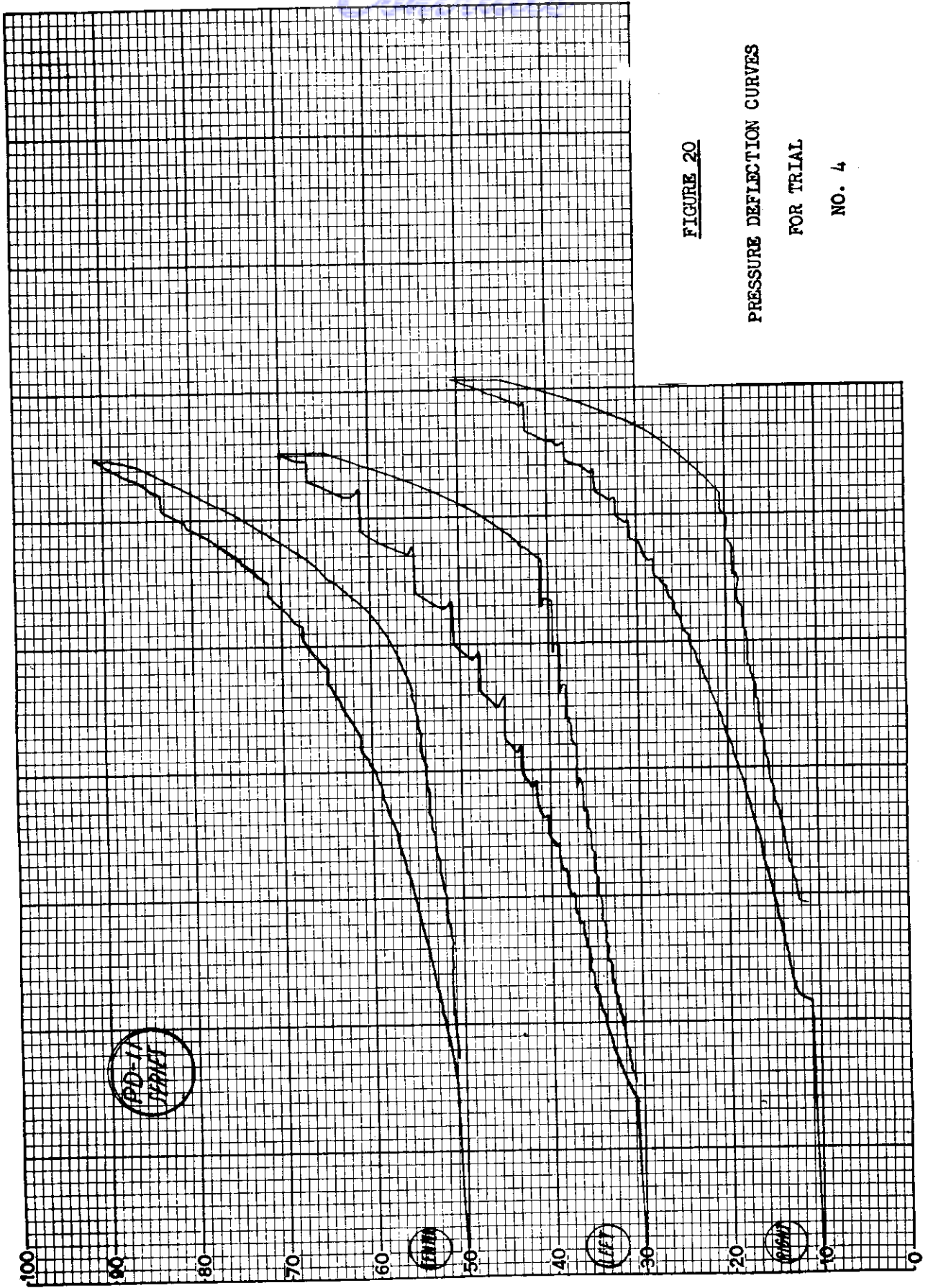


FIGURE 20

PRESSURE DEFLECTION CURVES

FOR TRIAL

NO. 4

DEFLECTION

WADC TR 54-474 Pt 2

LOAD (PSI)  
39

*Centrair*

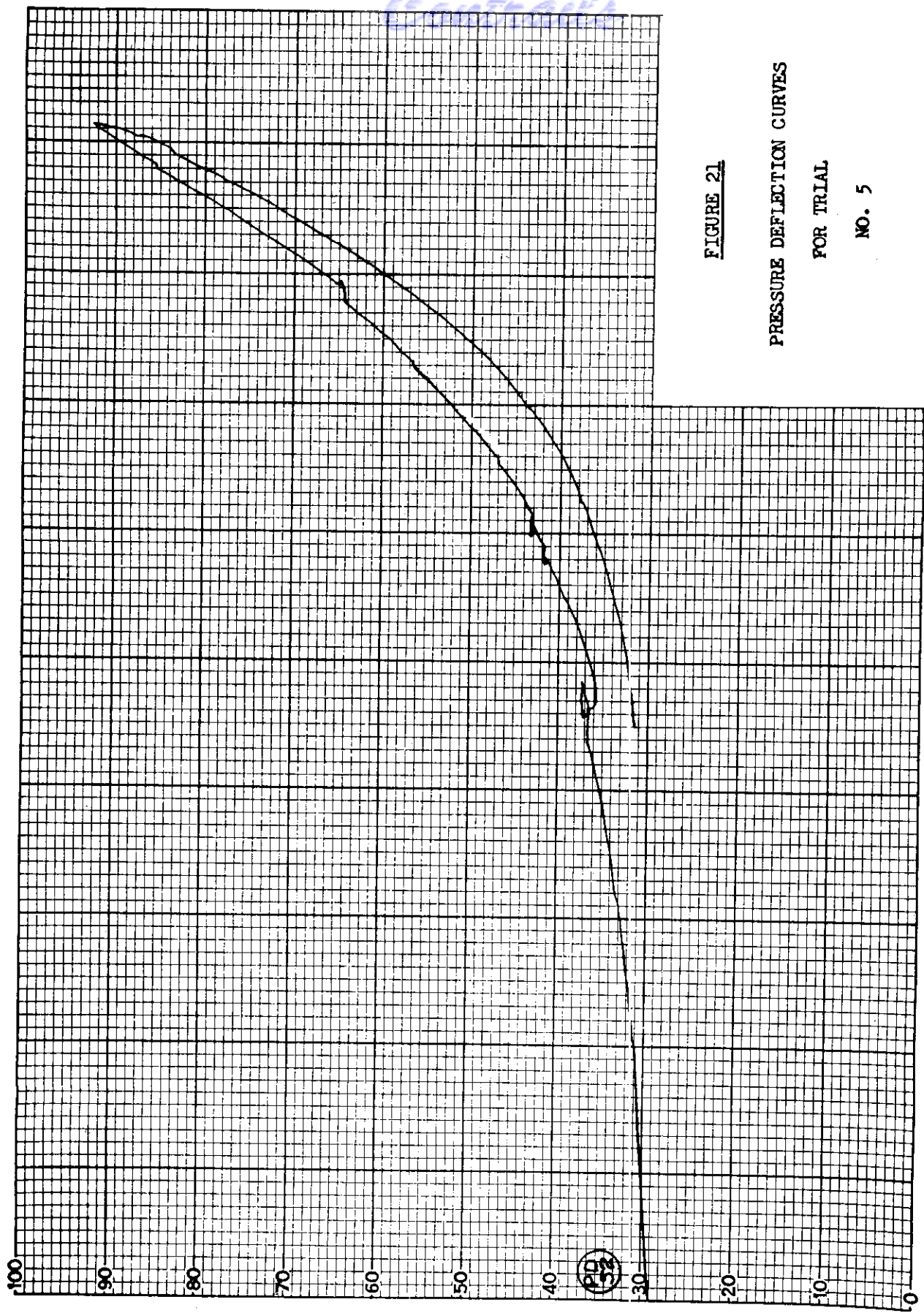


FIGURE 21  
PRESSURE DEFLECTION CURVES  
FOR TRIAL  
NO. 5

DEFLECTION

WADC TR 54-474 Pt 2

LOAD (PSI)  
40



*Control*

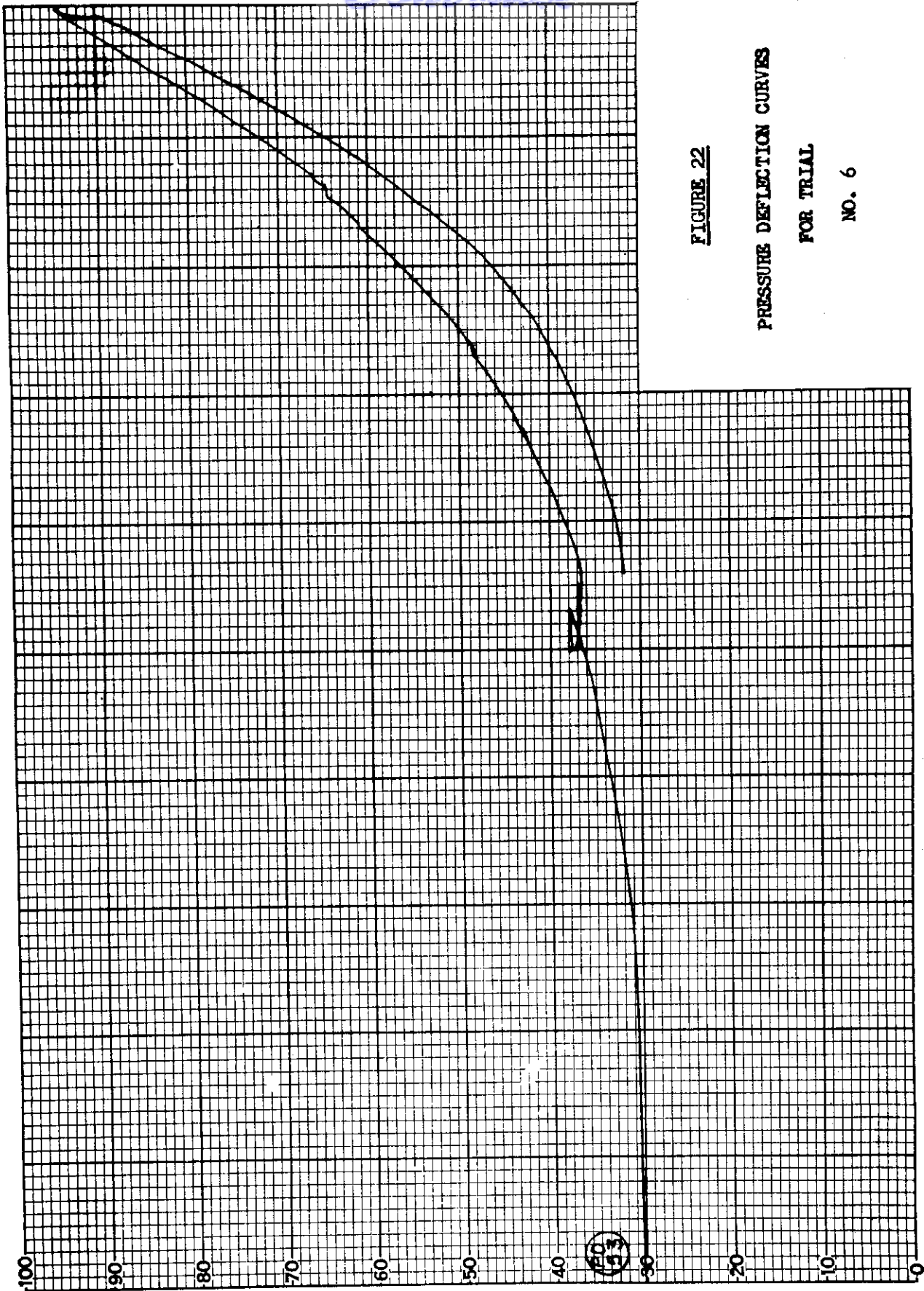


FIGURE 22

PRESSURE DEFLECTION CURVES

FOR TRIAL

NO. 6

DEFLECTION

LOAD (PSI)

41

WADC TR 54-474 Pt 2

*Centrals*

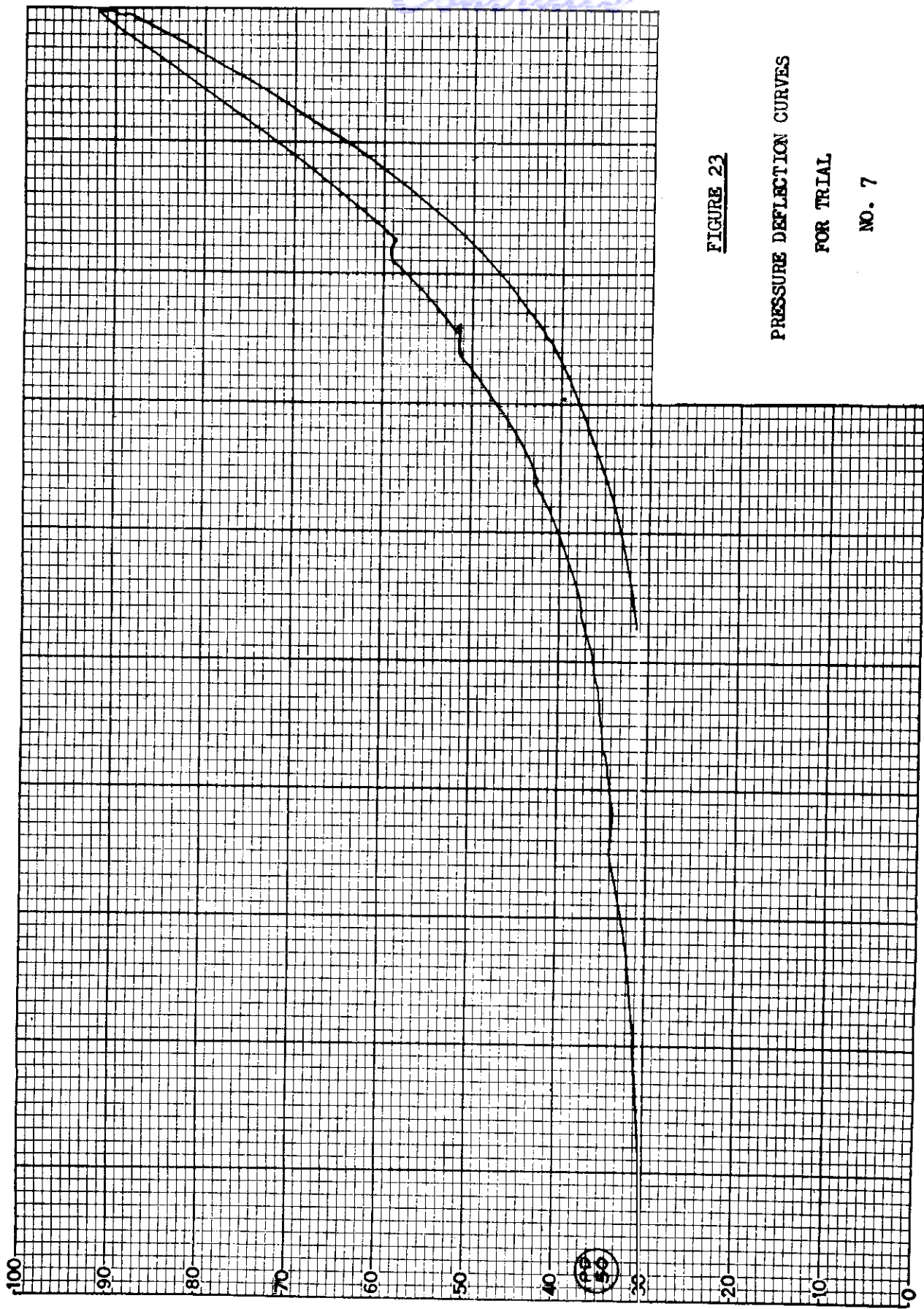


FIGURE 23

PRESSURE DEFLECTION CURVES

FOR TRIAL

NO. 7

DEFLECTION

WADC TR 54-474

LOAD (PSI)  
42

*Conrails*

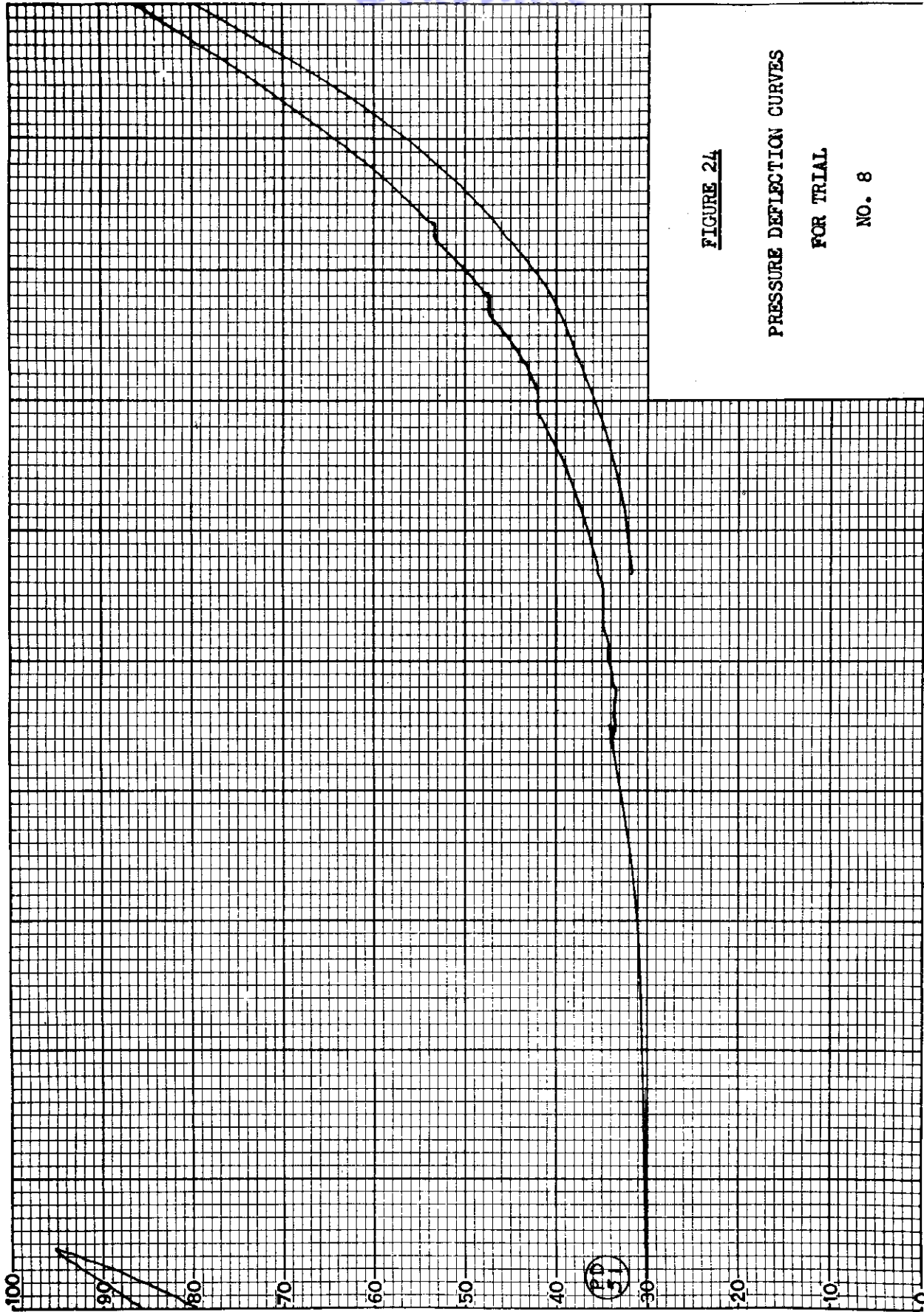


FIGURE 24

PRESSURE DEFLECTION CURVES

FOR TRIAL

NO. 8

DEFLECTION

*Contours*

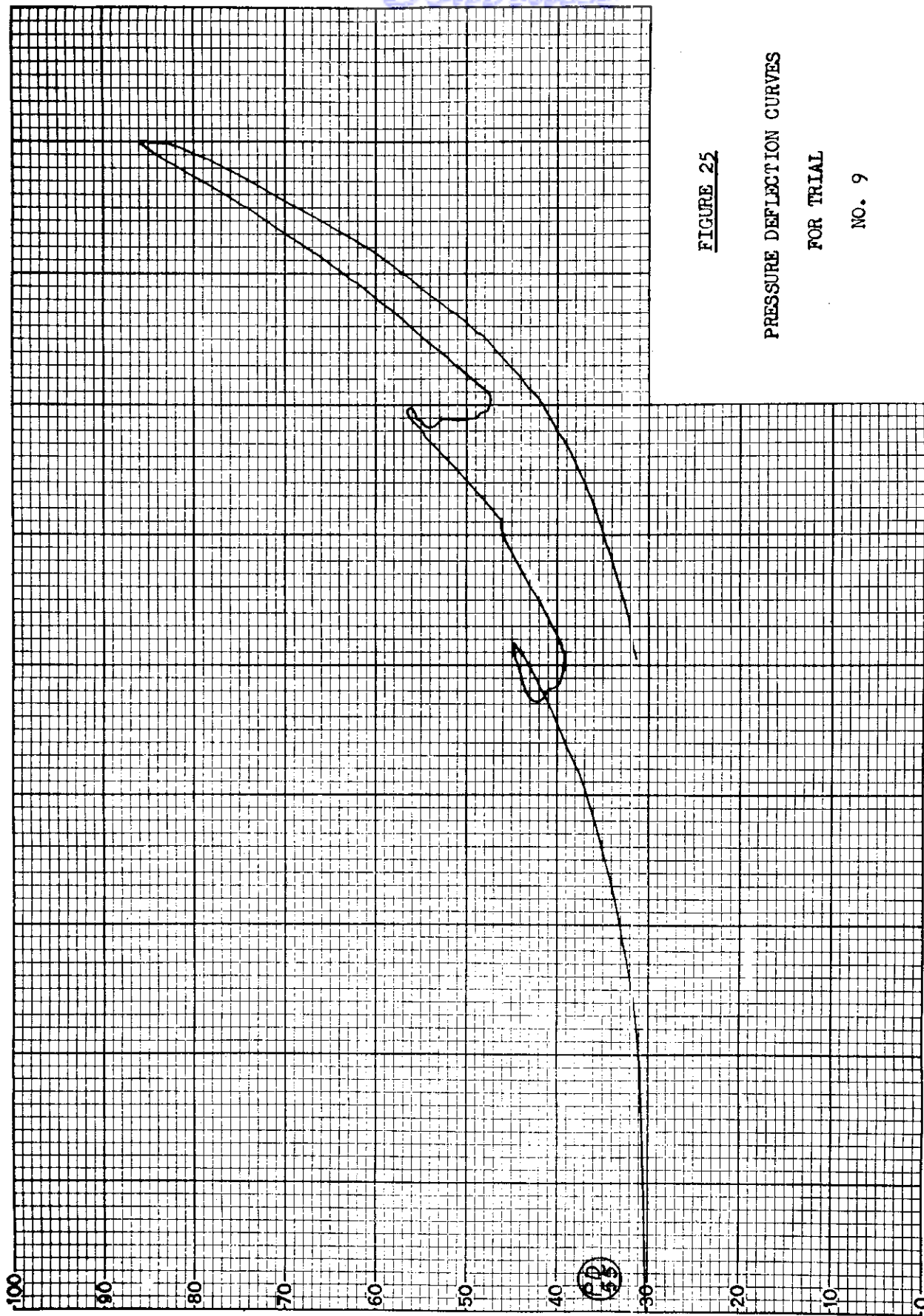


FIGURE 25

PRESSURE DEFLECTION CURVES

FOR TRIAL

NO. 9

DEFLECTION

WADC TR 54-474 Pt 2

LOAD (PSI)  
44

*Control*

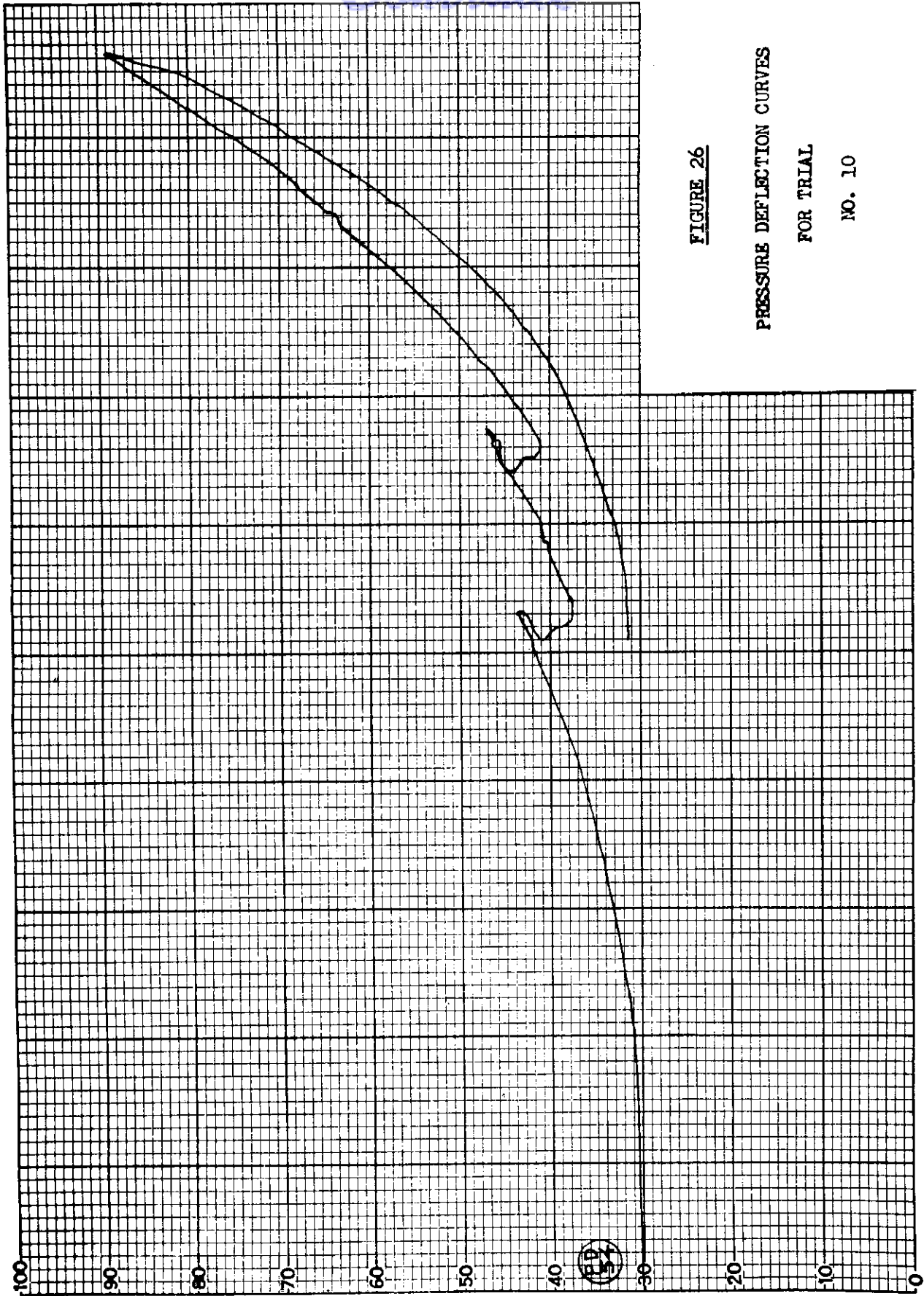


FIGURE 26

PRESSURE DEFLECTION CURVES

FOR TRIAL

NO. 10

DEFLECTION

*Control*

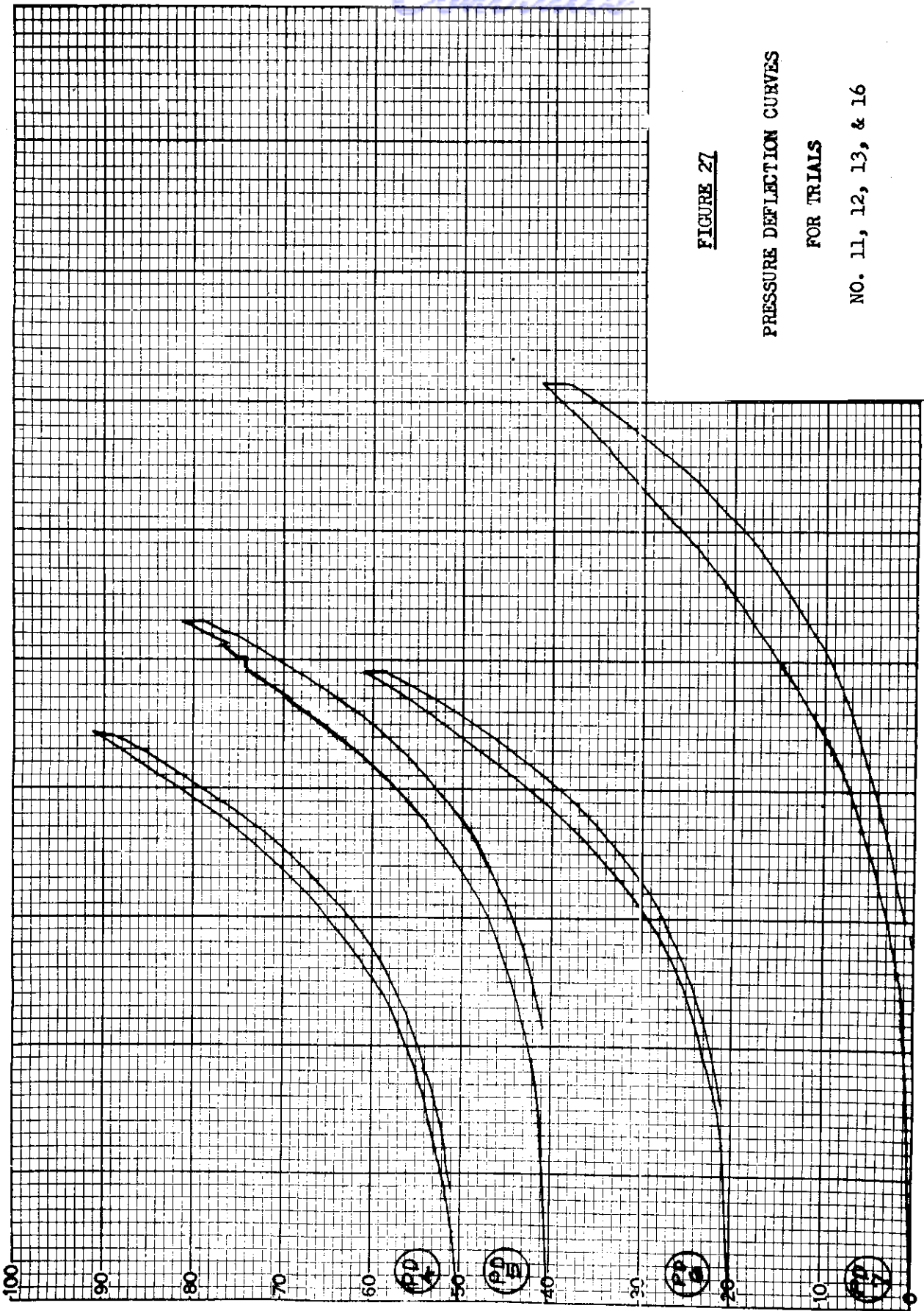


FIGURE 27

PRESSURE DEFLECTION CURVES

FOR TRIALS

NO. 11, 12, 13, & 16

DEFLECTION

*Controls*

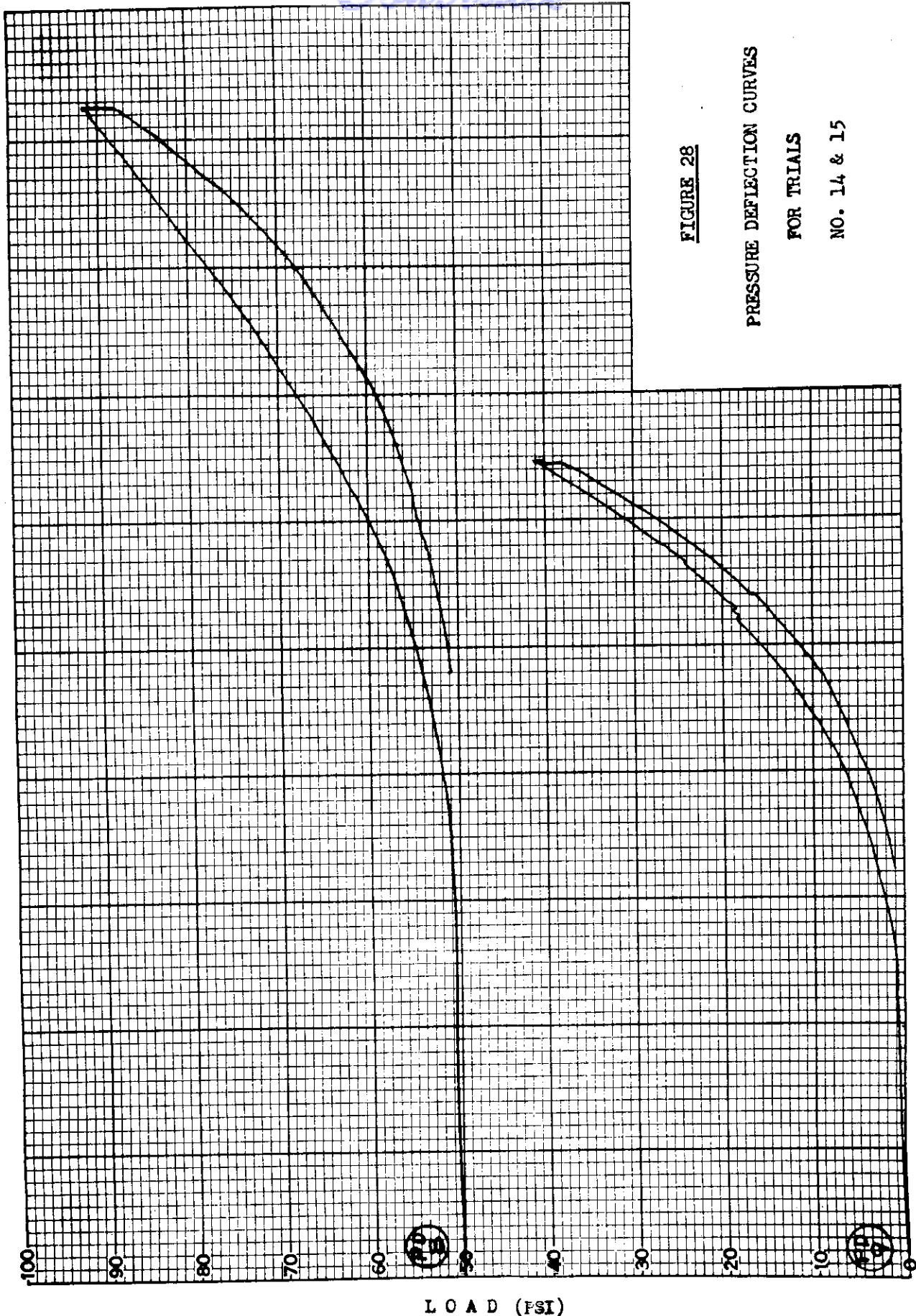


FIGURE 28

PRESSURE DEFLECTION CURVES

FOR TRIALS

NO. 14 & 15

DEFLECTION

*Contours*

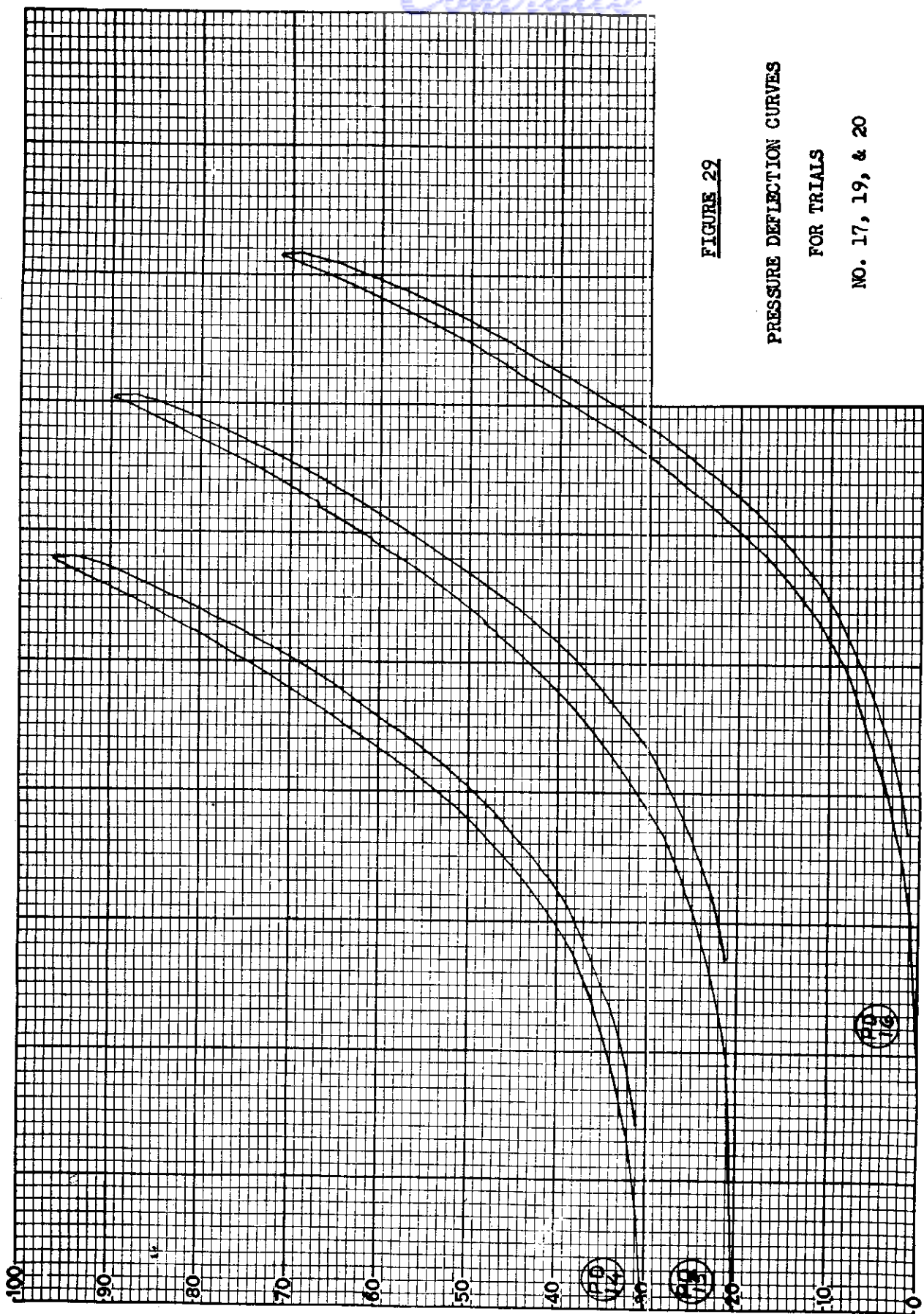


FIGURE 29

PRESSURE DEFLECTION CURVES

FOR TRIALS

NO. 17, 19, & 20

DEFLECTION



*Controls*

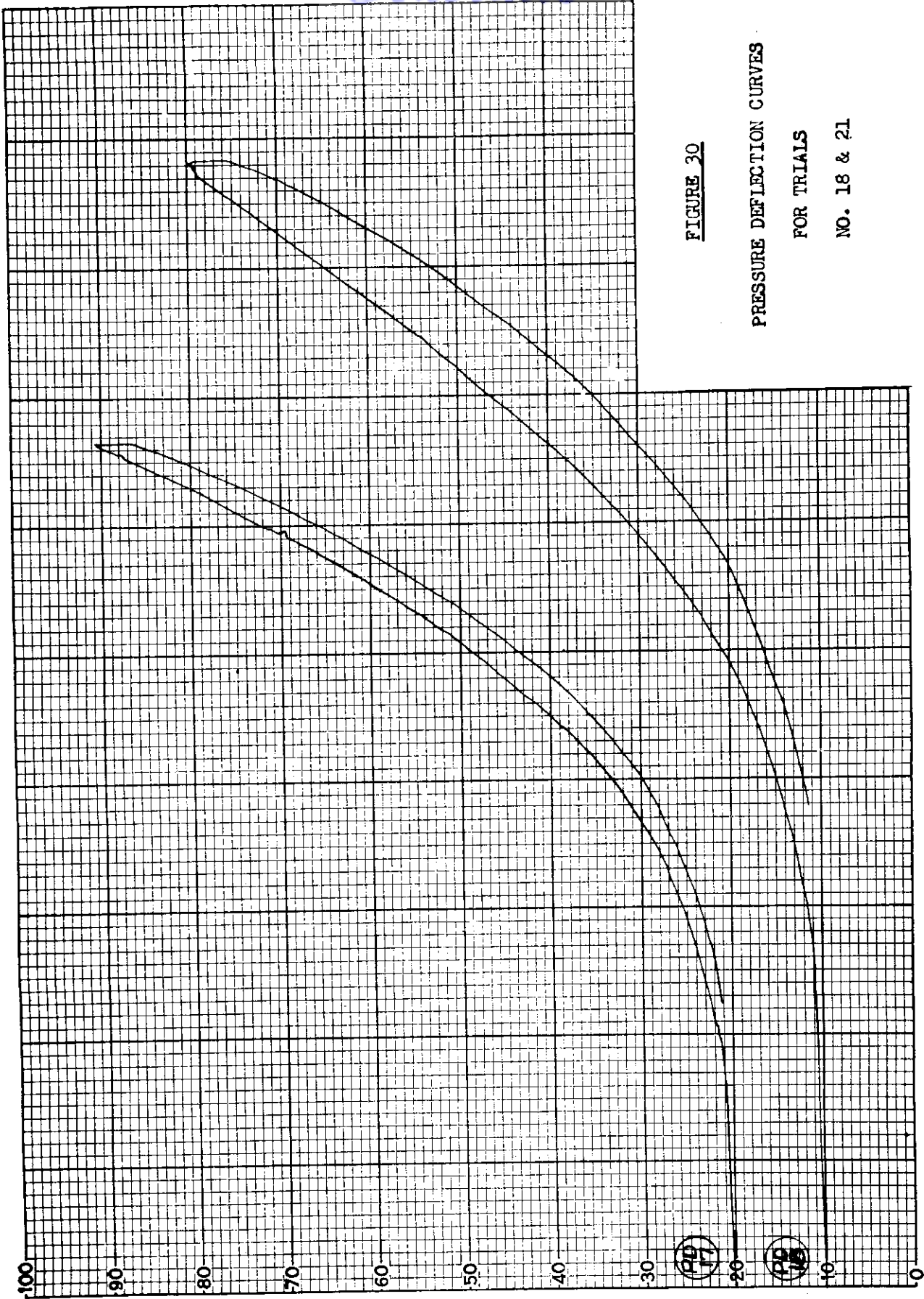


FIGURE 30

PRESSURE DEFLECTION CURVES

FOR TRIALS

NO. 18 & 21

DEFLECTION

MADC TR 24-474 Pt 2

LOAD (PSI)  
49

*Contrails*

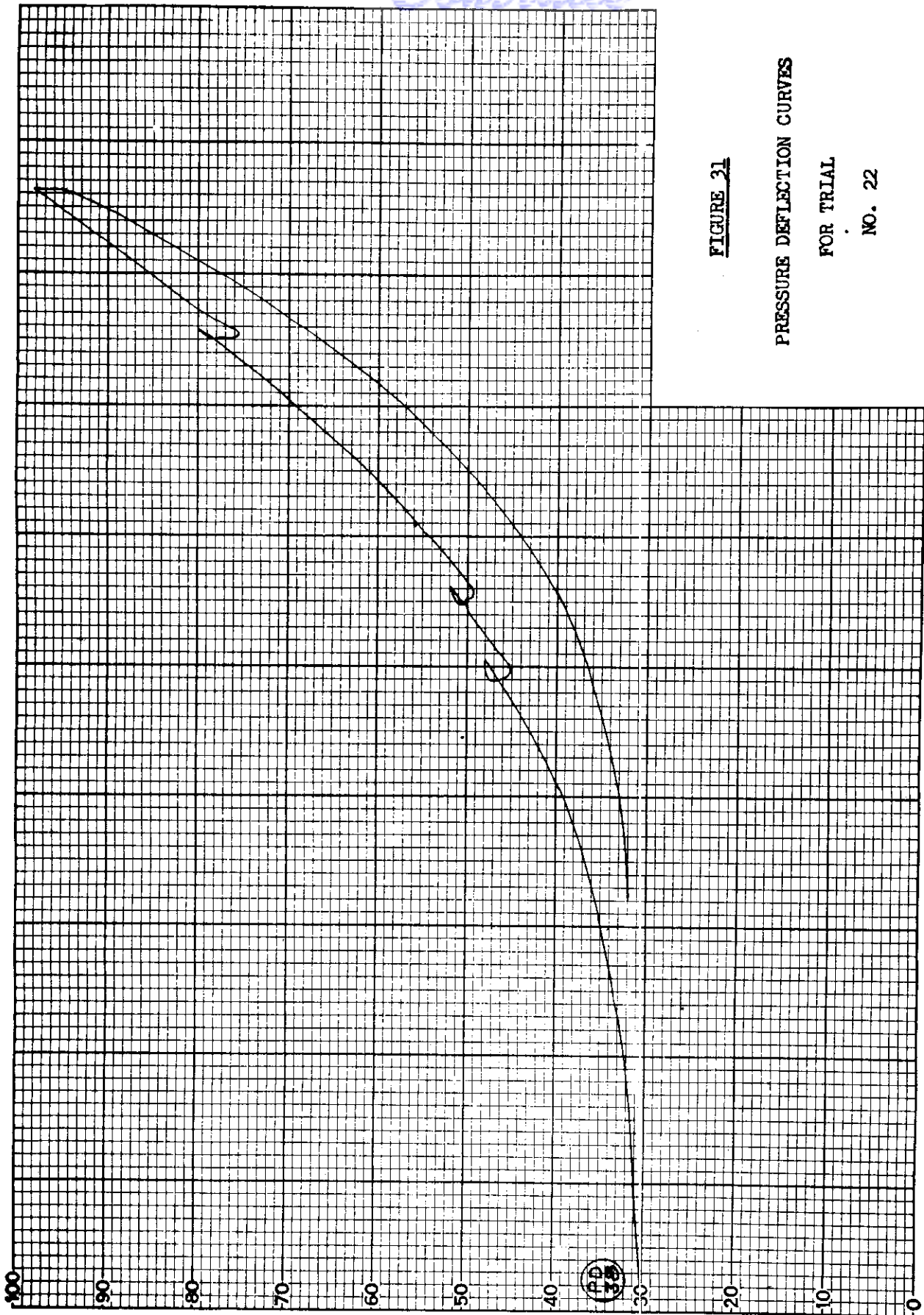


FIGURE 31

PRESSURE DEFLECTION CURVES

FOR TRIAL

NO. 22

DEFLECTION

*Controls*

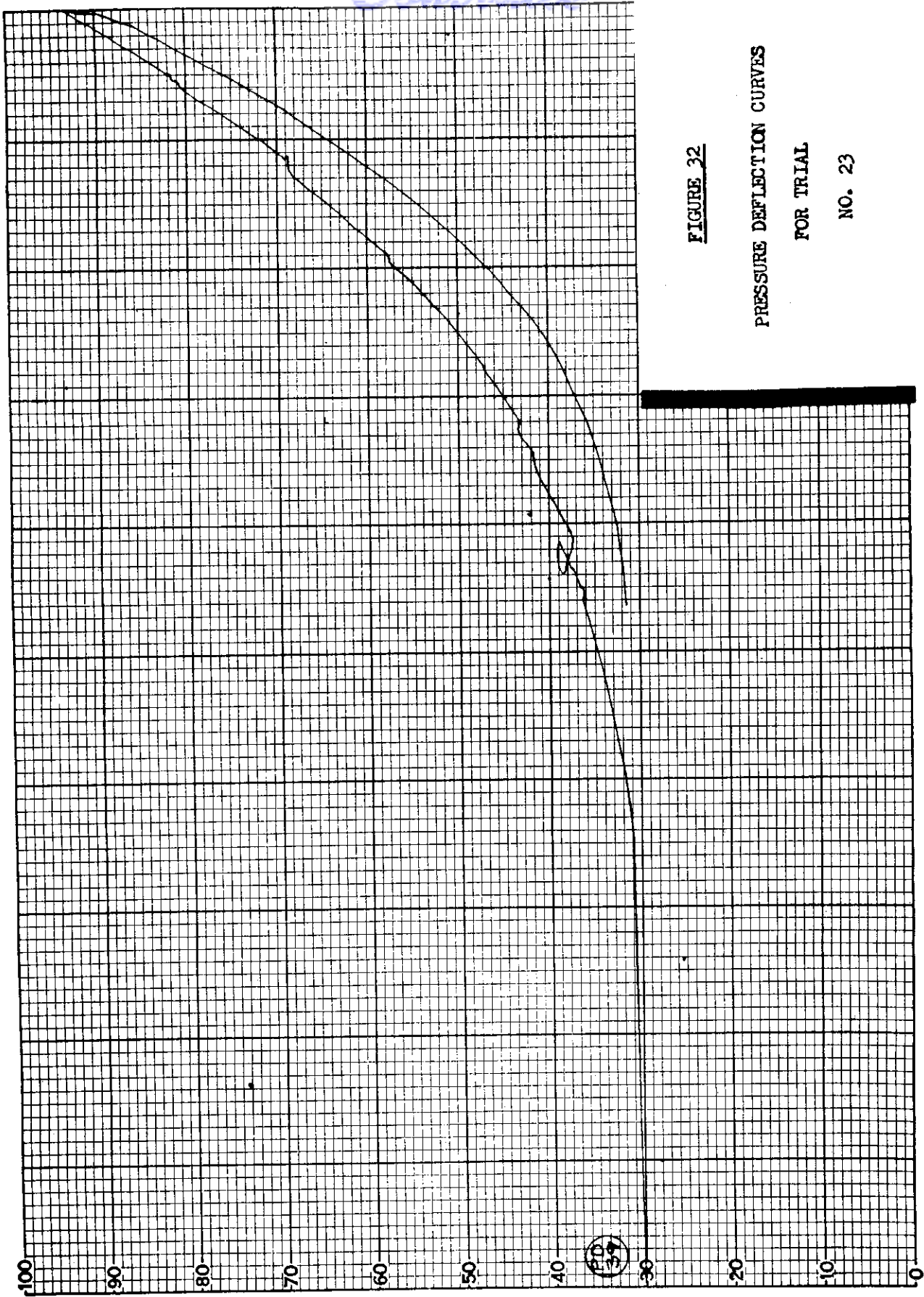


FIGURE 22

PRESSURE DEFLECTION CURVES

FOR TRIAL

NO. 23

DEFLECTION

*Control*

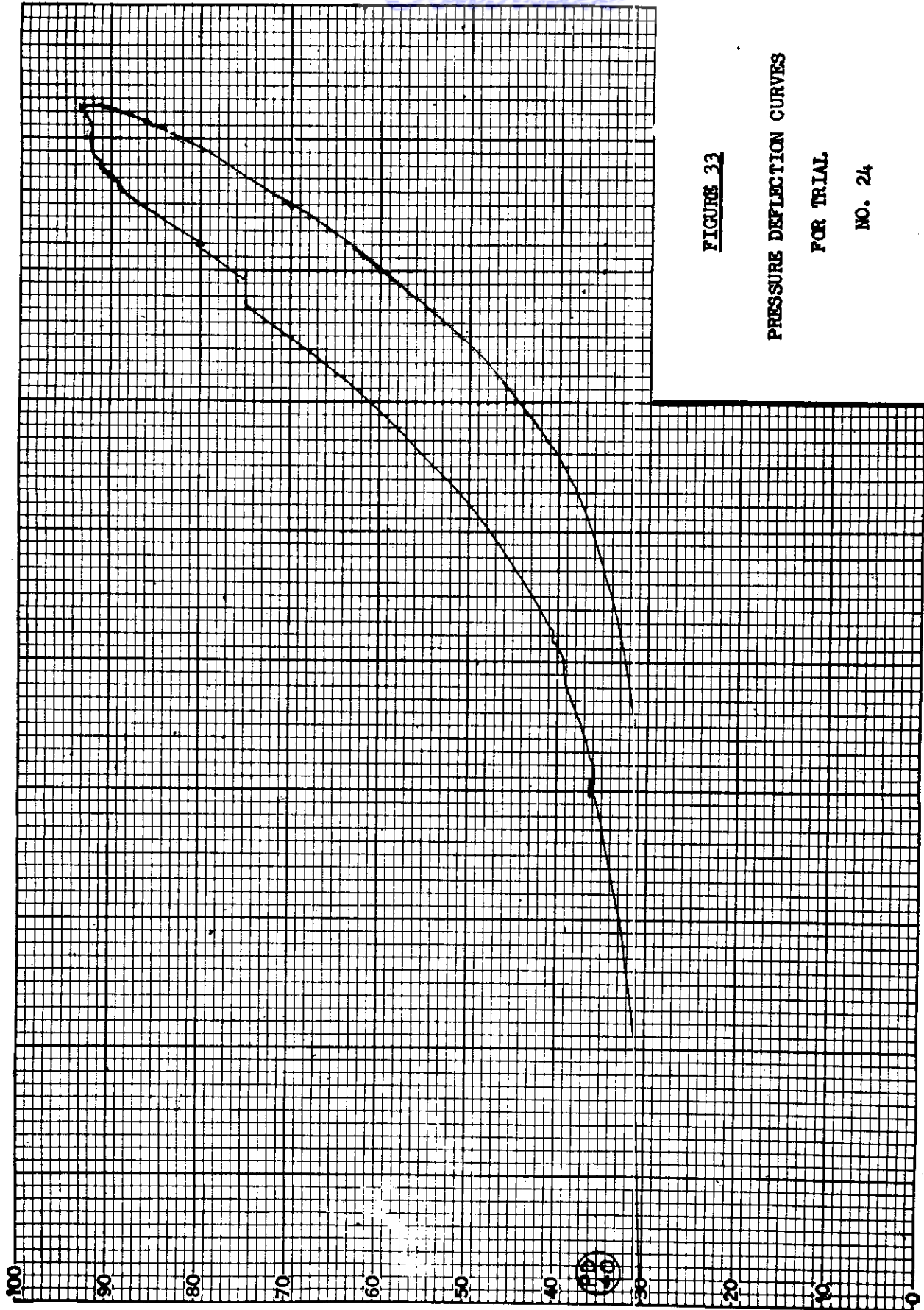


FIGURE 33

PRESSURE DEFLECTION CURVES

FOR TRIAL

NO. 24

DEFLECTION

*Control*

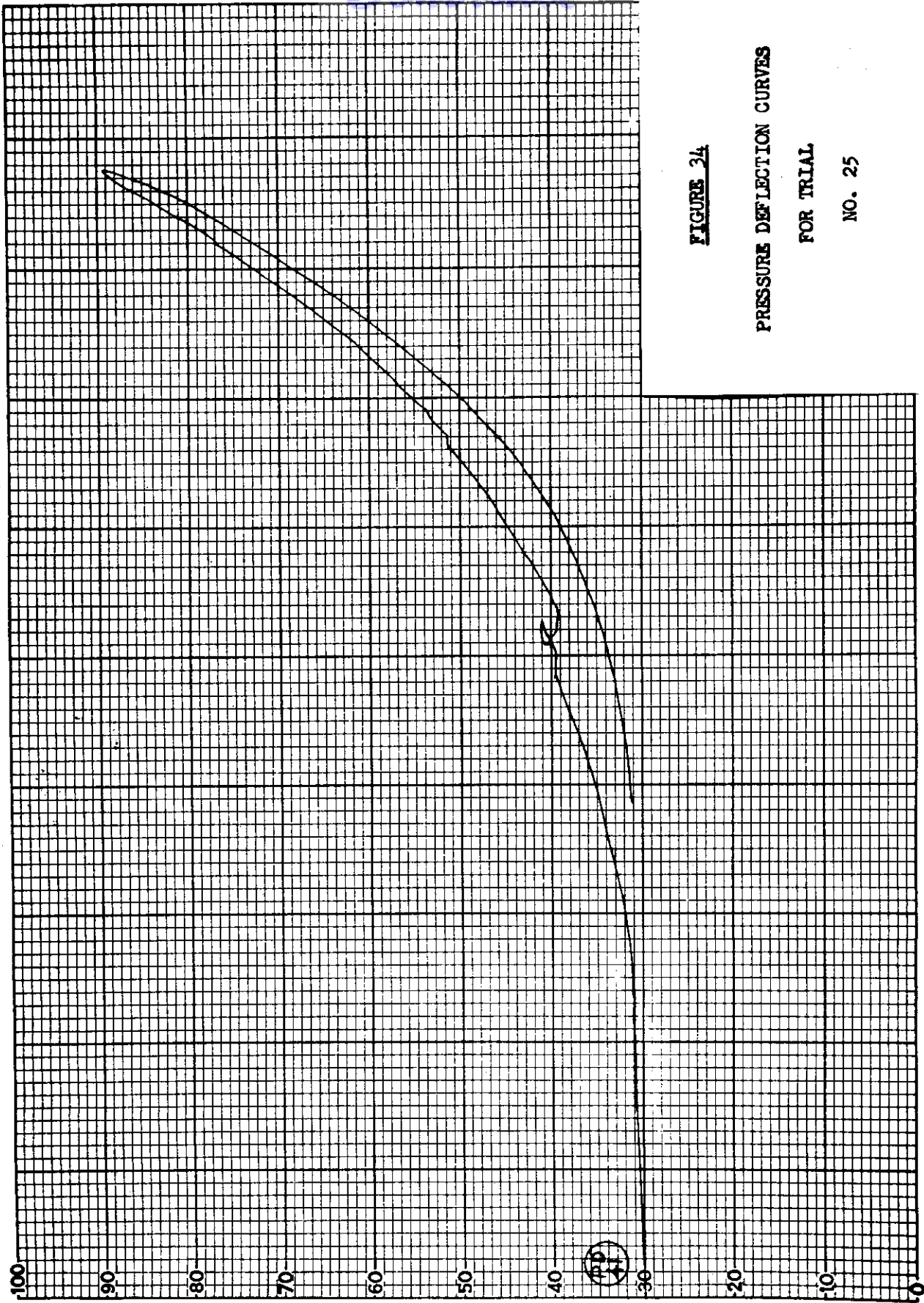


**FIGURE 34**

**PRESSURE DEFLECTION CURVES**

**FOR TRIAL**

**NO. 25**

**DEFLECTION**

*Contours*

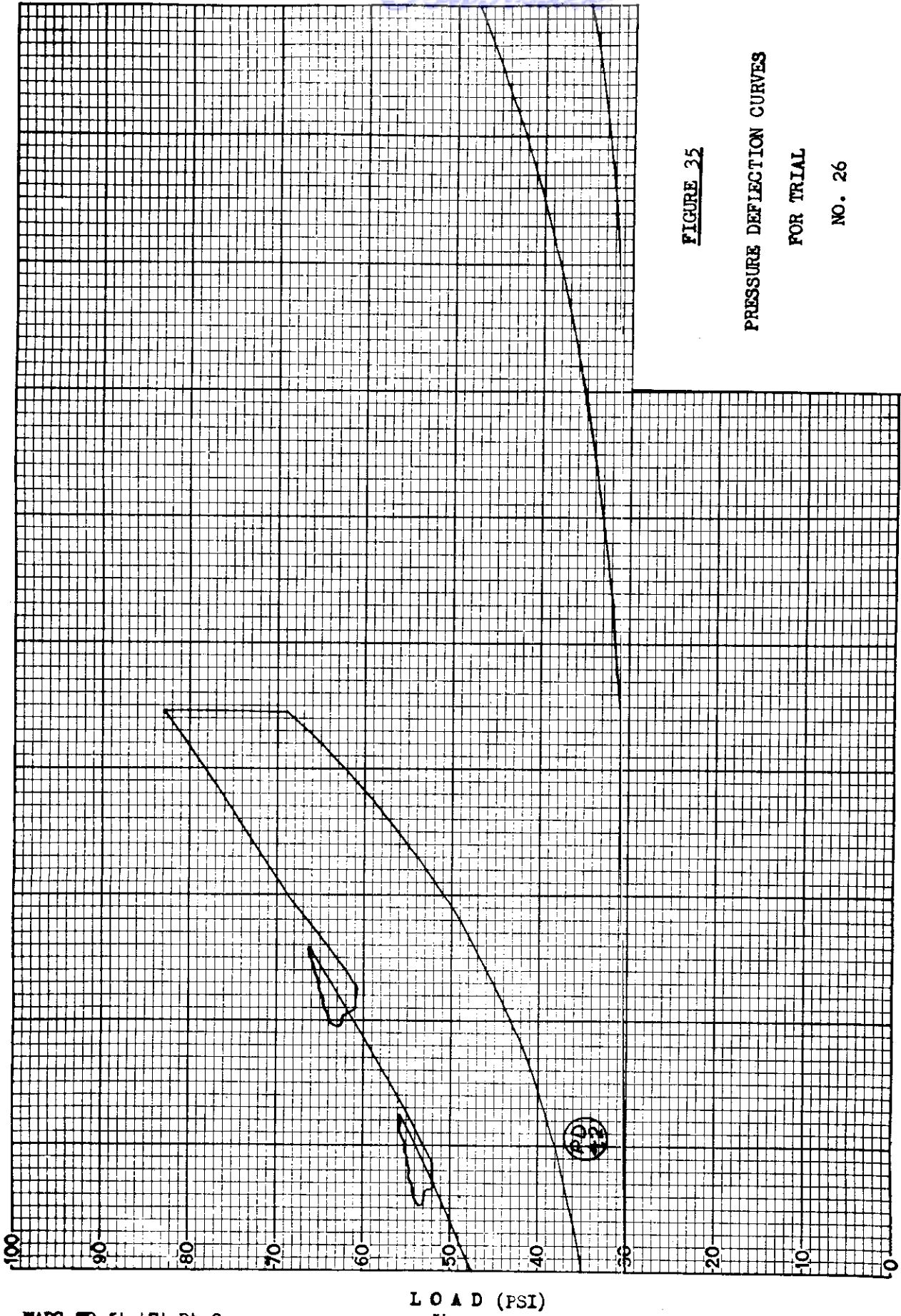


FIGURE 35

PRESSURE DEFLECTION CURVES

FOR TRIAL

NO. 26

DEFLECTION

*Continued*

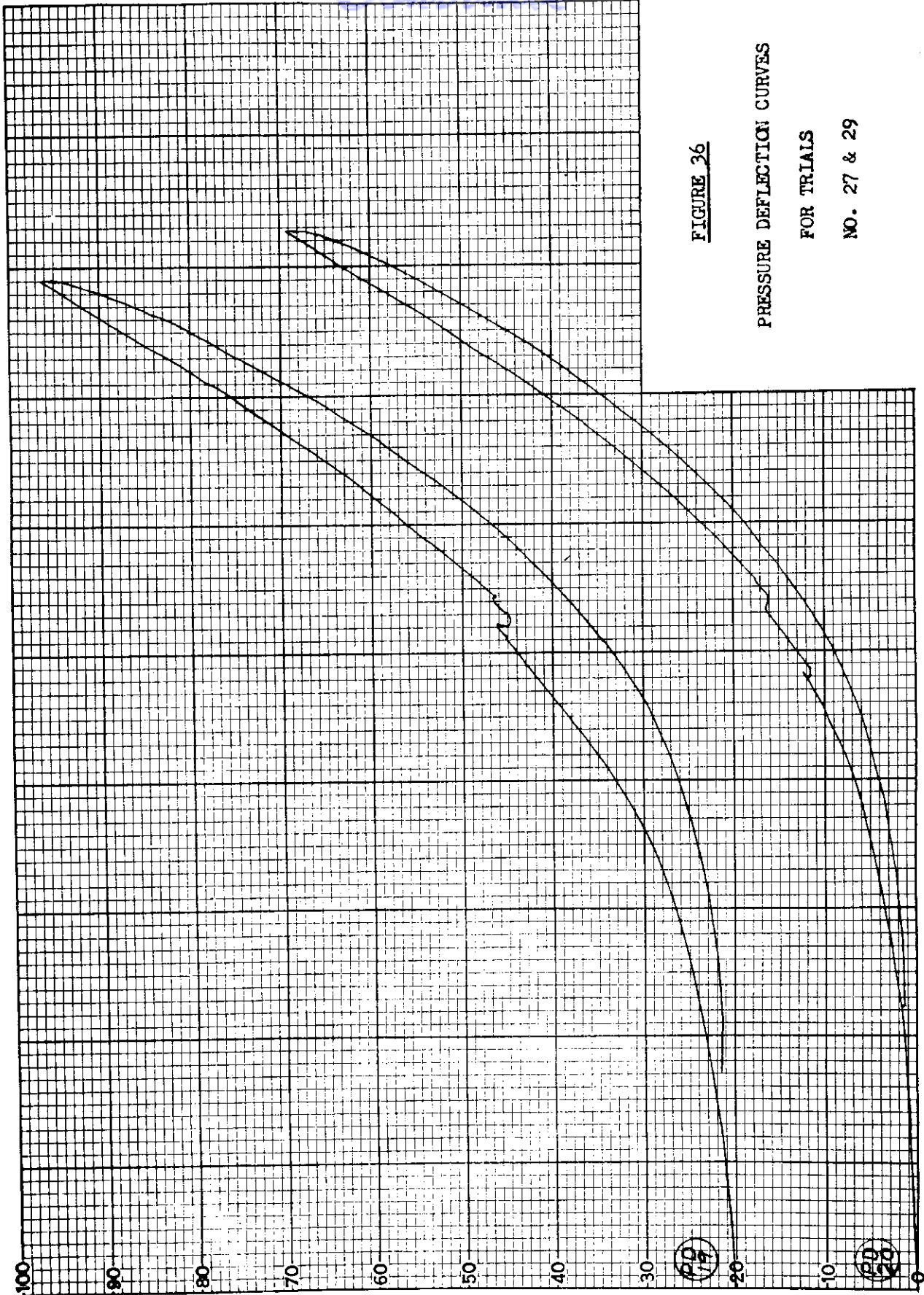


FIGURE 36

PRESSURE DEFLECTION CURVES

FOR TRIALS

NO. 27 & 29

DEFLECTION

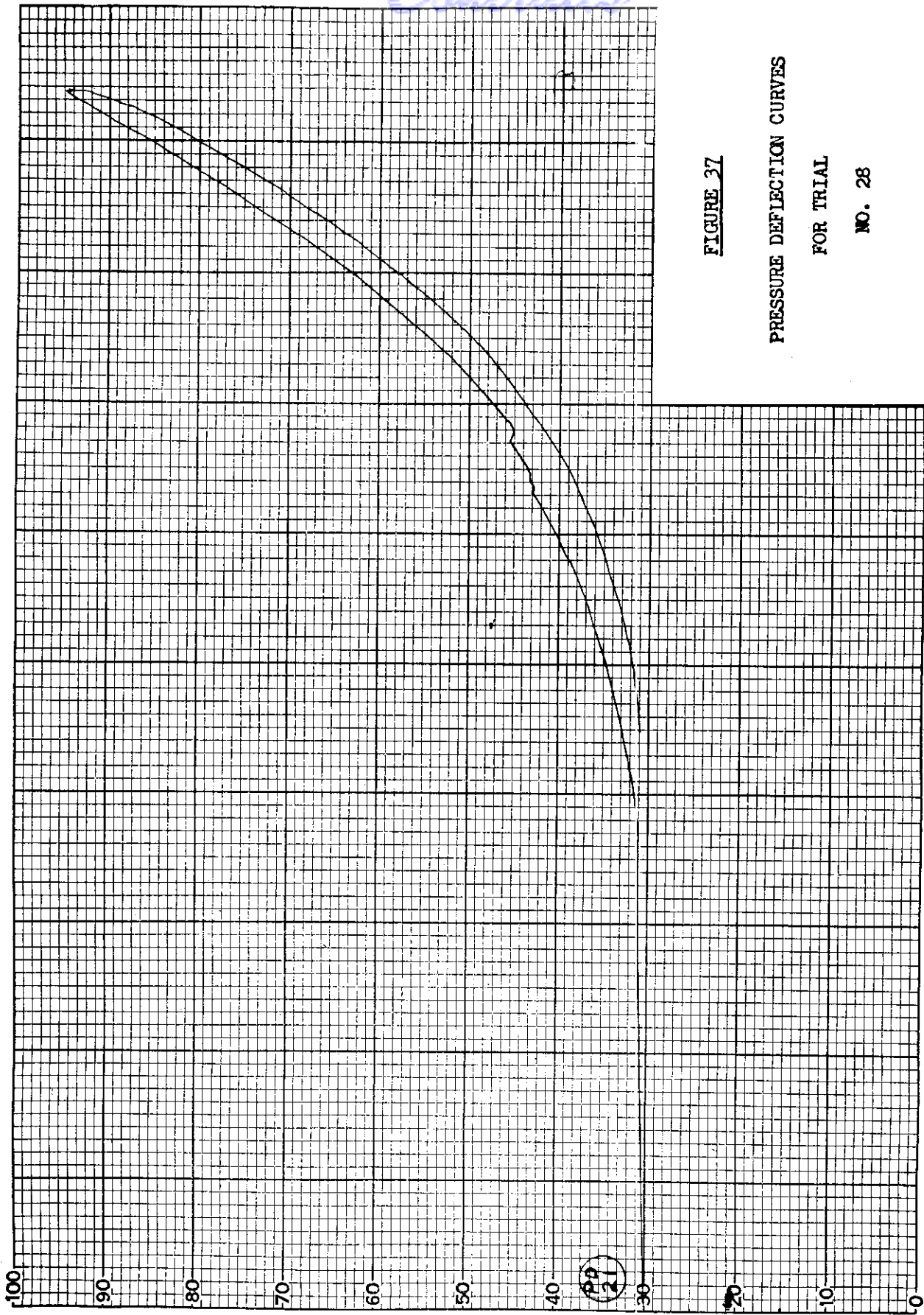
*Controls*

FIGURE 37

PRESSURE DEFLECTION CURVES

FOR TRIAL

NO. 28



DEFLECTION



*Controls*

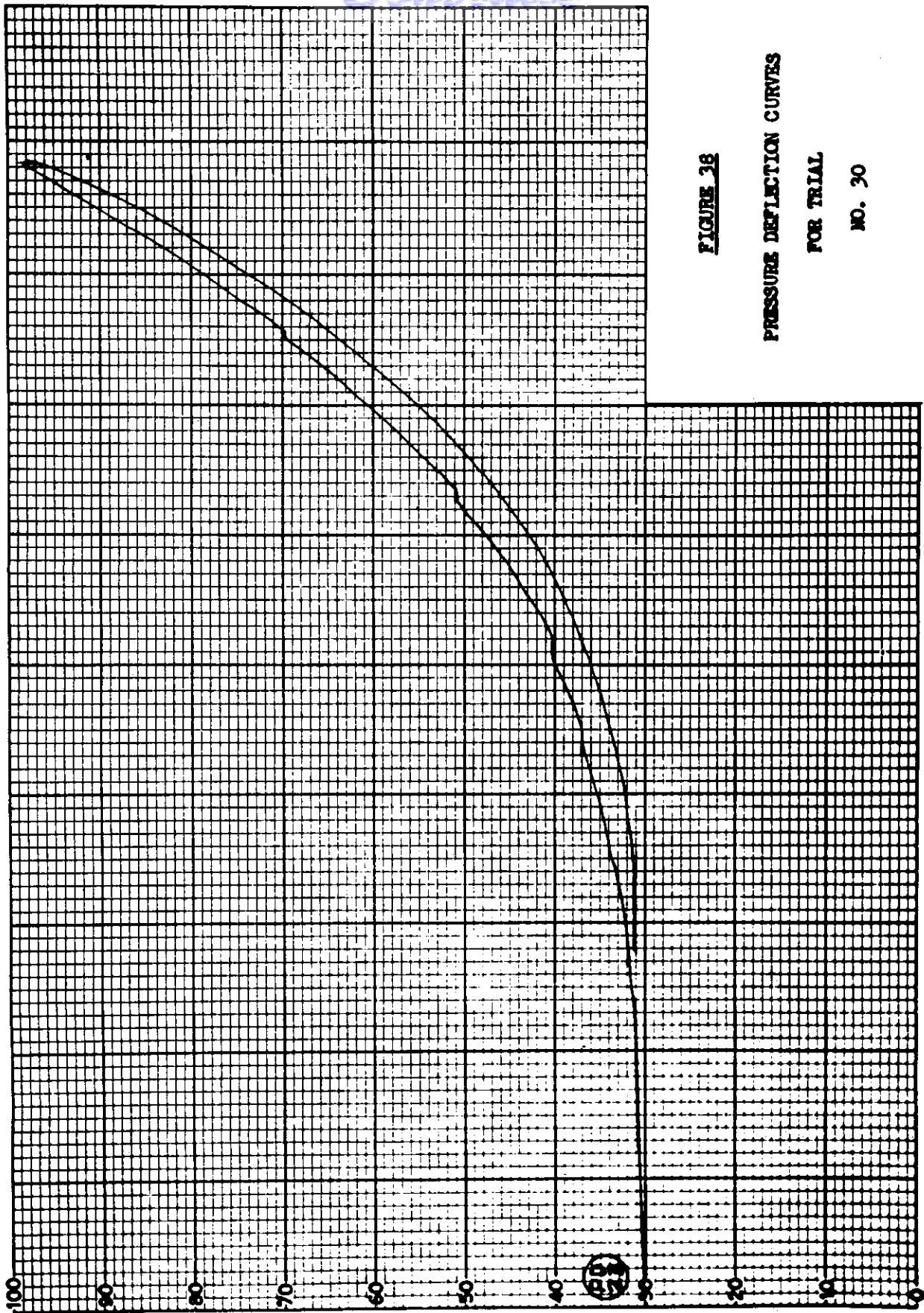


FIGURE 38

PRESSURE DEFLECTION CURVES

FOR TRIAL

NO. 30

DEFLECTION

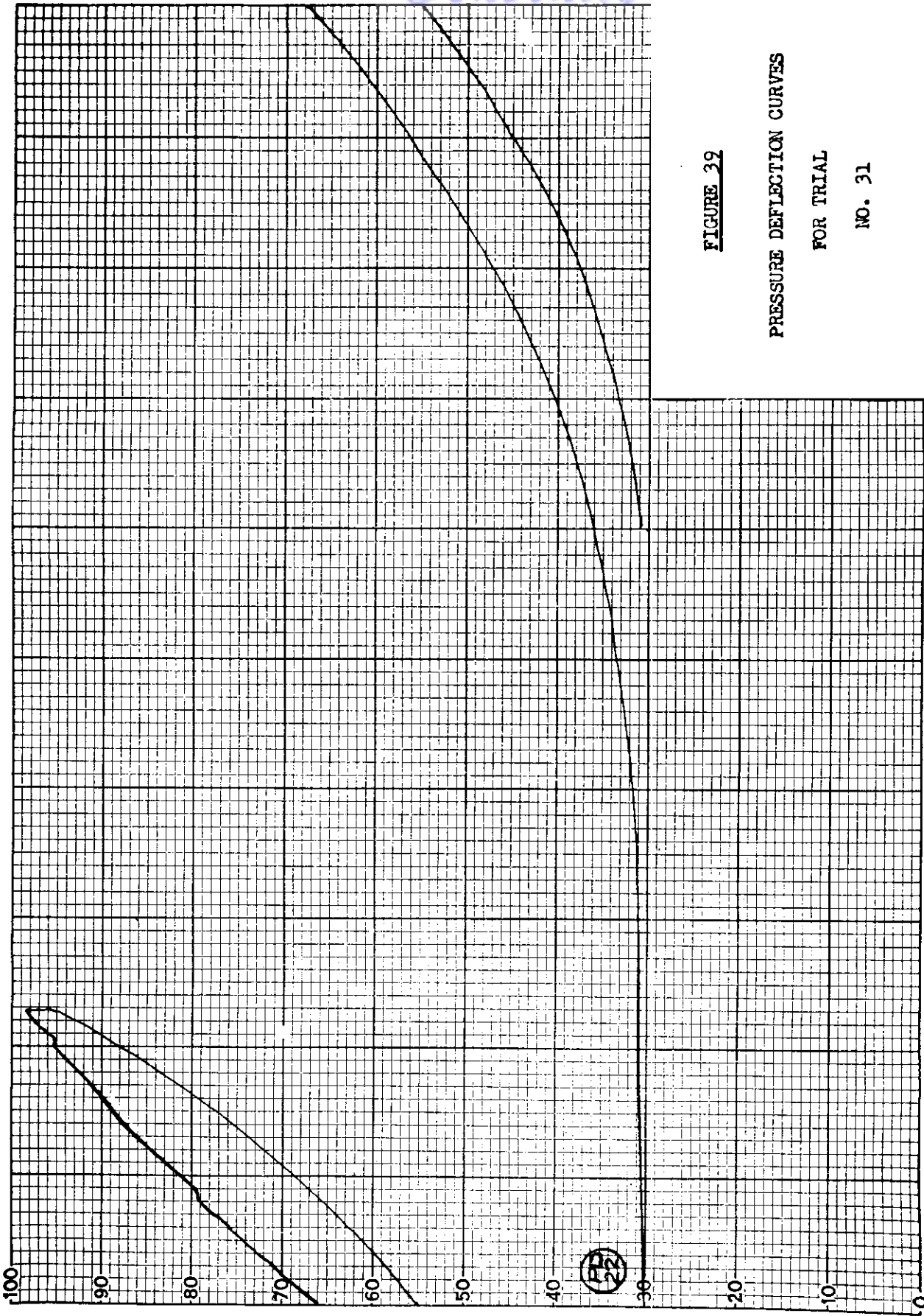


FIGURE 39

PRESSURE DEFLECTION CURVES

FOR TRIAL

NO. 31

DEFLECTION

*Contrails*

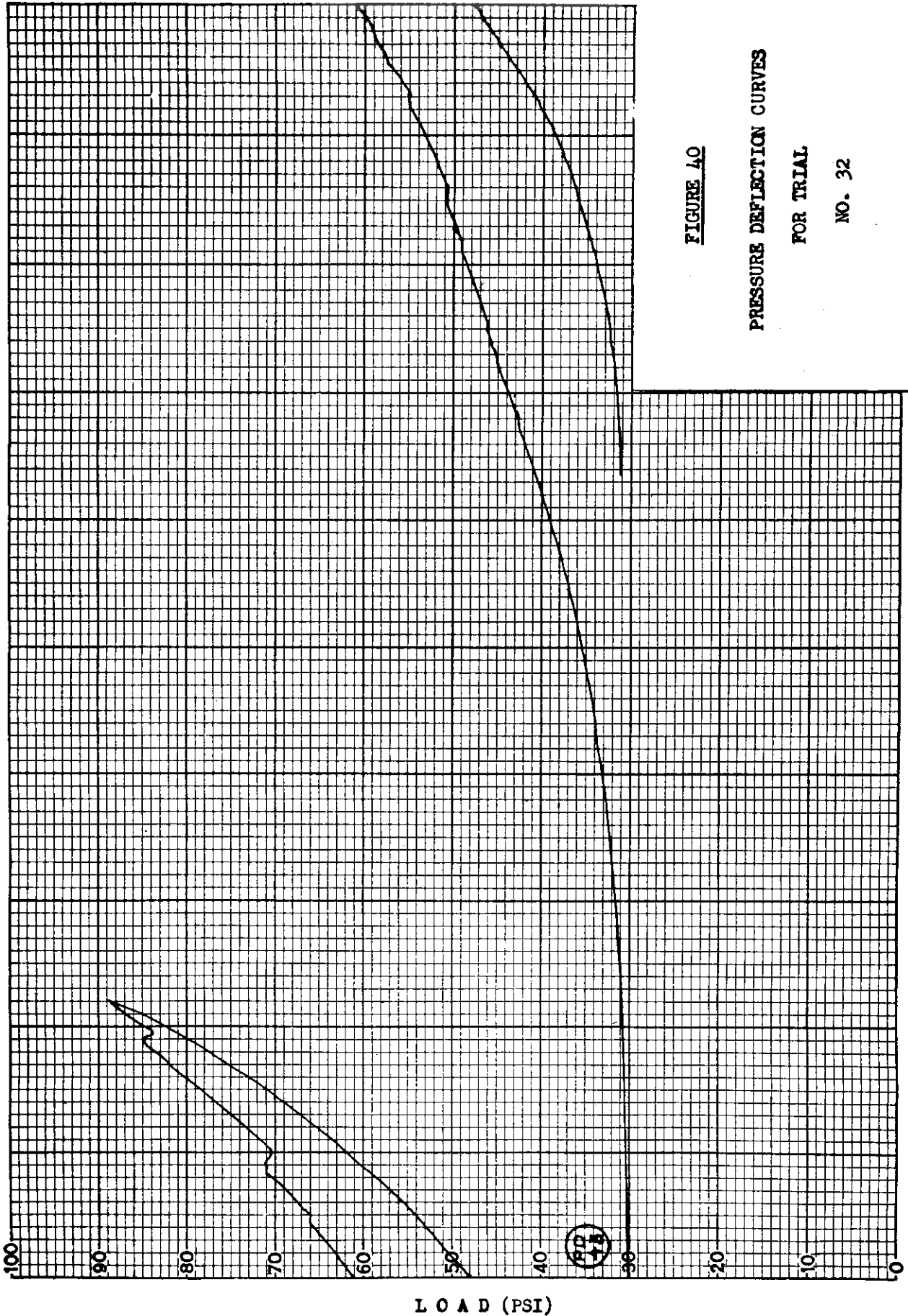


FIGURE 40

PRESSURE DEFLECTION CURVES

FOR TRIAL

NO. 32

DEFLECTION

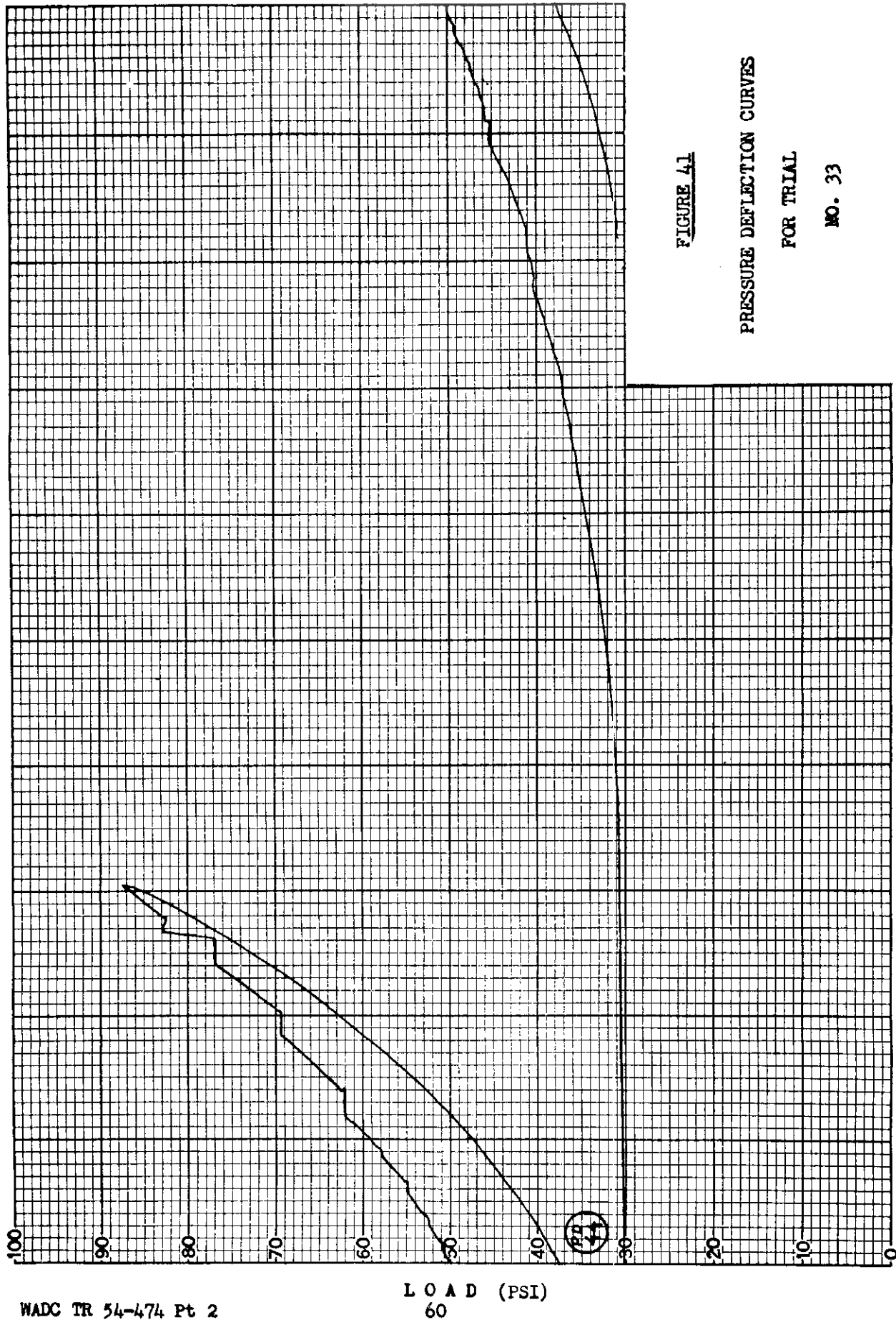


FIGURE 41

PRESSURE DEFLECTION CURVES

FOR TRIAL

NO. 33

DEFLECTION

*Control*

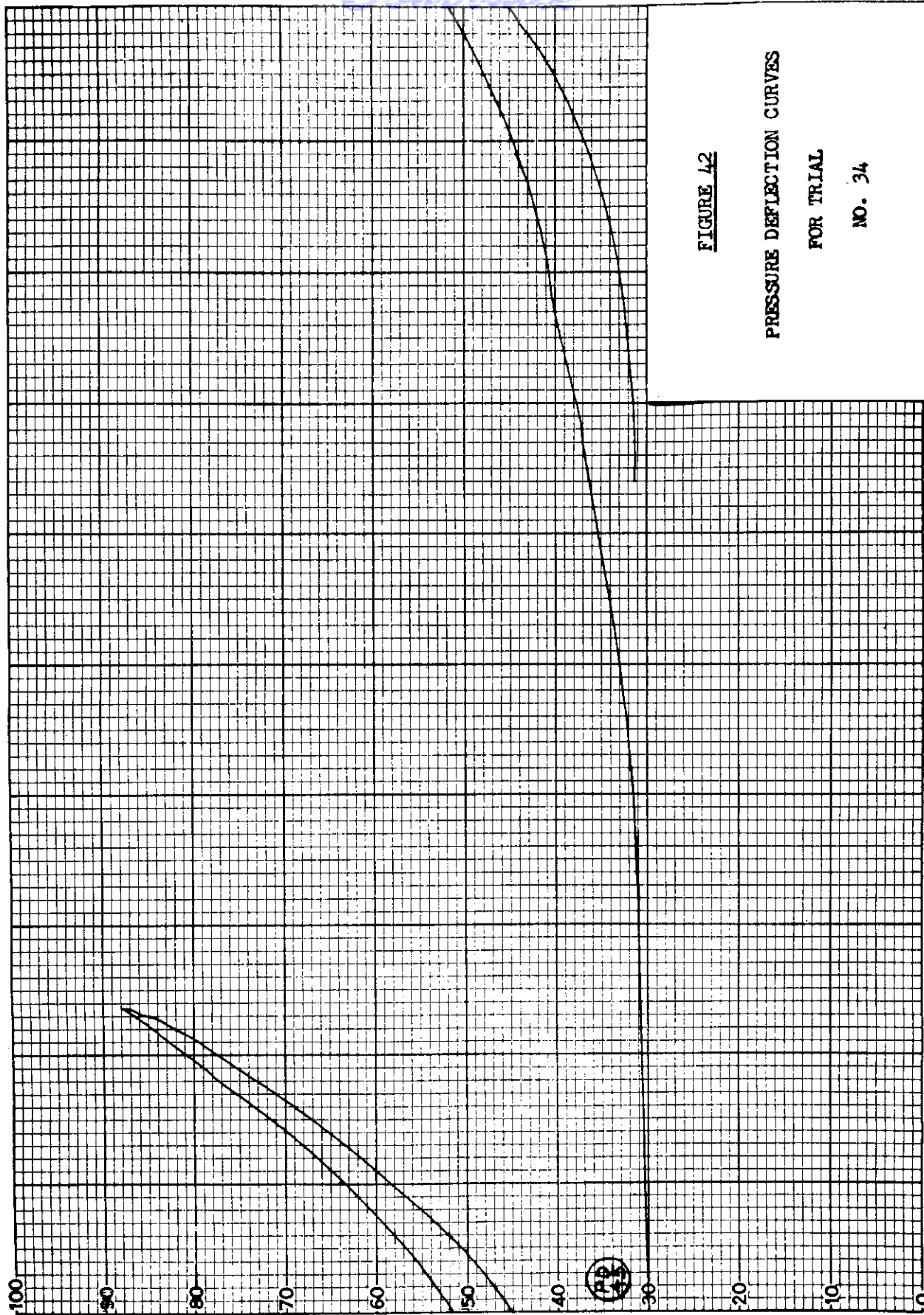


FIGURE 42

PRESSURE DEFLECTION CURVES

FOR TRIAL

NO. 34

DEFLECTION

*Continued*

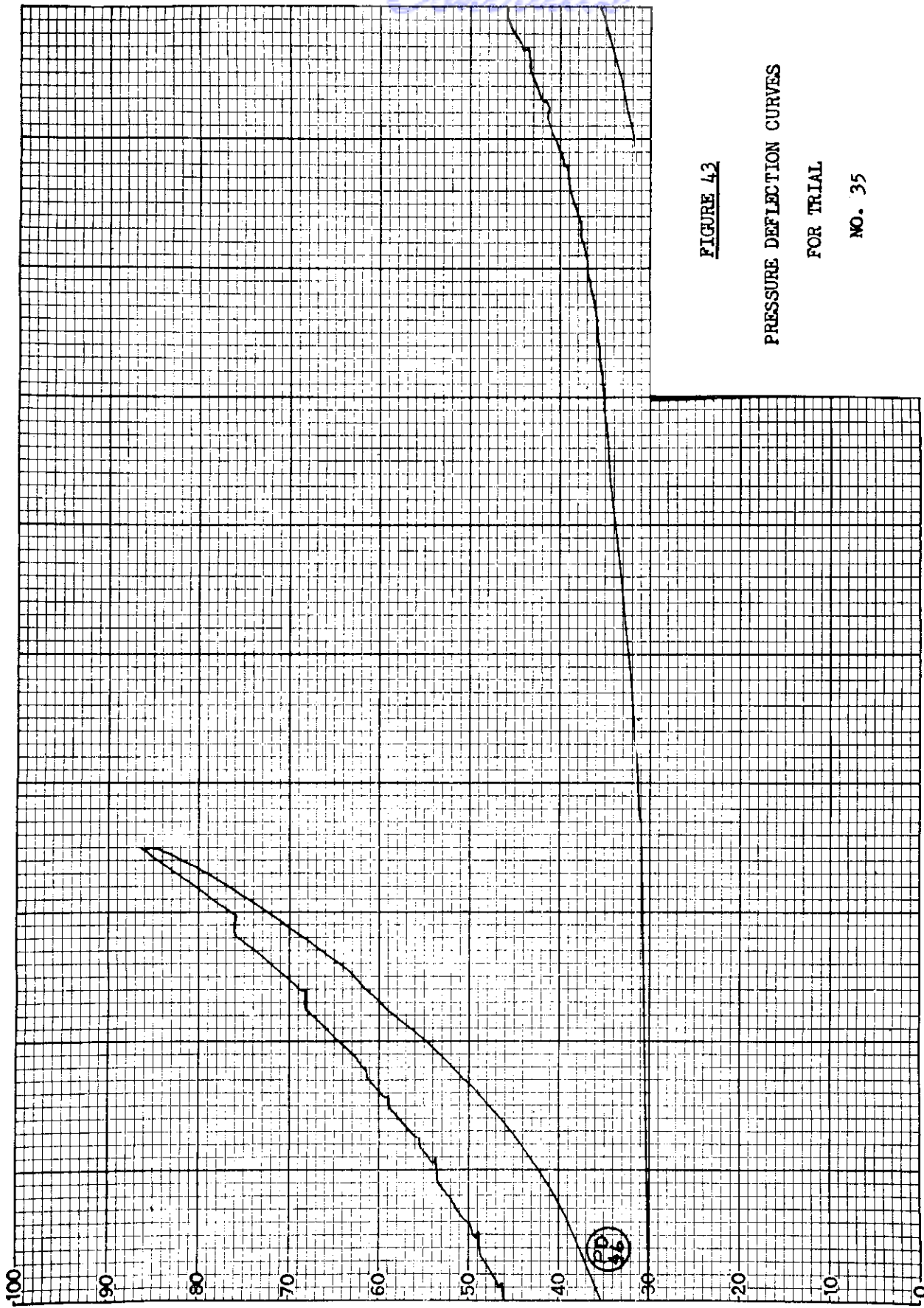


FIGURE 43

PRESSURE DEFLECTION CURVES

FOR TRIAL

NO. 35

DEFLECTION

LOAD (PSI)  
62

WADC TR 54-474 Pt 2

Continued

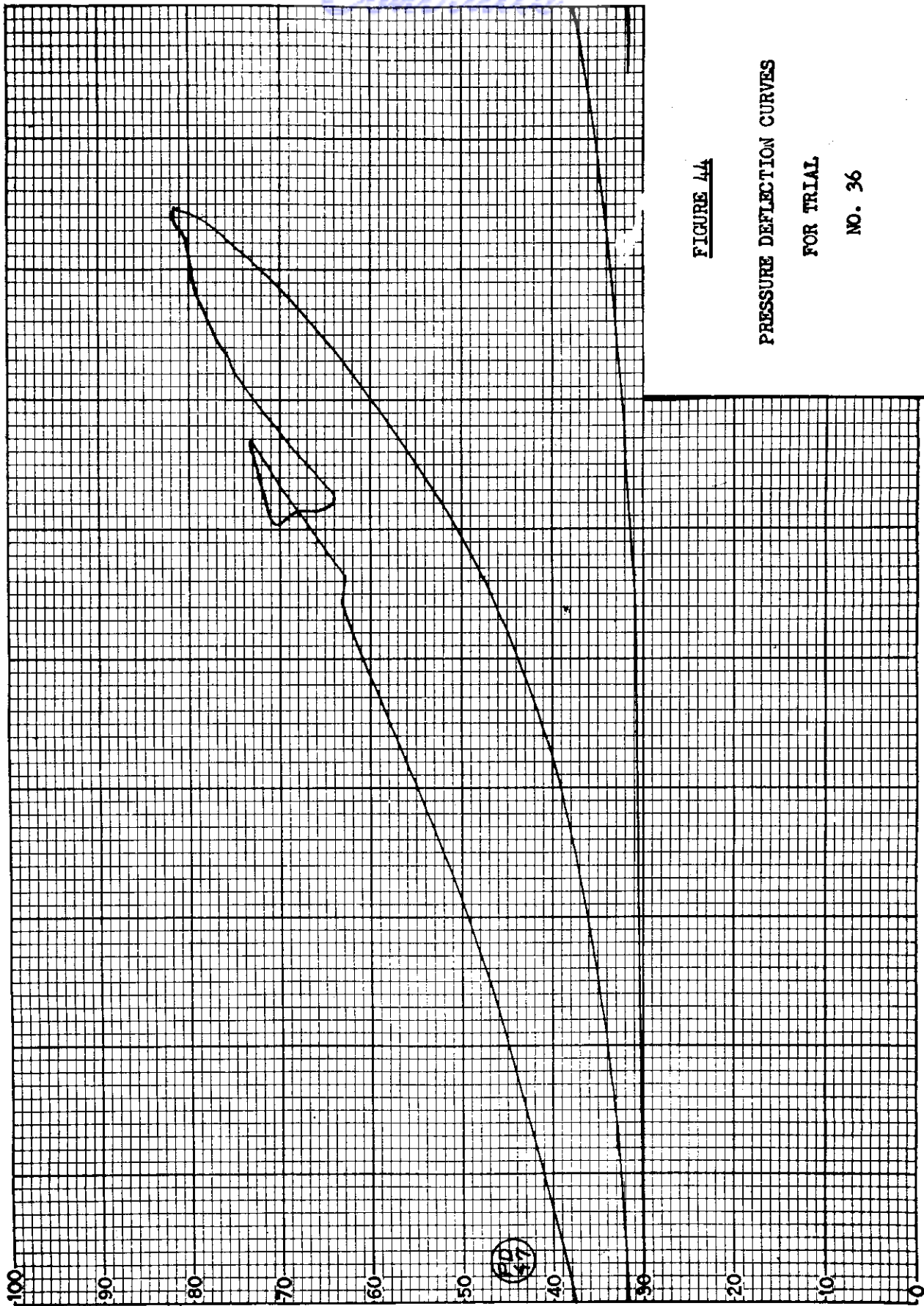


FIGURE 44

PRESSURE DEFLECTION CURVES

FOR TRIAL

NO. 36

DEFLECTION

*Conrails*

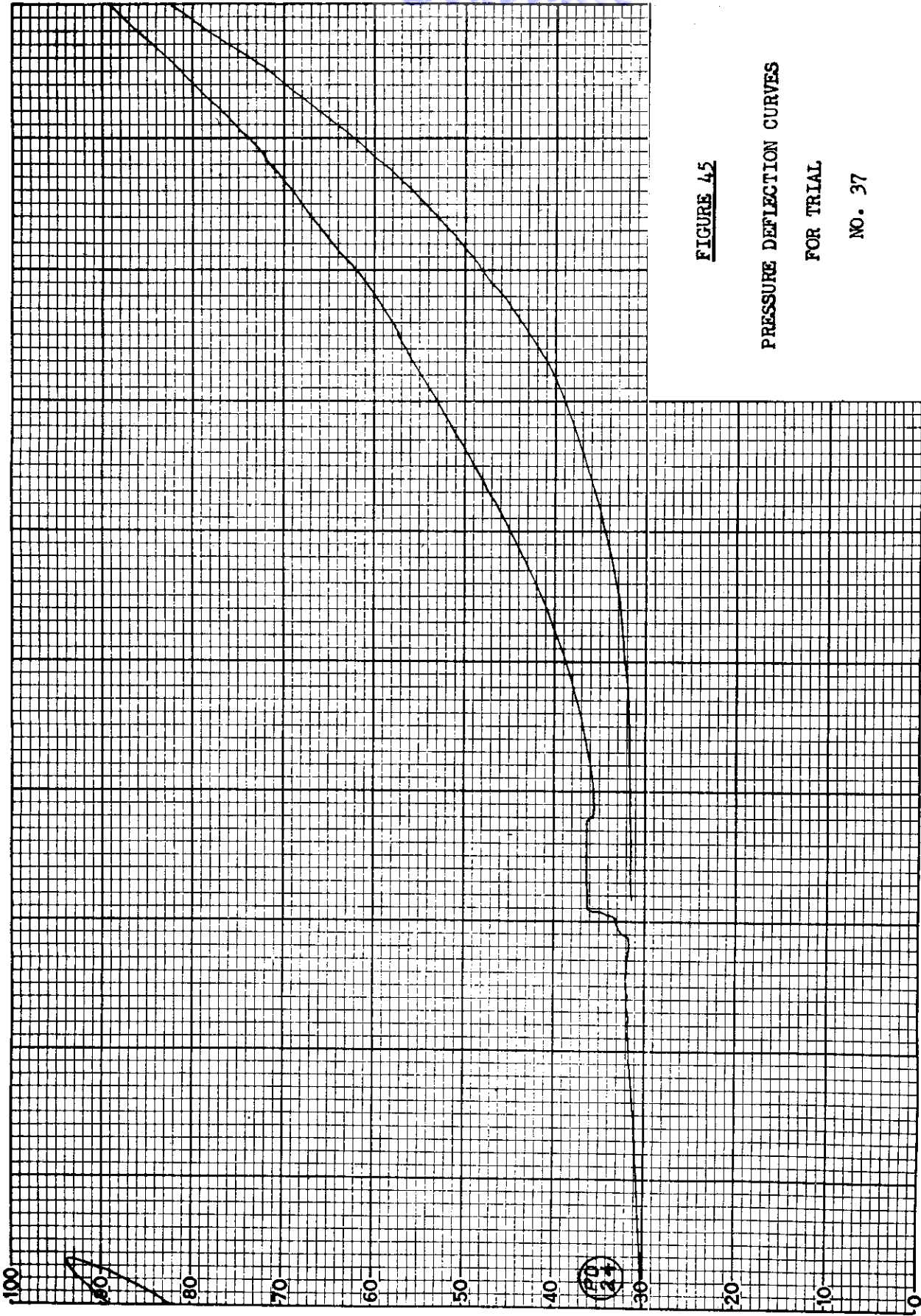


FIGURE 45

PRESSURE DEFLECTION CURVES

FOR TRIAL

NO. 37

DEFLECTION



*Control*

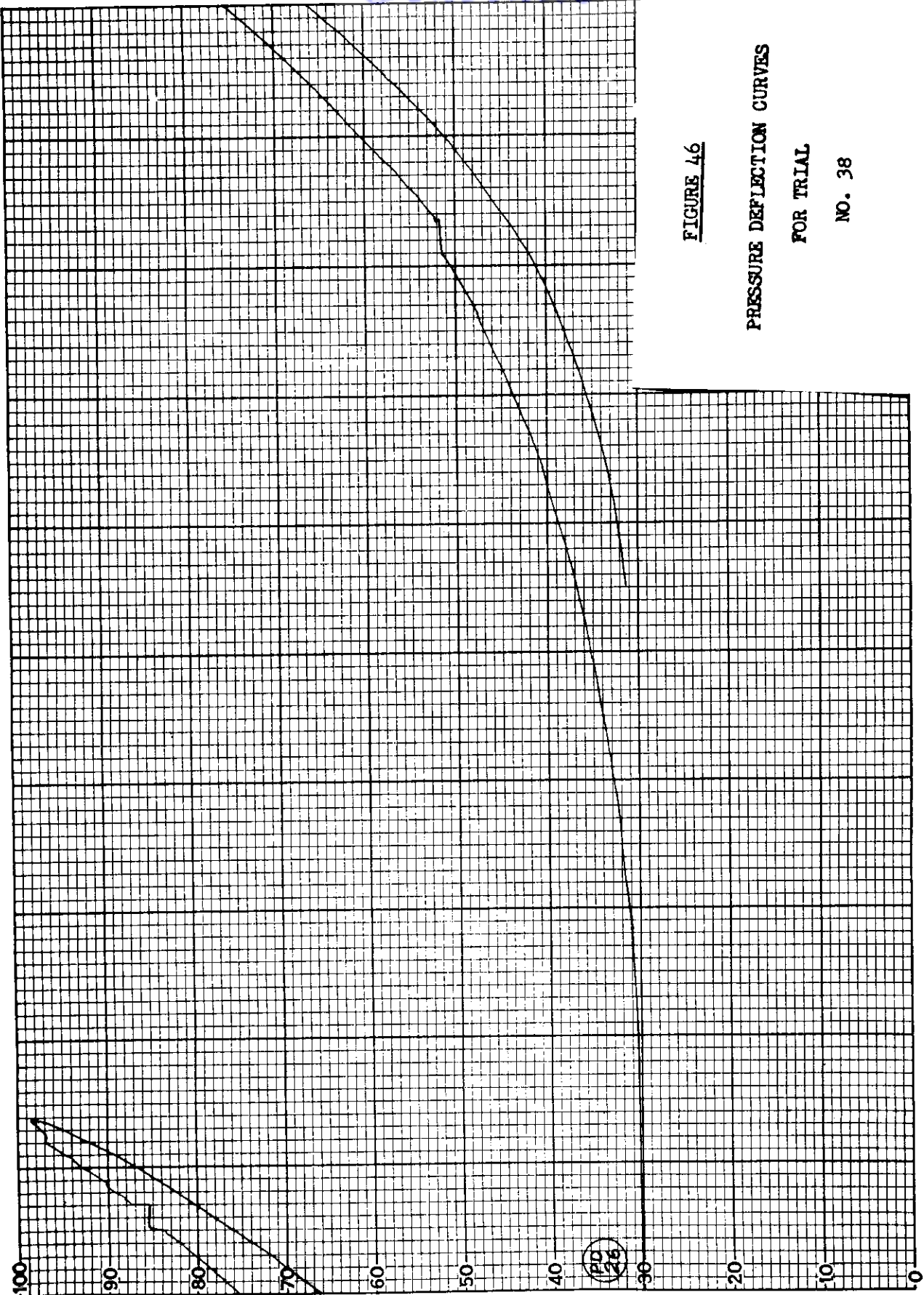


FIGURE 46

PRESSURE DEFLECTION CURVES

FOR TRIAL

NO. 38

DEFLECTION

*Control*

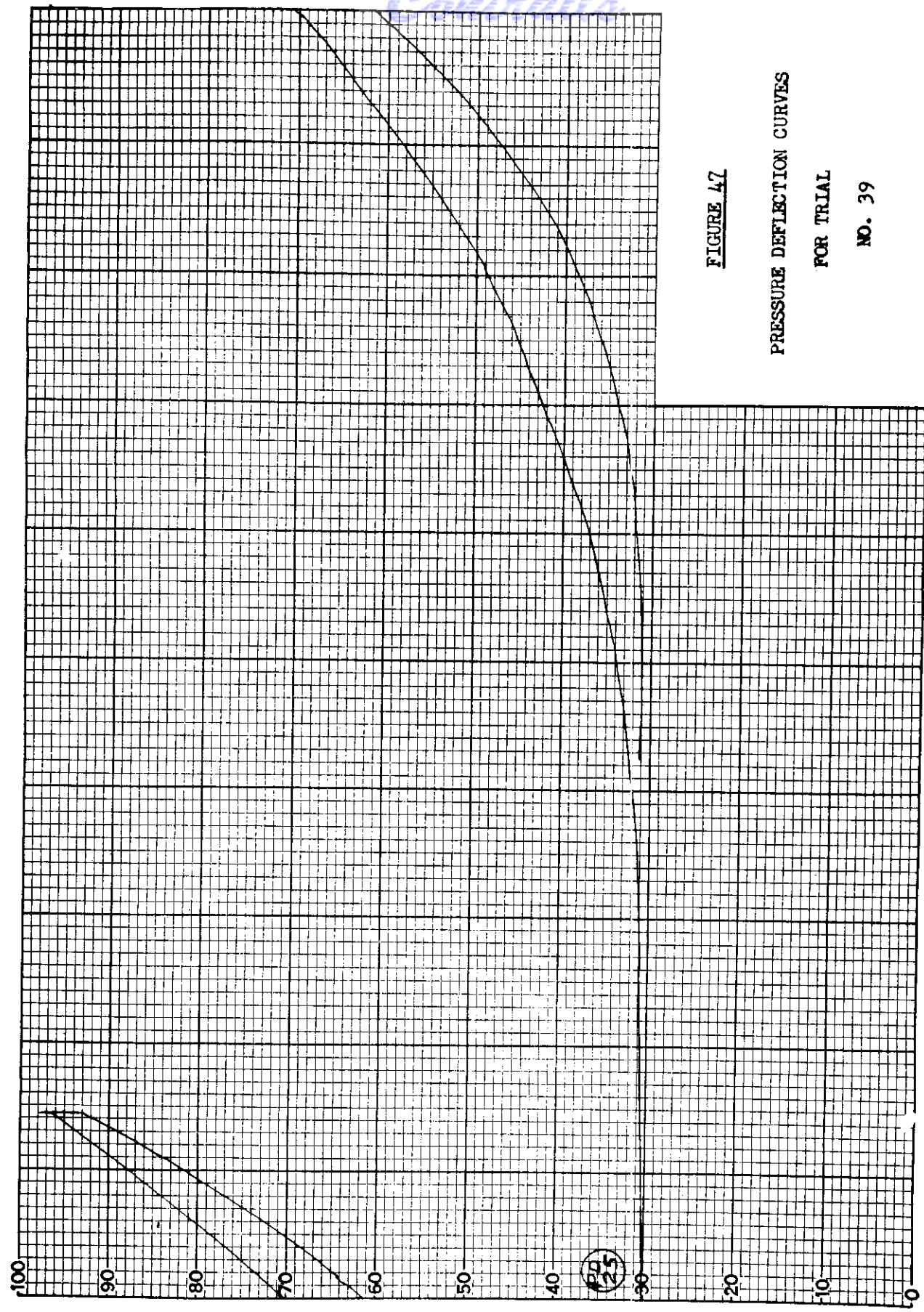


FIGURE 47

PRESSURE DEFLECTION CURVES

FOR TRIAL

NO. 39

DEFLECTION

*Centrair*

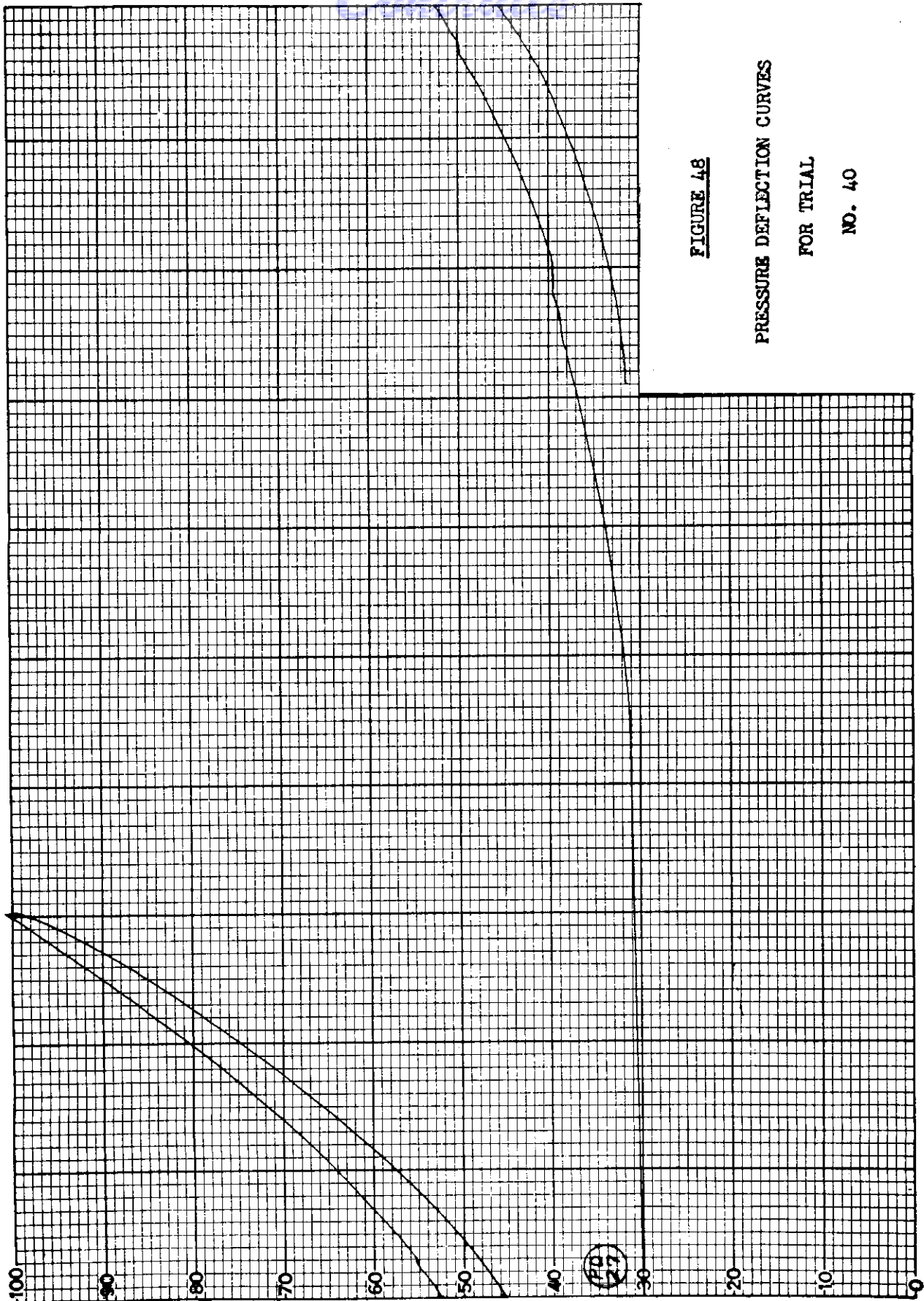


FIGURE 48

PRESSURE DEFLECTION CURVES

FOR TRIAL

NO. 40

DEFLECTION

WADC TR 54-474 Pt 2

LOAD (PSI)  
67

*Controls*

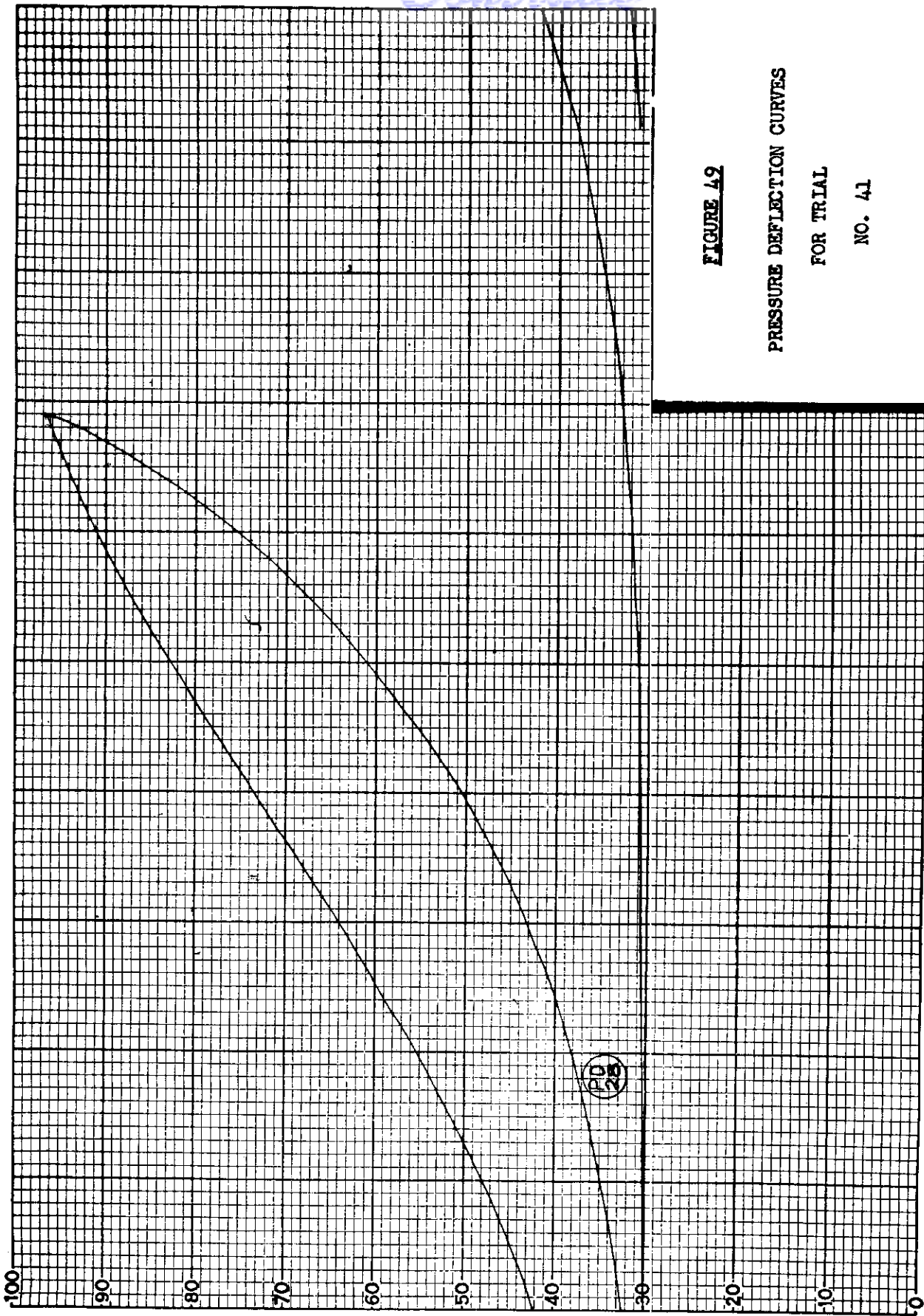


**FIGURE 49**

**PRESSURE DEFLECTION CURVES**

**FOR TRIAL**

**NO. 41**

**DEFLECTION**

*Continued*

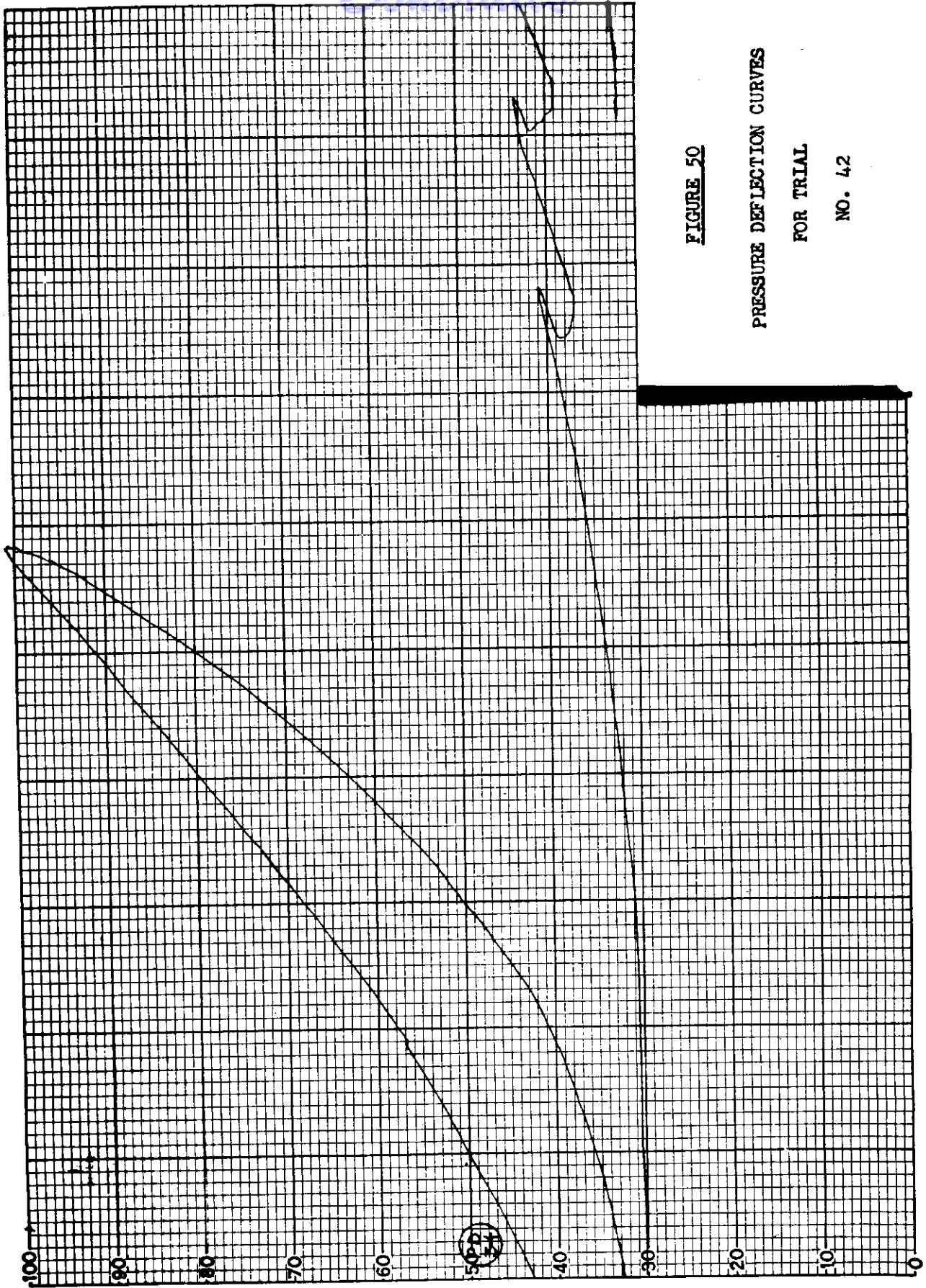


FIGURE 50

PRESSURE DEFLECTION CURVES

FOR TRIAL

NO. 42

DEFLECTION

*Controls*

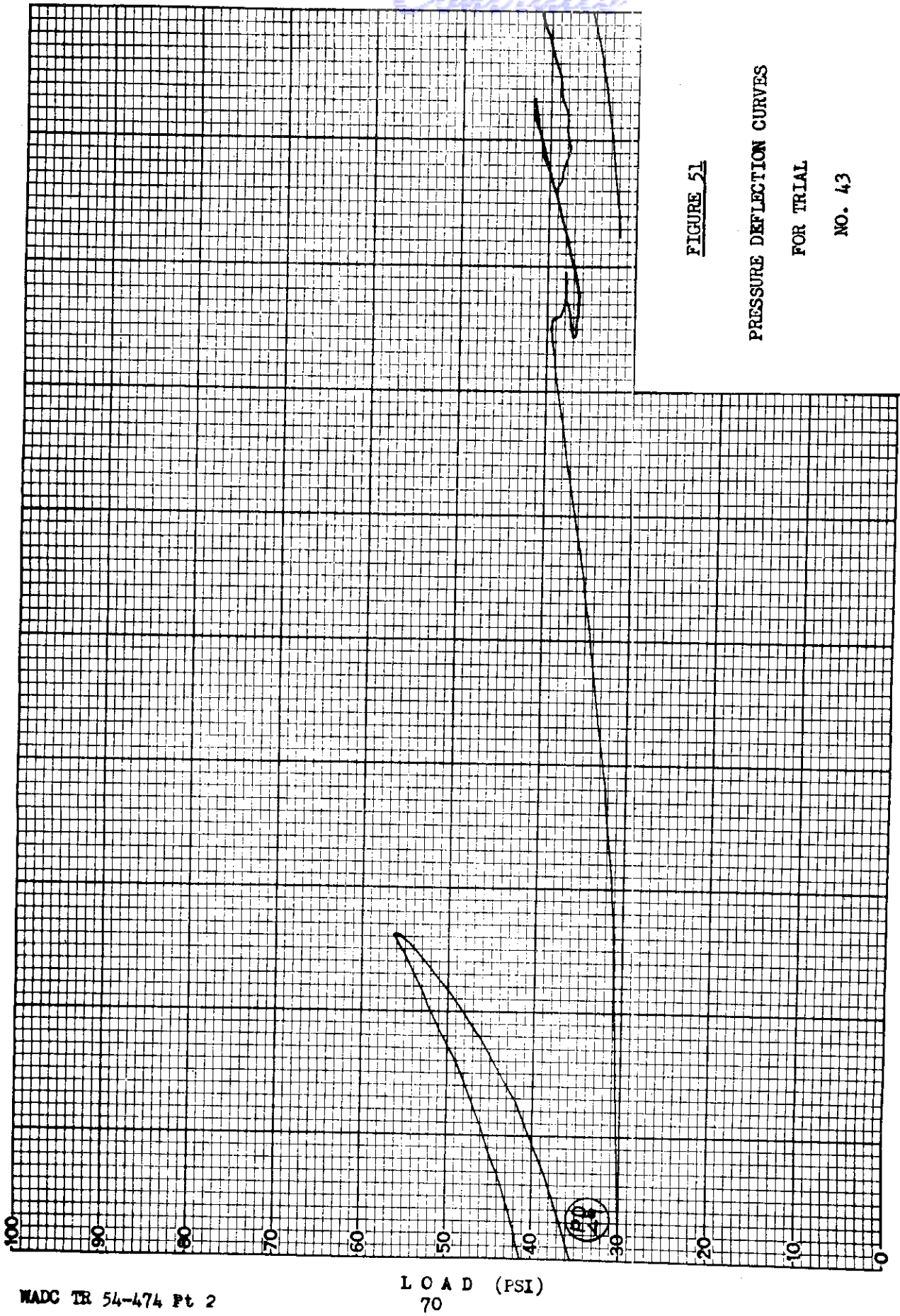


FIGURE 51

PRESSURE DEFLECTION CURVES

FOR TRIAL

NO. 43

DEFLECTION

*Cartridge*

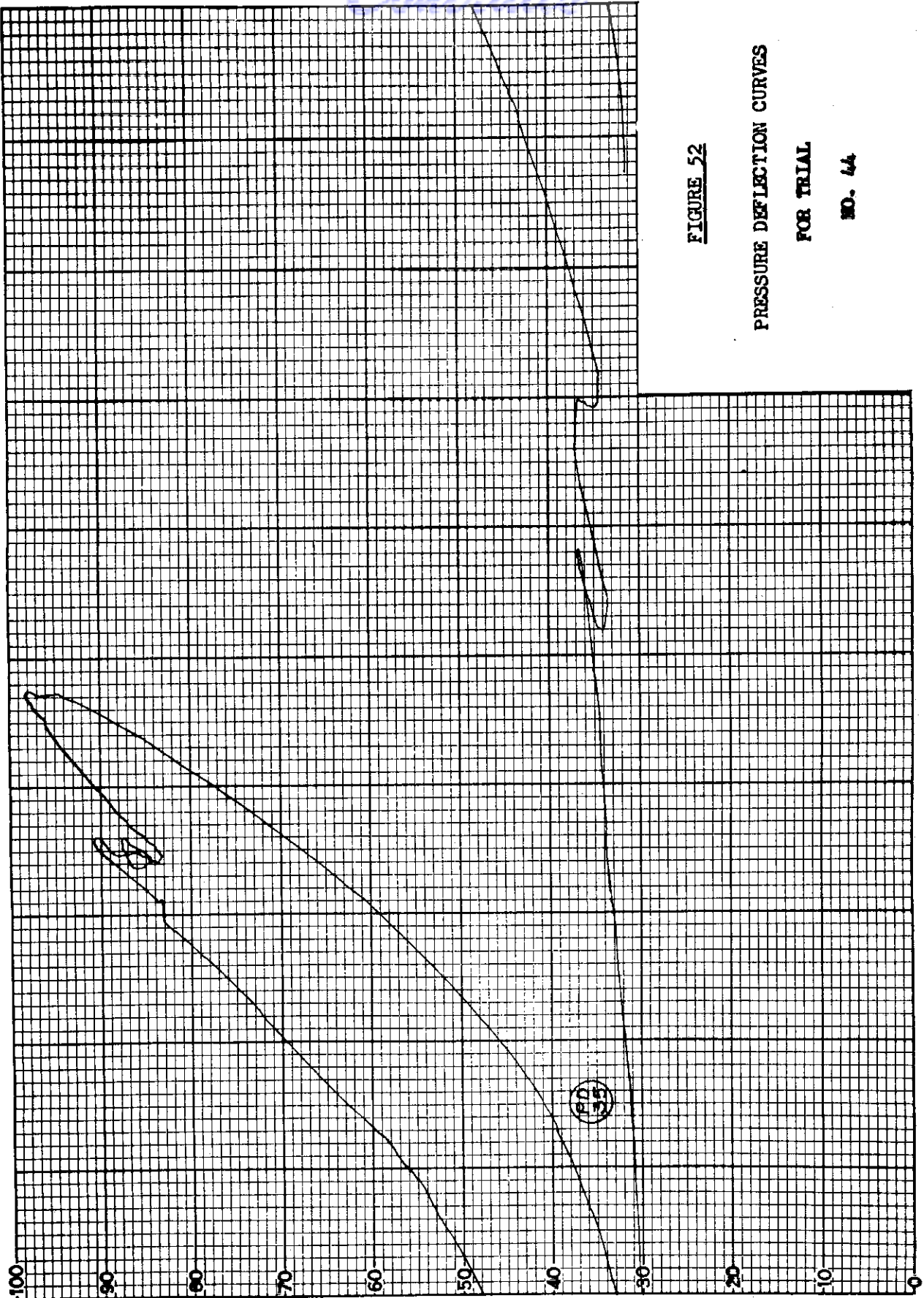


FIGURE 52

PRESSURE DEFLECTION CURVES

FOR TRIAL

NO. 44

DEFLECTION

*Control*

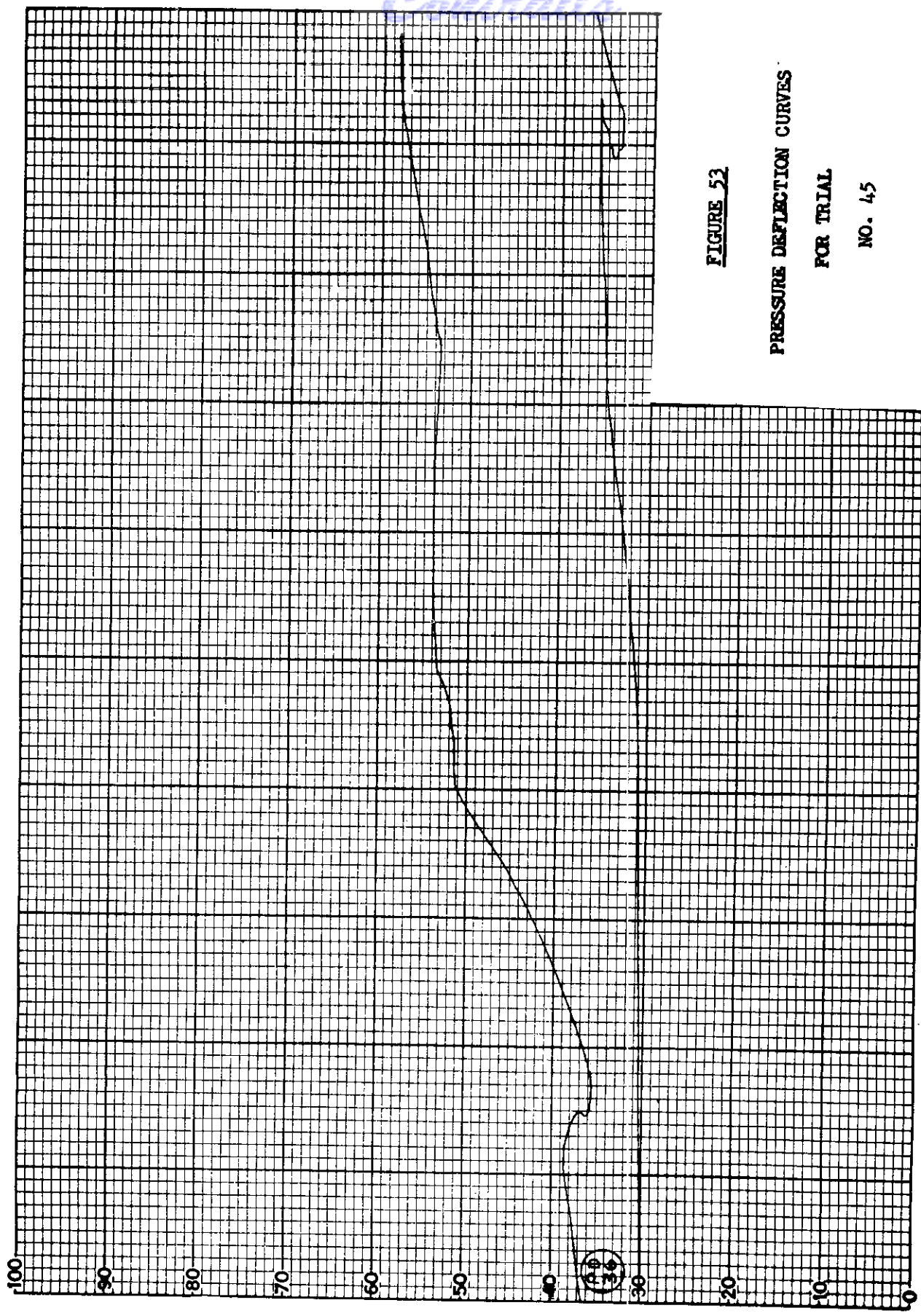


FIGURE 53

PRESSURE DEFLECTION CURVES

FOR TRIAL

NO. 45

DEFLECTION



*Controls*

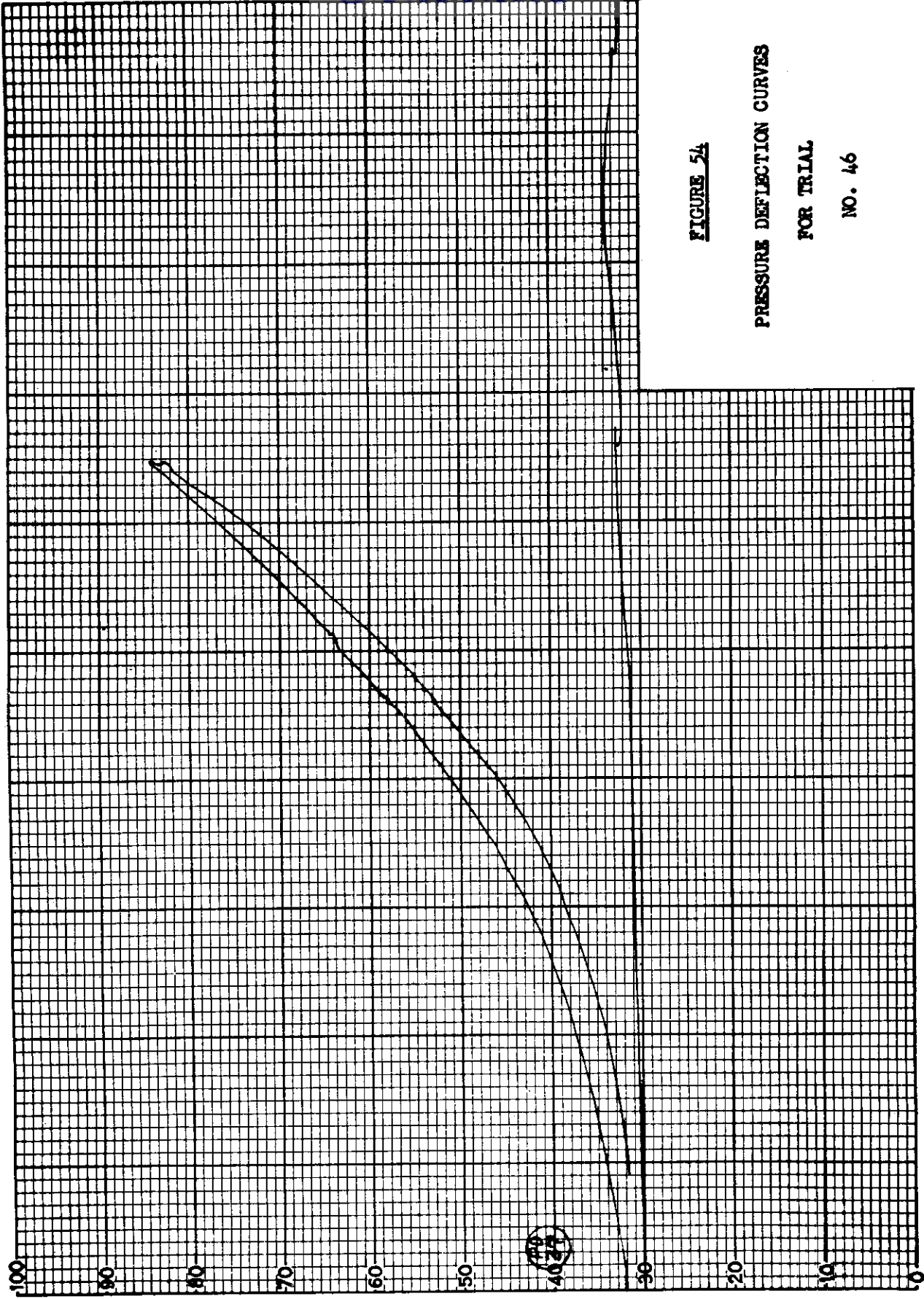


FIGURE 54

PRESSURE DEFLECTION CURVES

FOR TRIAL

NO. 46

DEFLECTION

MDC IR 51-174 Pt 2

LOAD (PSI)  
73

*Contrails*

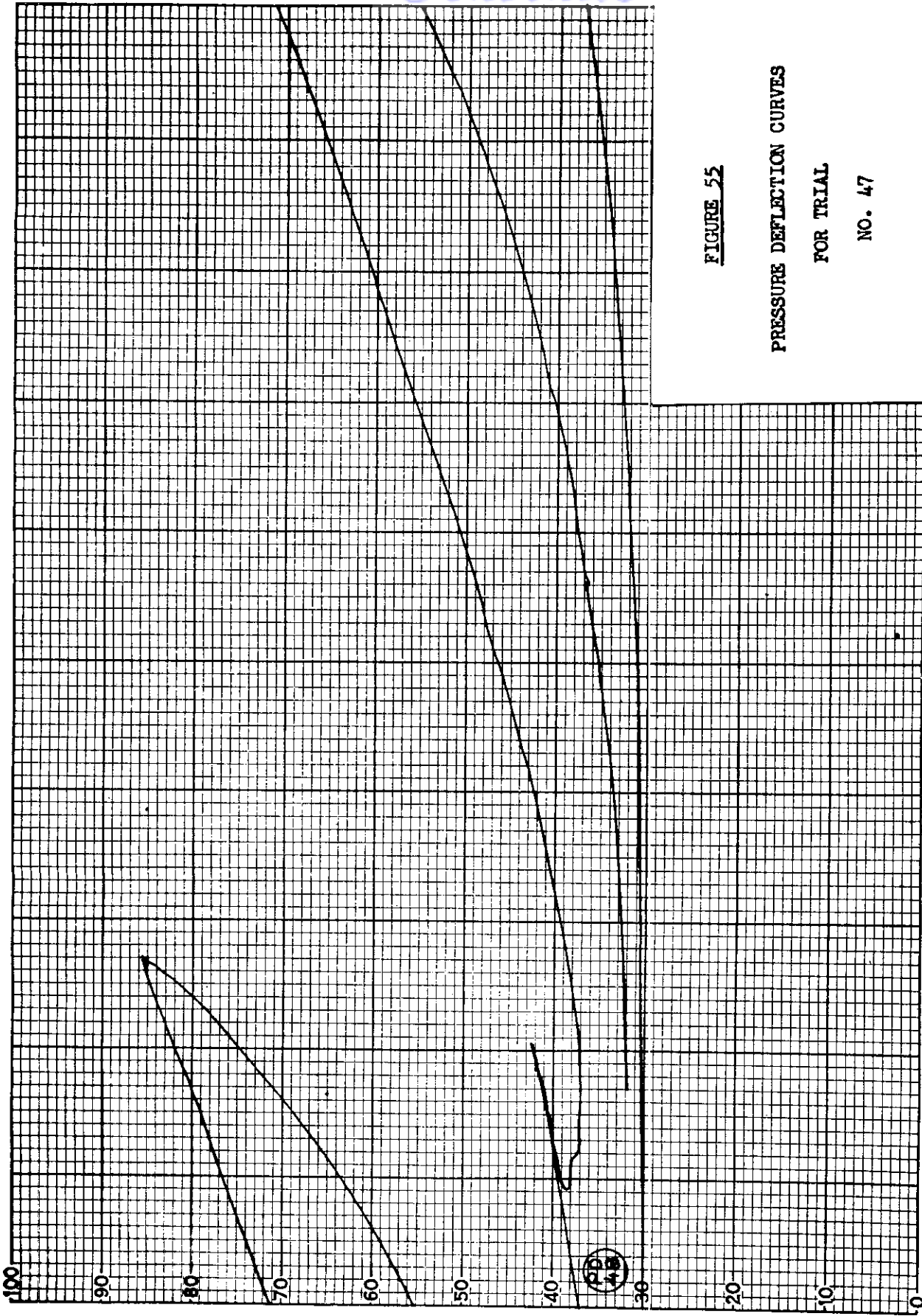


FIGURE 55

PRESSURE DEFLECTION CURVES

FOR TRIAL

NO. 47

DEFLECTION

WADC TR 54-474 Pt 2

LOAD (PSI)  
74

*Control*

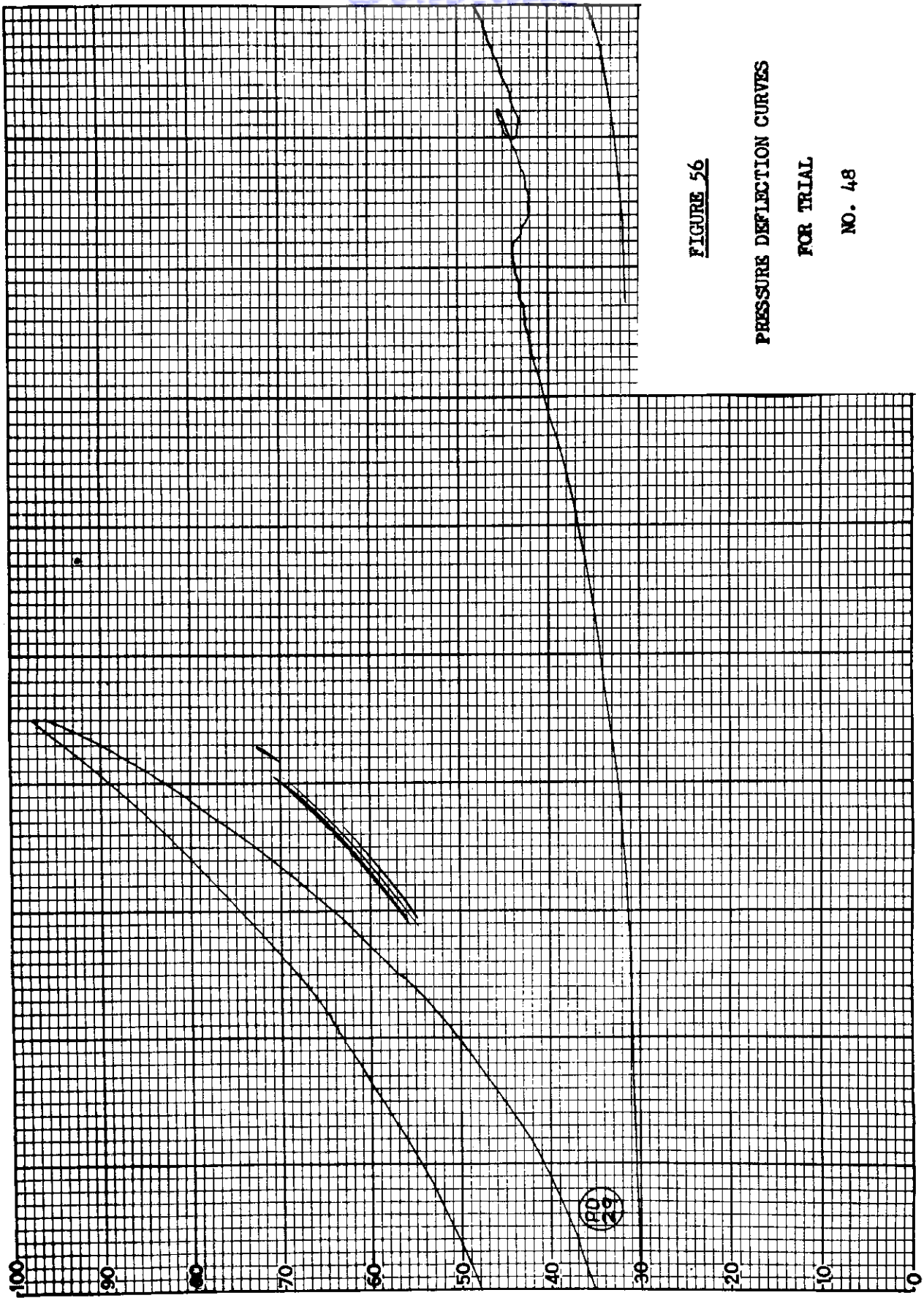


FIGURE 56

PRESSURE DEFLECTION CURVES

FOR TRIAL

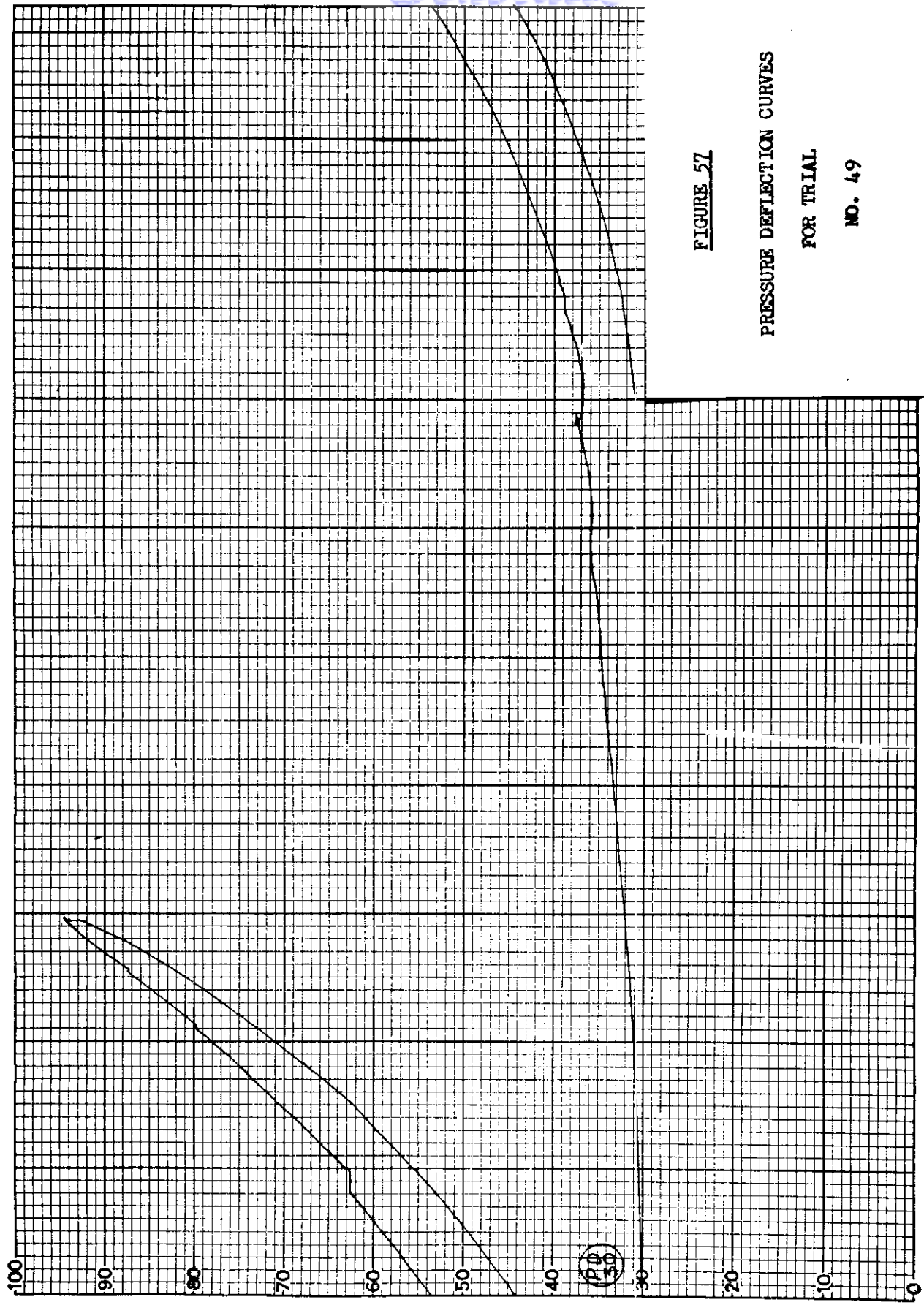
NO. 48

DEFLECTION

*Contrails*

FIGURE 57

PRESSURE DEFLECTION CURVES  
FOR TRIAL  
NO. 49



DEFLECTION

*Continued*

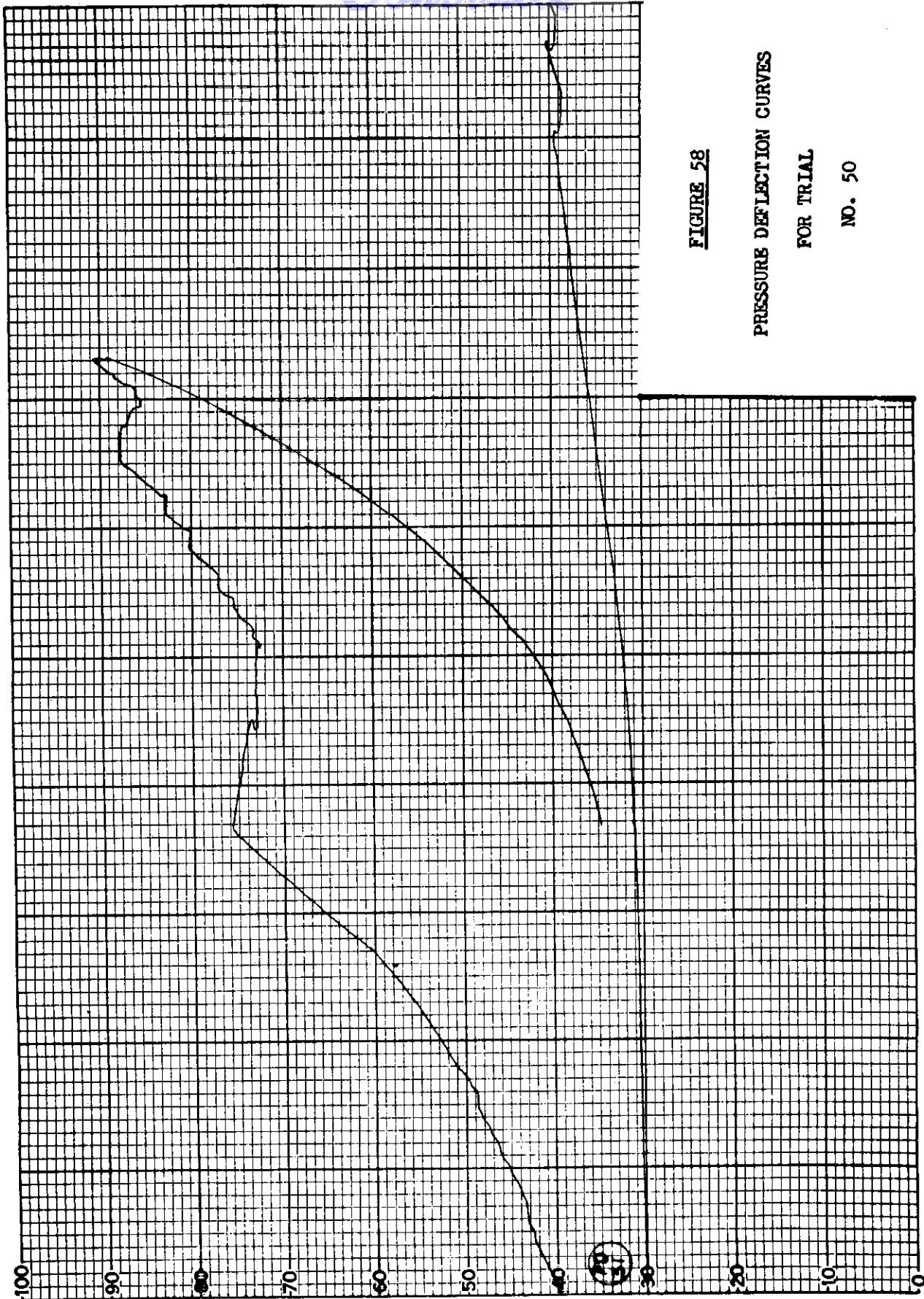


FIGURE 58

PRESSURE DEFLECTION CURVES

FOR TRIAL

NO. 50

DEFLECTION

*Continuity*

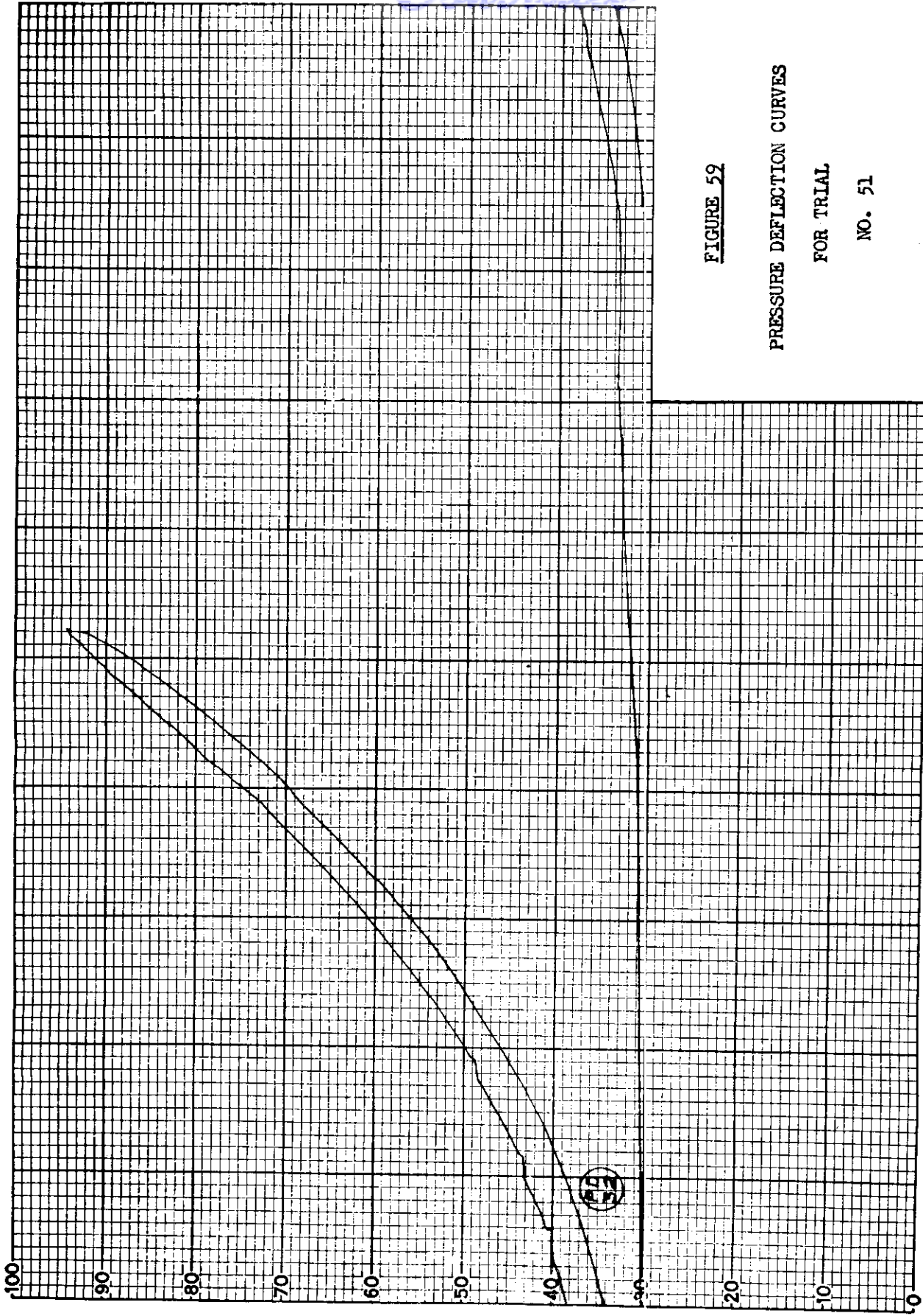


FIGURE 59

PRESSURE DEFLECTION CURVES

FOR TRIAL

NO. 51

DEFLECTION

WADC TR 54-474 Pt 2

LOAD (PSI)  
78

*Contrails*

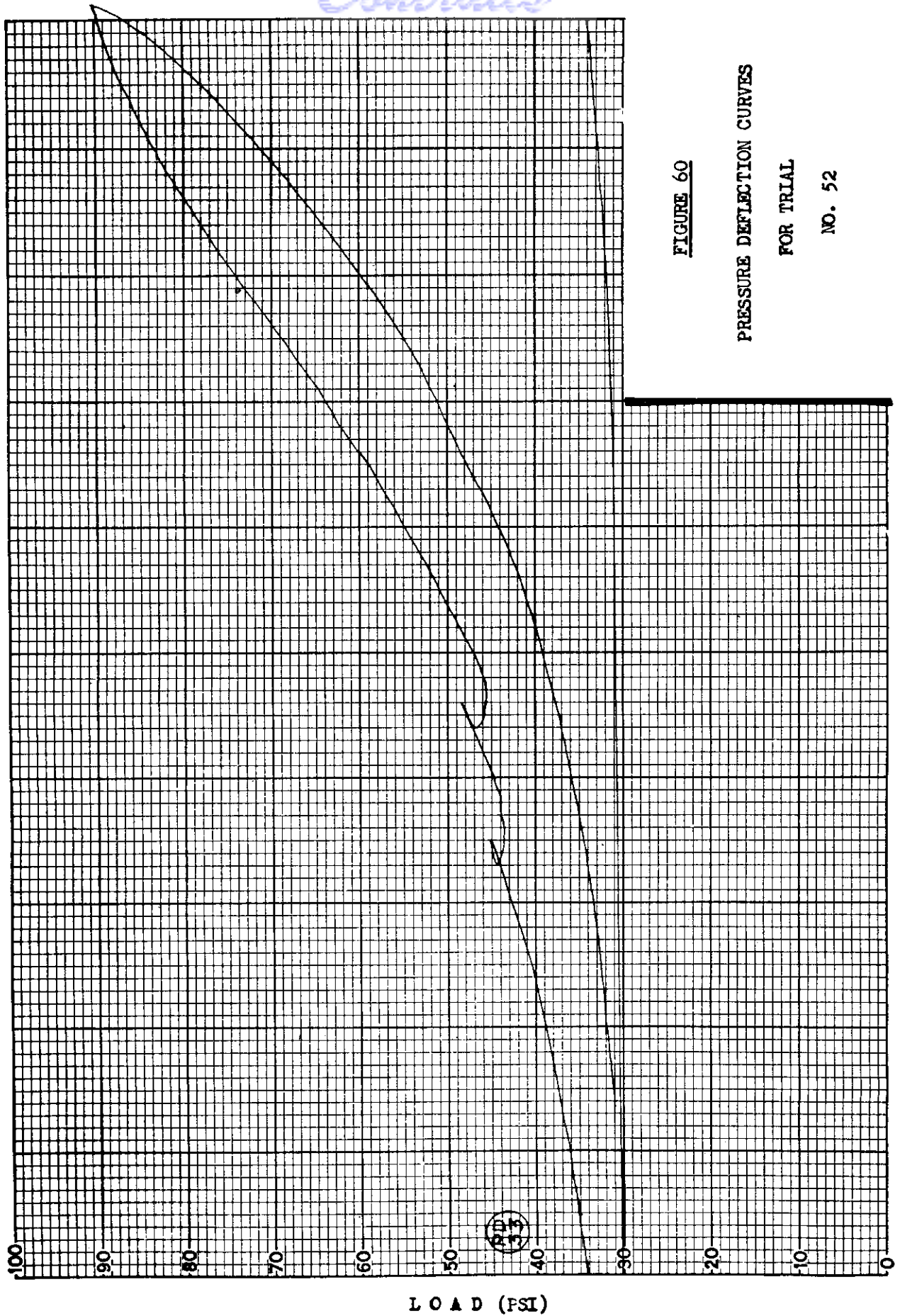


FIGURE 60

PRESSURE DEFLECTION CURVES  
FOR TRIAL  
NO. 52

DEFLECTION

*Control*

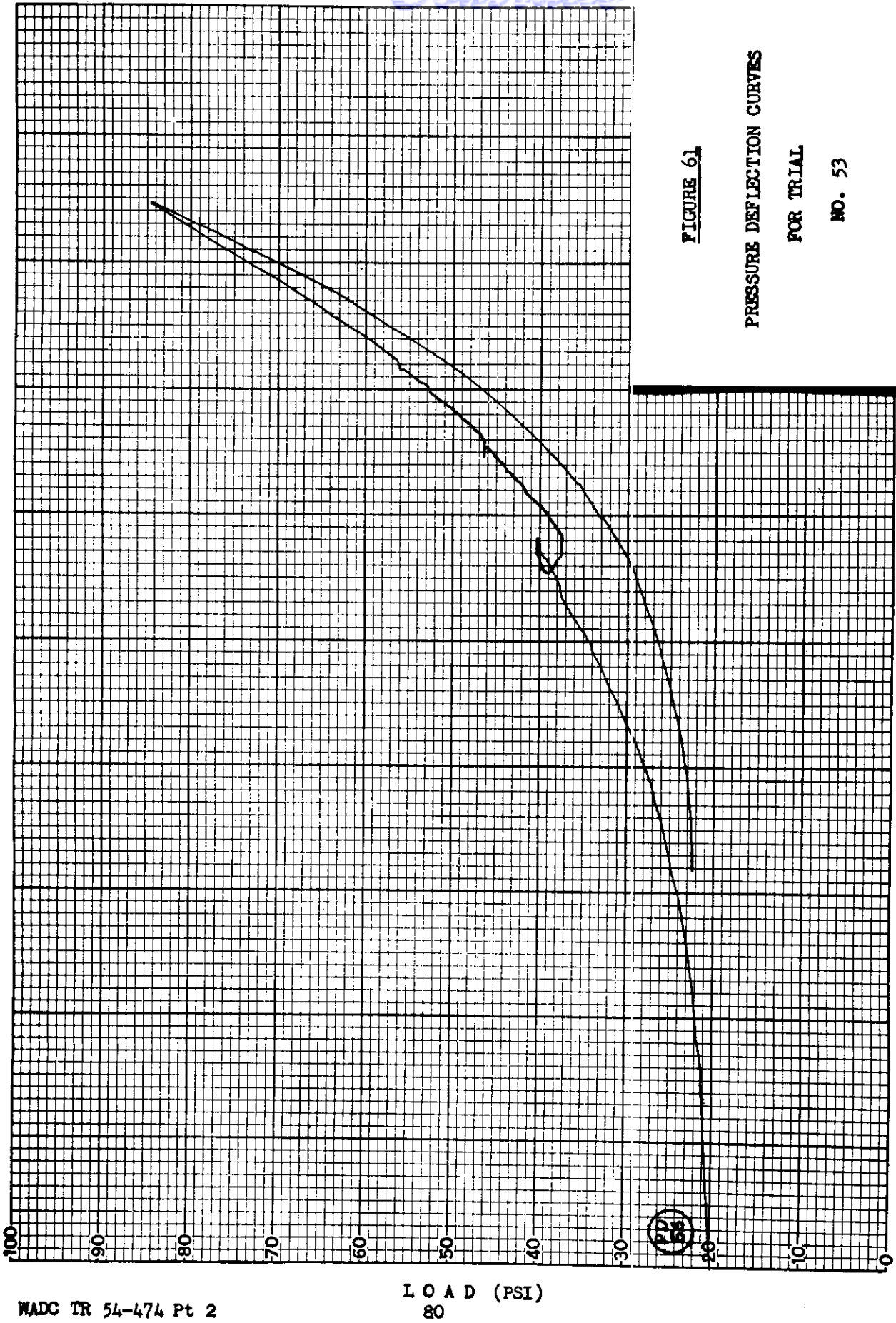


FIGURE 61

PRESSURE DEFLECTION CURVES

FOR TRIAL

NO. 53

DEFLECTION



*Contours*

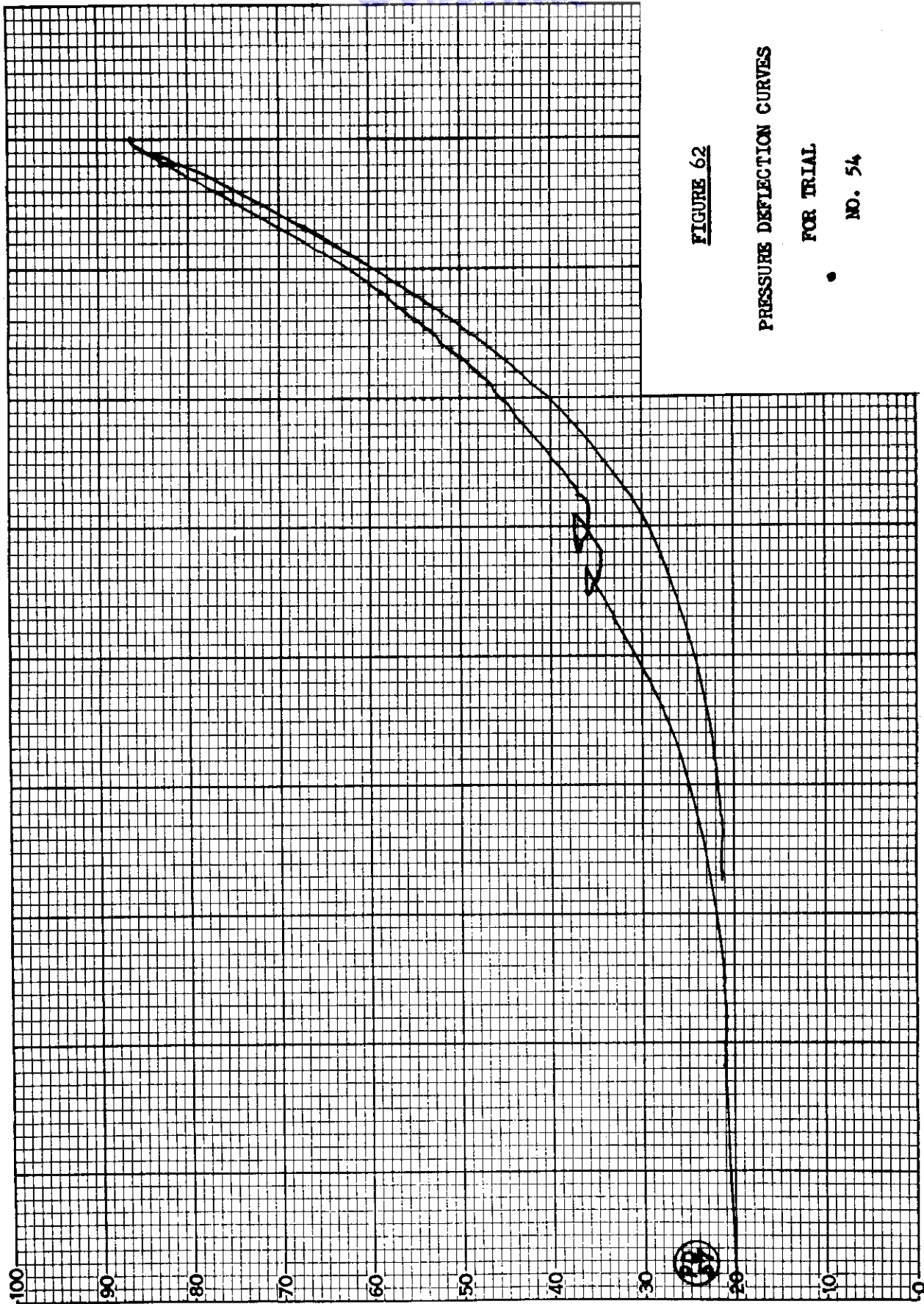


FIGURE 62

PRESSURE DEFLECTION CURVES

FOR TRIAL

NO. 54

DEFLECTION

LOAD (PSI)  
81

WADC TR 54-474 Pt 2

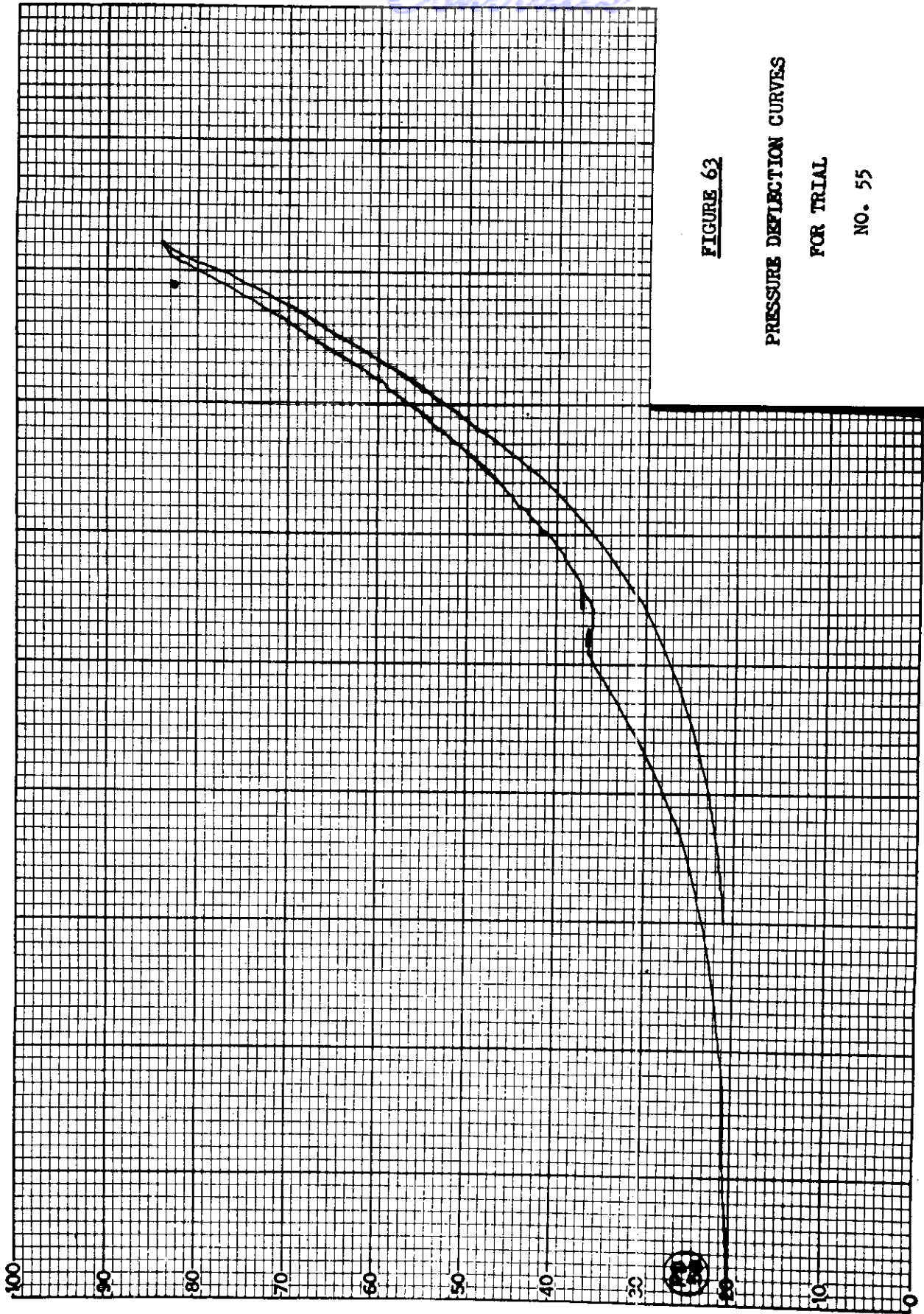
*Continuity*

FIGURE 63

PRESSURE DEFLECTION CURVES

FOR TRIAL

NO. 55



DEFLECTION

*Control*

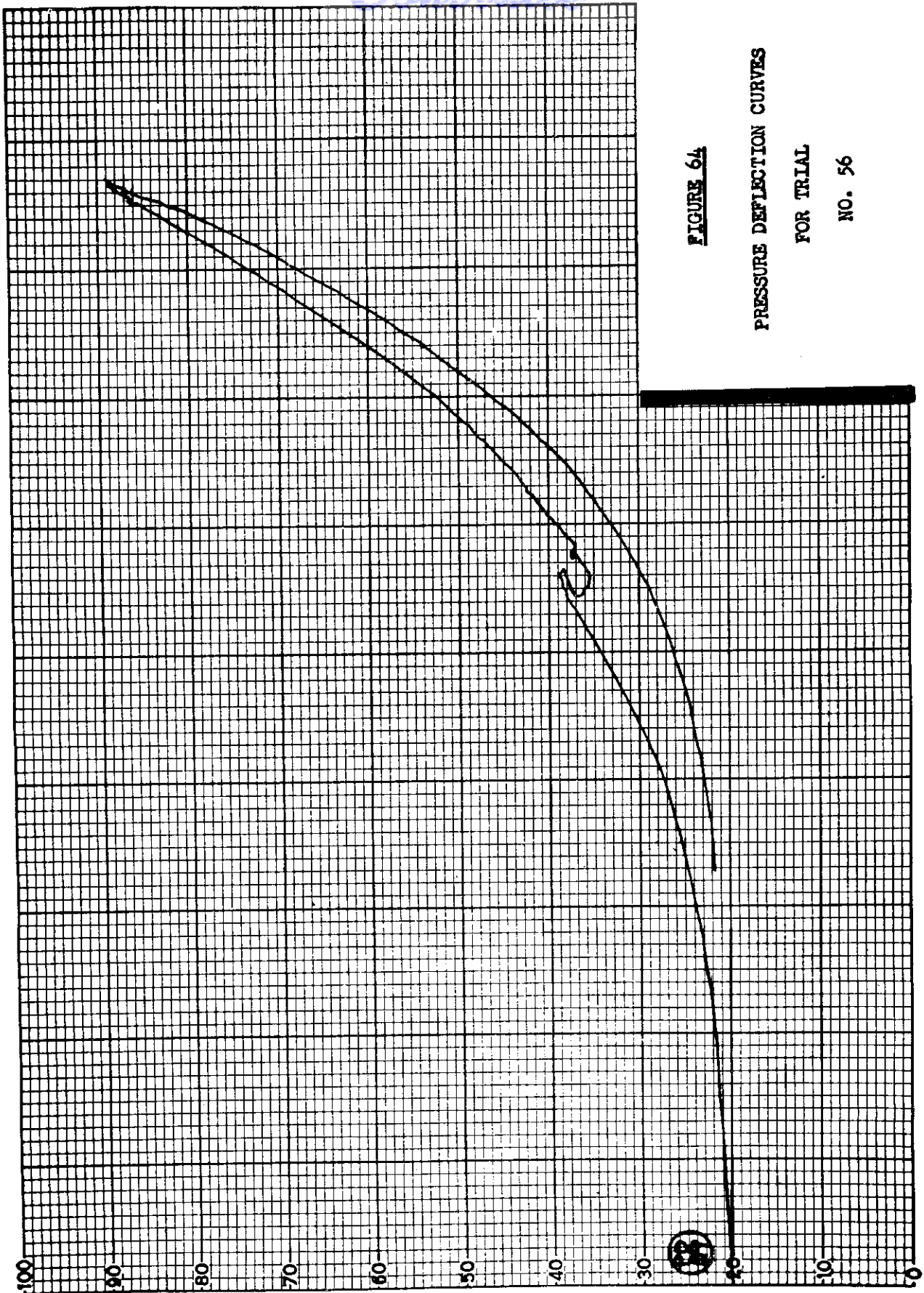


**FIGURE 64**

**PRESSURE DEFLECTION CURVES**

**FOR TRIAL**

**NO. 56**

**DEFLECTION**

*Control*

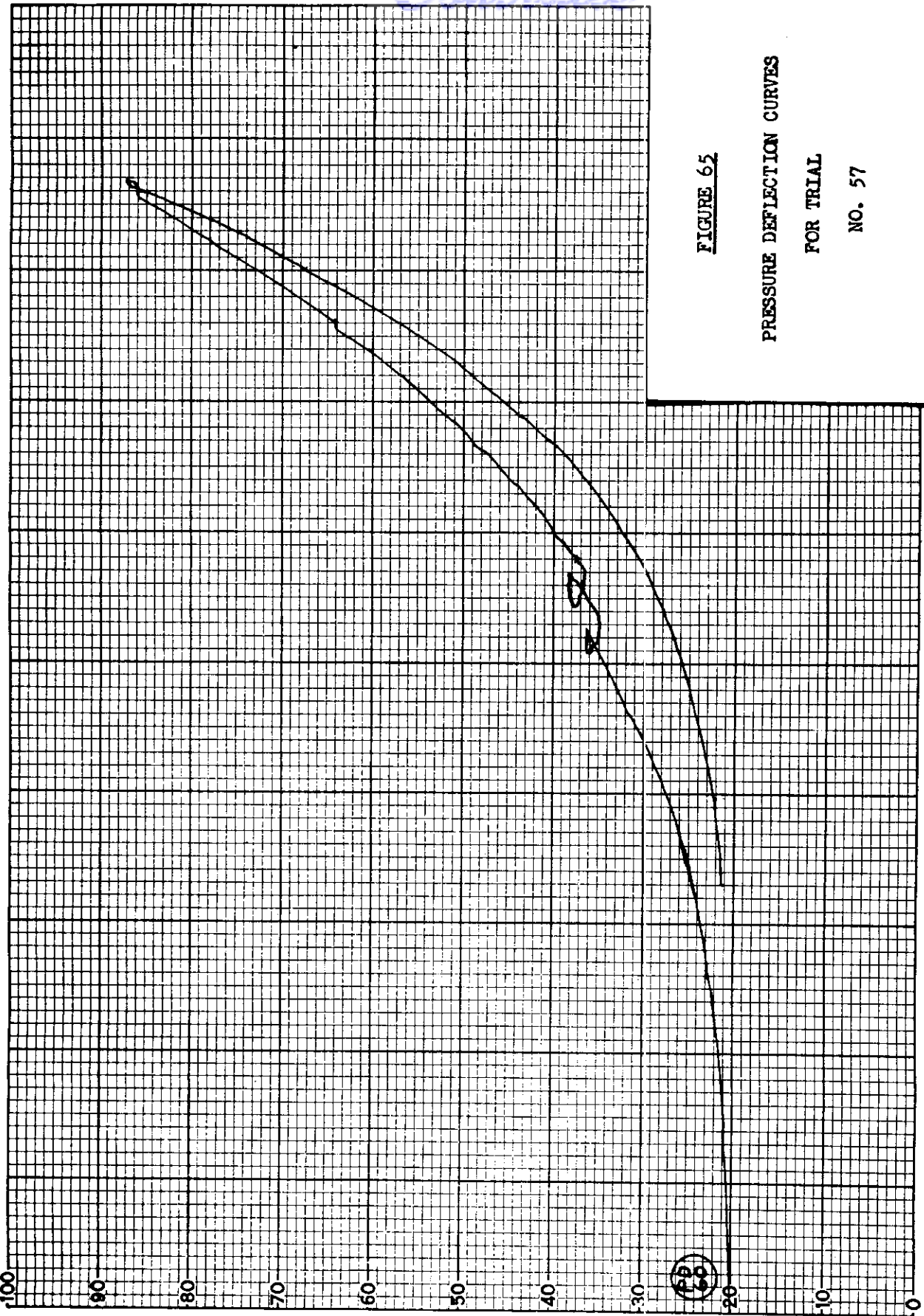


FIGURE 65

PRESSURE DEFLECTION CURVES

FOR TRIAL

NO. 57

DEFLECTION

WADC TR 54-474 Pt 2

LOAD (PSI)  
84

*Control*

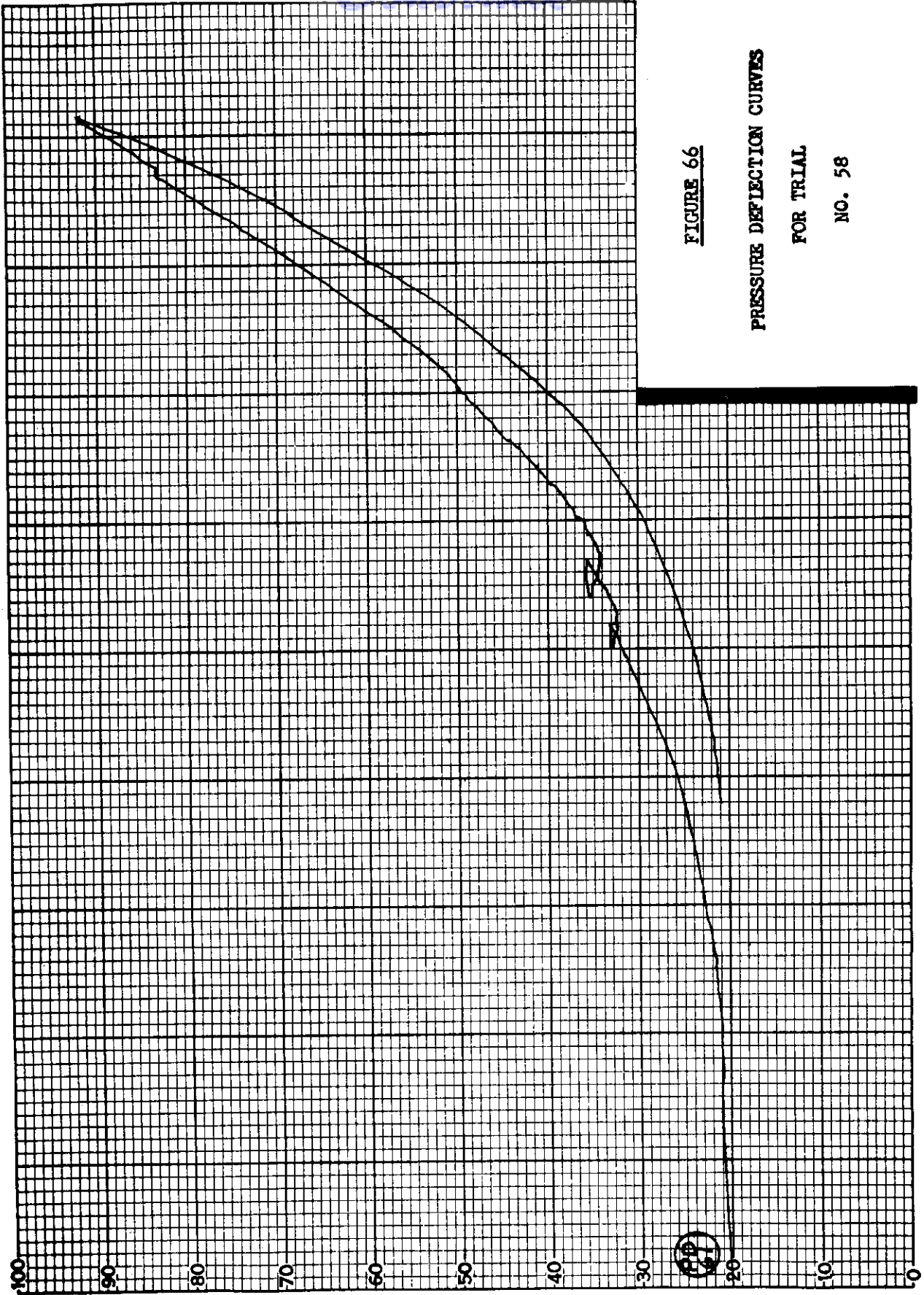


FIGURE 66

PRESSURE DEFLECTION CURVES

FOR TRIAL

NO. 58

DEFLECTION

WADC TR 54-474 Pt 2

LOAD (PSI)  
85

*Control*

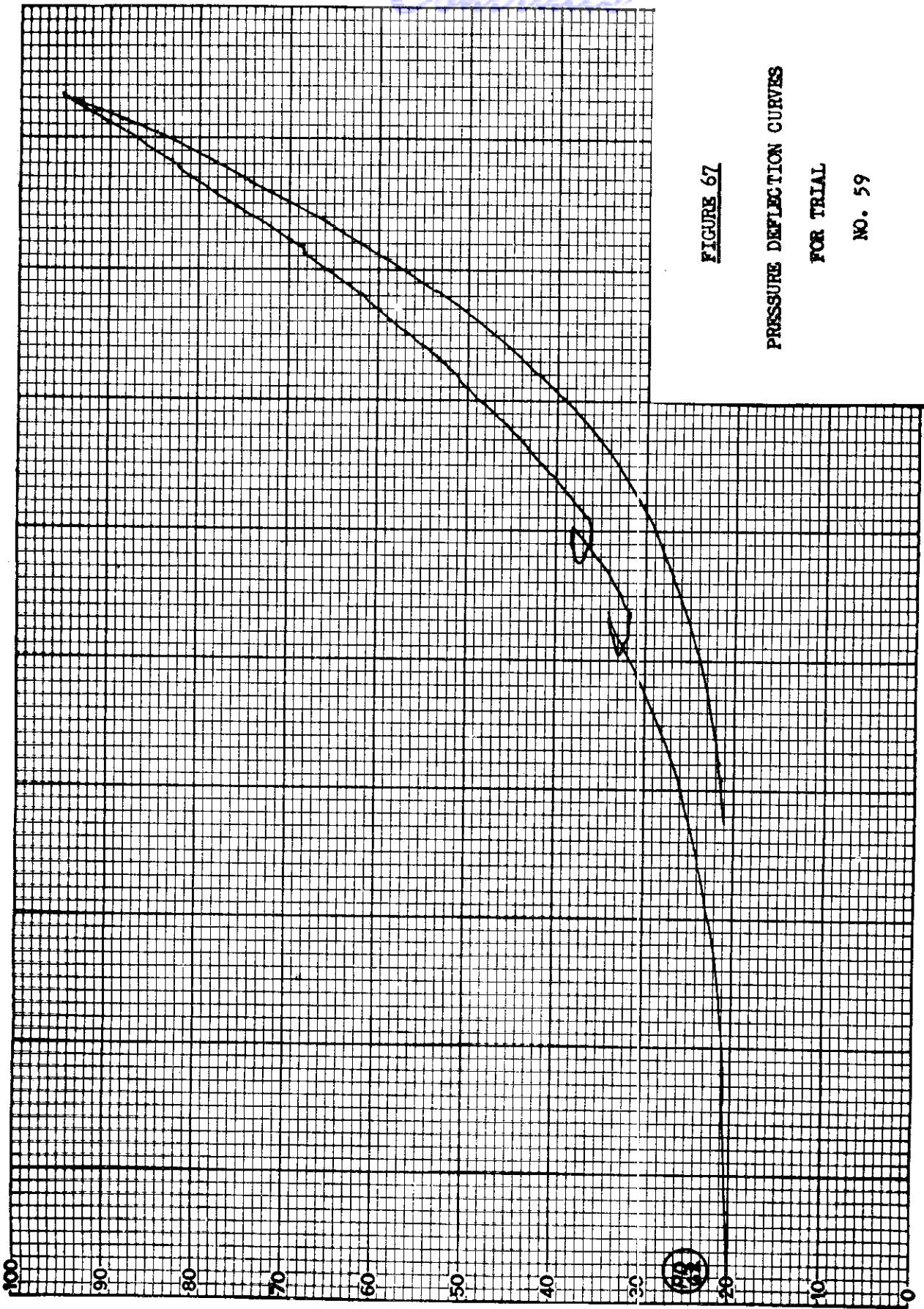


FIGURE 67

PRESSURE DEFLECTION CURVES

FOR TRIAL

NO. 59

DEFLECTION

*Continued*

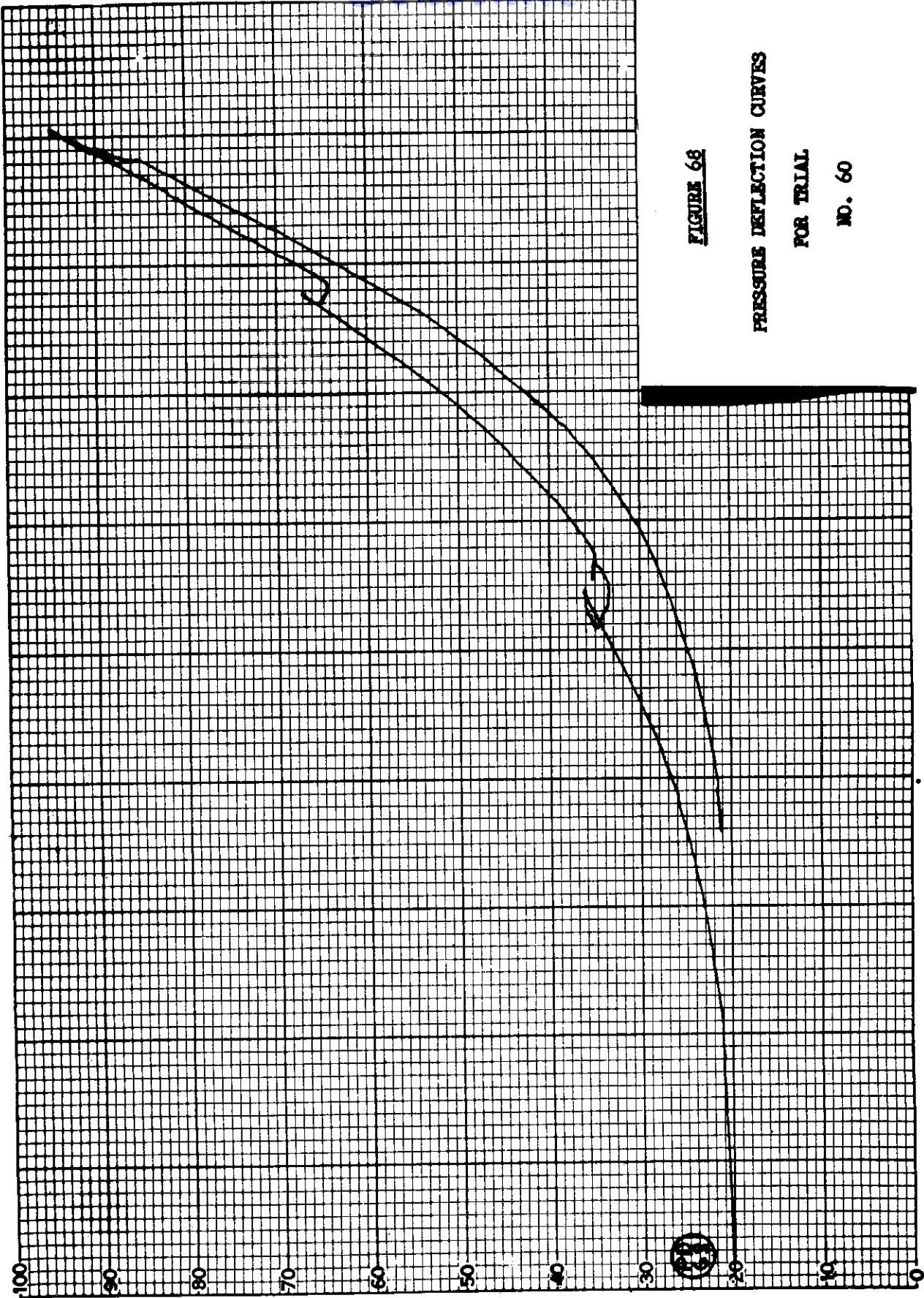


FIGURE 68

PRESSURE DEFLECTION CURVES

FOR TRIAL

NO. 60

DEFLECTION

*Continued*

This same dependence of the results on the fastening method is demonstrated by comparing the results of trials 5 thru 10. These panels were installed as Type III backing boards. The effect of changing the number of fasteners on trials 9 and 10 can be seen by noting the decreased deflection of these panels compared with trials 5 thru 8. The spacing of fasteners was reduced to two inches on the outer hat sections of trials 9 and 10 by adding two fasteners between the regularly spaced fasteners.

Trials numbered 11 thru 52 compare the five test materials installed as Type III backing boards. Tests were made on each material with hat section spacings of 6, 8, 10, and 12 inches using both self-sealing, and bladder type fuel cells.

Trials numbered 53 thru 60 indicate the reproducibility of the test method. It can be seen that the curves for the most part are quite similar. However, it is evident that trials 54, 58, and 59 have noticeably greater deflections for given pressures than the rest of the series. Discussion of this variability will be delayed until a further description of the method used to analyze the data is presented.

### ANALYTICAL METHODS

The previously stated purpose of the pressure-deflection testing involved the determination of empirical equations to fit the pressure-deflection curves obtained from the test jig. These equations would satisfy two needs. One, provide a means of extrapolating experimental data. Two, relate certain properties of the test materials to their deflection under load characteristics. It was desired to examine this type of information as a basis for specifying a backing board construction for service uses. It is known that the serviceability of a backing board is related to its ability to support the fuel cell under various conditions of loading and also have maximum resistance to gunfire damage. In the cases where resistance to gunfire is part of the specification, this property would have to be the primary consideration.

The entire work of this program was undertaken with the understanding that certain variables in the installation of backing board materials for fuel cells, such as the type and number of fasteners which hold the material to the air frame, are of extreme significance to the performance of any given material in service. However, it seemed expedient to hold the number of experimental cases to a minimum by varying only what seemed to be the most influential variables.

To accomplish this end, the pressure-deflection testing was arranged to examine the effect of backing boards with widely different constructions and properties. The variables of air frame construction chosen for investigation were, the spacing across which the boards would be installed, and the pressures that might be exerted by the fuel cell in service.

Other variables that are undoubtedly important in performance but whose effects were minimized include the elasticity of the foundation and the type



and distribution of the fasteners. In this investigation these factors were standardized about an essentially inelastic hat section or support, characterized in the equipment by the solid steel hat sections mounted on the one inch steel test frame. The fastening system described in Appendix II, page 109, is common in the aircraft industry and also used for gunfire and qualification testing.

The problem of relating the deflection that occurs in a backing board material subjected to fluid pressures through a fuel cell construction, to its mechanical properties, is essentially one of a plate subjected to normal fluid pressures. References 1 thru 10, page 131, relate to much of the analysis that has been done on this subject.

It is known that the deflection of a plate within its elastic limits occurs in two essential modes. In the first, the deflections at the center are small in comparison with the thickness of the plate and similar to the bending of a beam. In the second, the deflection grows large with respect to the thickness and the action is similar to the stretching of a membrane.

The classical conditions which apply to the tests under analysis here are not well defined, in that the backing board may not be classified as a simply supported plate, but rather a combination of simply supported and built in edge. In addition, the distribution of stresses involved in the rivet like manner of fastening and the plastic qualities of the materials, in the pressure ranges of interest, pose problems of straightforward analysis beyond the scope of this work.

The equations of Table V, page 94, were devised to provide an analytical means of comparing the reactions of the five backing board materials to various test conditions. Also, it was intended to compare the different properties of the test materials under the same test conditions. These equations are essentially empirical expressions relating the deflection of the backing board material at the center of the test span to the fluid pressure that produced this deflection.

The equations are polynomial expressions patterned after the solutions to differential equations which describe the deflection at the center of thin plates subjected to fluid pressures to produce large deflections. The classical meaning of large deflections is employed, where deflections of the plate in excess of three to five times their thickness is classified as a large deflection. This is in opposition with the term as employed in the analysis of beams, where the deflection is generally a small fraction of the thickness of the test material.

The manner in which the equations of Table V, were developed is given in the discussion that follows. Timoshenko, Reference 1, and Den Hartog, Reference 10, have indicated expressions for solutions of the basic differential equations for the bending of plates, which approximate the action of plates subjected to lateral uniform loads to produce large deflections.

# Contrails

These equations have the general form:

$$(1) P = \frac{Eh^3}{a^4} (Aw + \frac{Bw^3}{h^2})$$

Where:

- P - The lateral Load (psi)
- E - Modulus of Elasticity (psi)
- a - One-half the shorter dimension of a rectangular plate - taken here as one-half the hat section spacing (in.)
- h - The thickness of the plate (in.)
- w - The deflection at the center of the span (in.)
- A & B - Constants that depend on the properties of the plate, and the boundary conditions or fastening system.

This combines the equations for bending of a plate with small deflections, and the stretching of a membrane under uniform lateral loads.

The first term of equation (1) is significant when the deflection w is small and the bending moments of the panel at the center and at the fastened edges resist the loading. The second term becomes increasingly significant as the deflections become large. This suggests that in the initial stages of loading a linear relation exists between load and deflection, but that these parameters are cubically related as the deflections become large.

To examine the pressure deflection data for such action curves of the data were plotted on logarithmic paper to examine the power relationship of w and p in the early and final stages of loading. This showed the pressure deflection relationship to have linear tendencies in the initial stages reverting to a near cubical relationship as the deflections become large. An equation of the form:

$$(2) P = Aw + Bw^3$$

can be fitted to the data of Trial No. 11. This equation is found to be:

$$(3) P = 7.84 w + 181 w^3$$

## SAMPLE CALCULATIONS

The pressure (p) and deflection (w) data from the stress strain curves were used to develop equations. Reading from the stress strain chart at .05 inch intervals in the w direction, the corresponding values of p are read on the p-w curve and these pairs of values are plotted on

# Contrails

logarithmic paper. The properties of the line through the plotted points reveal much about the nature of the p-w curve.

For the derivation of equations the "method of averages" was used, whereby values of the rectifying functions, arranged in ascending order with respect to w, were divided into two sets containing approximately the same number of pairs of values. Equations of the form  $P = Aw + Bw^3$  were fitted to the data by substituting values of p and w, giving as many linear equations in two unknowns, A and B, as there are pairs of values of p and w.

## DATA

<u>W (in)</u>	<u>P (lbs)</u>
.20	2.96
.25	4.71
.30	7.21
.35	10.71
.40	15.71
.45	21.46

Substituting these values into equations as in (2), the following 6 equations are obtained:

$$(4) \quad 2.96 = .20 A + .008 B$$

$$(5) \quad 4.71 = .25 A + .016 B$$

$$(6) \quad 7.21 = .30 A + .027 B$$

---

$$(7) \quad 10.71 = .35 A + .043 B$$

$$(8) \quad 15.71 = .40 A + .064 B$$

$$(9) \quad 21.46 = .45 A + .091 B$$

The three equations in each group are added, resulting in the two summation equations:

$$(10) \quad 14.88 = .75 A + .051 B$$

$$(11) \quad 47.88 = 1.20 A + .198 B$$

---

which solved simultaneously for A and B, yield

$$A = 5.77$$

$$B = 209$$

# Contrails

The percent deviation between the values calculated by the equation and the experimental values shows the manner in which the equation fits the data.

<u>w</u>	<u>% Deviation of p</u>
.20	- 4.19
.25	- .40
.30	1.80
.35	1.77
.40	- 1.11
.45	- .39

From .10 - .20 deflection, the linear equations

$$(12) \quad p = 20w - 1.04$$

fits the curve within readable limits. An equation of the form

$$(13) \quad p = aw^b$$

expresses the relationship between w and p satisfactorily in the region where the membrane effect dominates the deflection.

Taking log of both sides of (5), we have:

$$(14) \quad \log p = \log a + b \log w$$

which is linear in log p and log w. That means that p and w form a straight line when plotted on full logarithmic paper. This effect is produced by plotting any of the pressure deflection curves on logarithmic paper.

Taking the log of the set of values in the data of page 91, we obtain the following equations:

$$(15) \quad a. \quad .474 = \log a - .699 b$$

$$(16) \quad .674 = \log a - .602 b$$

$$(17) \quad .858 = \log a - .523 b$$

---

$$(18) \quad b. \quad 1.030 = \log a - .456 b$$

$$(19) \quad 1.196 = \log a - .398 b$$

$$(20) \quad 1.332 = \log a - .347 b$$

---

*Calculations*

solving the two summation equations

$$(21) \quad 2.004 = 3 \log a - 1.8246$$

$$(22) \quad 3.558 = 3 \log a - 1.2016$$

---

for a and b, they yield

$$a = 152$$

$$b = 2.49$$

giving the equation:

$$(23) \quad p = 152 w^{2.49}$$

The percent deviation table shows:

<u>w</u>	<u>% Deviation in p</u>
.20	- 7.09
.25	+ 2.34
.30	+ 5.13
.35	+ 4.01
.40	- 1.34
.45	- 2.98

Equations for all the test panels of Table IV were developed in the form of Equation (2). These are listed in Table V, page 94.

#### SUMMARY DISCUSSION

Comparison of action of the materials evaluated under the pressure deflection test conditions by means of the equations of Table V, with the physical properties of these materials given in Table VIII, is the basis for judging the correlation of these two sets of information.

The reliability of the pressure deflection data is illustrated by the repetitive tests in the design of the pressure-deflection experiment, particularly tests numbered 53 through 60. The variation existing in this data will be discussed in detail. However, it must be emphasized that the normal variation of the dimensions and physical properties of the non-homogenous constructions of the backing board materials, certainly contributes in part to variations in test results.

The matter of variability of physical properties is illustrated in the data of Table VII, page 118, for two thickness ranges of USV CR 88 backing board. The wide variations exhibited here are attributed in part to the normal causes, such as placement and relative amounts of high strength fabric with lower order strength resin. More particularly however, in the

*Contrails*  
TABLE V

PRESSURE DEFLECTION EQUATIONS

<u>NO.</u>	<u>CODE</u>	<u>PANEL</u>	<u>STRESS STRAIN CURVE (FIGURE)</u>	<u>EQUATION</u>	<u>EQUATION RANGE</u>
1	PD-2	USV 747-5	17	$p - 11.4 w / 218 w^3$ $p - 13.8 w / 244 w^3$ $p - 13.2 w / 249 w^3$	.05 - .40 .05 - .40 .05 - .40
2	PD-3	USV 747-5	18	$p - 13.7 w / 290 w^3$	.05 - .35
3	PD-10	USV 747-5	19	$p - 5.51 w / 95.8 w^3$	.10 - .30
4	PD-11	USV 747-5	20	$p - 9.72 w / 63.3 w^3$	.10 - .35
5	PD-52	USV CR 88	21	$p - 2.30 w / 26.7 w^3$	.25 - .35
6	PD-53	USV CR 88	22	$p - .32 w / 22.7 w^3$	.35 - .45
7	PD-50	USV 33	23	$p - 2.30 w / 26.7 w^3$	.25 - .35
8	PD-51	USV 33	24	$p - .50 w / 19.1 w^3$	.35 - .45
9	PD-55	USV CR 88	25	$p - 1.10 w / 49.1 w^3$	.25 - .50
10	PD-54	USV 33	26	$p - 1.64 w / 42.4 w^3$	.25 - .50
11	PD-4	USV 747-5	27	$p - 7.84 w / 181 w^3$	.05 - .40
12	PD-6	USV CR 88	27	$p - 1.84 w / 170 w^3$	.15 - .45
13	PD-5	USV 55A	27	$p - -.10 w / 136 w^3$	.20 - .45

*Continued*  
TABLE V (Cont.)

PRESSURE DEFLECTION EQUATIONS

<u>NO.</u>	<u>CODE</u>	<u>PANEL</u>	<u>STRESS STRAIN CURVE (FIGURE)</u>	<u>EQUATION</u>	<u>EQUATION RANGE</u>
14	PD-9	USV 33	28	$p = -.68 w / 130 w^3$	.20 - .40
15	PD-8	S 2N	28	$p = -2.86 w / 30.4 w^3$	.40 - .90
16	PD-7	S 3N	27	$p = -.51 w / 61.0 w^3$	.25 - .70
17	PD-14	USV 747-5	29	$p = 4.77 w / 159 w^3$	.05 - .55
18	PD-17	USV CR 88	30	$p = -1.25 w / 122 w^3$	.15 - .65
19	PD-16	USV 55A	29	$p = 2.08 w / 147 w^3$	.10 - .60
20	PD-15	USV 33	29	$p = -1.42 w / 100 w^3$	.15 - .70
21	PD-18	S 2N	30	$p = -2.72 w / 58 w^3$	.25 - .85
22	PD-38	USV 747-5	31	$p = 3.76 w / 50.2 w^3$	.15 - .50
23	PD-39	USV CR 88	32	$p = -1.65 w / 26.3 w^3$	.40 - .50
24	PD-40	USV 55A	33	$p = 1.39 w / 38.6 w^3$	.25 - .40
25	PD-41	USV 33	34	$p = .86 w / 46.1 w^3$	.30 - .45
26	PD-42	S 2N	35	$p = .68 w / 9.62 w^3$	.50 - 1.10
27	PD-19	USV 747-5	36	$p = 6.21 w / 67.5 w^3$	.05 - .50

*Contrails*  
TABLE V (Cont.)

PRESSURE DEFLECTION EQUATIONS

<u>NO.</u>	<u>CODE</u>	<u>PANEL</u>	<u>STRESS STRAIN CURVE (FIGURE)</u>	<u>EQUATION</u>	<u>EQUATION RANGE</u>
28	PD-21	USV CR 88	37	$p - -2.87 w / 31.6 w^3$	.35 - .65
29	PD-20	USV 55A	36	$p - 1.96 w / 43.1 w^3$	.15 - .45
30	PD-23	USV 33	38	$p - -1.03 w / 46.3 w^3$	.25 - .40
31	PD-22	S 2N	39	$p - - .91 w / 18.5 w^3$	.30 - 1.00
32	PD-43	USV 747-5	40	$p - .53 w / 19.2 w^3$	.30 - .55
33	PD-44	USV CR 88	41	$p - - .30 w / 10.8 w^3$	.45 - .75
34	PD-45	USV 55A	42	$p - - .39 w / 13.1 w^3$	.40 - .65
35	PD-46	USV 33	43	$p - .89 w / 6.1 w^3$	.45 - .60
36	PD-47	S 2N	44	$p - -1.02 w / 5.1 w^3$	.60 - 1.50
37	PD-24	USV 747-5	45	$p - 2.68 w / 27.0 w^3$	.15 - .70
38	PD-26	USV CR 88	46	$p - .37 w / 19.7 w^3$	.30 - .80
39	PD-25	USV 55A	47	$p - -1.44 w / 22.1 w^3$	.30 - 1.10
40	PD-27	USV 33	48	$p - -1.09 w / 12.0 w^3$	.45 - .75
41	PD-28	S 2N	49	$p - -2.23 w / 9.0 w^3$	.50 - 1.40



*Continued*  
TABLE V (Cont.)

PRESSURE DEFLECTION EQUATIONS

<u>NO.</u>	<u>CODE</u>	<u>PANEL</u>	<u>STRESS STRAIN CURVE (FIGURE)</u>	<u>EQUATION</u>	<u>EQUATION RANGE</u>
42	PD-34	USV 747-5	50	$p - 1.24 w / 9.75 w^3$	.35 - .75
43	PD-49	USV 747-5	51	$p - 2.52 w / 10.3 w^3$	.30 - .65
44	PD-35	USV CR 88	52	$p - 4.71 w / 1.82 w^3$	.15 - .30
45	PD-36	USV 55A	53	$p - .53 w / 7.89 w^3$	.50 - .70
46	PD-37	USV 33	54	$p - .17 w / 5.12 w^3$	.50 - .60
47	PD-48	S 2N	55	$p - .01 w / 3.47 w^3$	.60 - 1.20
48	PD-29	USV 747-5	56	$p - 1.17 w / 12.7 w^3$	.25 - .75
49	PD-30	USV CR 88	57	$p - 3.11 w / 6.9 w^3$	.20 - .55
50	PD-31	USV 55A	58	$p - .42 w / 6.8 w^3$	.40 - .85
51	PD-32	USV 33	59	$p - .04 w / 7.3 w^3$	.40 - .55
52	PD-33	S 2N	60	$p - -1.03 w / 3.32 w^3$	.70 - 1.30
53	PD-56	USV 747-5	61	$p - 3.13 w / 44.1 w^3$	.15 - .50
54	PD-57	USV 747-5	62	$p - .30 w / 34.2 w^3$	.20 - .55
55	PD-58	USV 747-5	63	$p - 1.04 w / 57.0 w^3$	.15 - .50

*Continued*  
TABLE V (Cont.)

PRESSURE DEFLECTION EQUATIONS

<u>NO.</u>	<u>CODE</u>	<u>PANEL</u>	<u>STRESS STRAIN CURVE (FIGURE)</u>	<u>EQUATION</u>	<u>EQUATION RANGE</u>
56	PD-59	USV 747-5	64	$p - 1.68 w / 56.0 w^3$	.15 - .55
57	PD-60	USV 747-5	65	$p - 1.85 w / 48.7 w^3$	.15 - .50
58	PD-61	USV 747-5	66	$p - .26 w / 45.7 w^3$	.20 - .50
59	PD-62	USV 747-5	67	$p - .26 w / 45.7 w^3$	.20 - .50
60	PD-63	USV 747-5	68	$p - .17 w / 50.9 w^3$	.20 - .50

case of the USV CR 88 construction, it is evident, that the greater departure from homogeneity represented in this construction by virtue of the wide spacings of the rovings and large areas of non-reinforced resin, contributes to wide variation in physical property tests that are made with conventional sample sizes and test methods.

For these reasons, the correlation of pressure deflection tests with physical property data, presents at the outset, a problem of considerable magnitude. However, with some consideration of this effect, the two sets of data seem to have a firm bearing on one another, which will be brought out in the discussion that follows.

The objectives of the pressure deflection testing included examination of the effect of various spans of support on the supporting properties of the materials. Although a standard fastening system was generally used, the examples for pressure deflection trials 8 and 9, of Table IV, where the outer hat section fasteners were spaced two inches apart, rather than 6 inches, show a discernible effect produced by this variation. These stated objectives were also to be examined with pressure applied through a heavy self-sealing fuel cell construction, and a lighter bladder cell construction.

Before proceeding with definite statements regarding the test results, the examination of several aspects of the form of the equations of Table V may be helpful.

The solutions to the differential equations that describe the action of plates subjected to fluid loads, Equation (1), page 90, relates to specific boundary conditions, such as the manner of fastening the edge of the test plate. In general, the restriction which was placed on the development of Equation (1), states that only two methods of support were applicable. One, a simply supported edge, free to rotate about the point of contact, or two, a built in edge, absolutely restrained from rotation beyond the point of edge contact away from the deflecting center of the plate. In both of these cases, slippage, or movement of the plate on its support, toward the center of support was negated.

To examine the validity with which the general form of the equations expresses the action of the test, attention is again directed to Equation (1), page 90. This form implies a fourth power reciprocal relationship between the pressures required to produce deflection and the span over which this deflection occurs. If the coefficients for the cubical deflection terms of equations, which represent its pressure deflection over 6, 8, 10, and 12 inch spans, are plotted for a given material, it is apparent that these factors have approximately a fourth power relationship. This is most easily observed by plotting the coefficients for the various spans against the span values on logarithmic paper. The average slope of this plot gives the power relationship of the terms. This has been found to vary considerably, particularly in the span from 6 to 8 inches. Again it must be assumed that other parameters are involved which are not accounted for in the present form of the equation.

If expressions of the form of Equation (1) fitted the data exactly, it would be possible to deduce from experimental data, constants for the deflection terms which would apply to all materials in a general way. This can be done by introducing into the specific equation for a given material, the values which represent the parameters, such as the test span, the thickness of the material, and the elastic modulus of the material.

It is convenient to choose two sets of data for the five materials; one, the pressure deflection curves for the self-sealing cell and six inch span; and two, the self-sealing cell and eight inch span. Equating the product of some constant B and the value of  $\frac{Eh}{a^4}$  with the co-

efficient of the cubical terms for the equations of trials 17, 18, 19, 20, 21, and trials 27, 28, 29, 30, 31, results in a specific value for this constant B for each of the equations. E represents the elastic modulus, h the thickness, and (a) one-half the test span, as on page 90. If the form of the equation represented the test exactly, constant B would have the same value for all the equations.

Performing the computations described above, the value for B for each of the trials mentioned is found to be approximately:

<u>Trials</u>	<u>Constant B</u>	<u>Trials</u>	<u>Constant B</u>
17	.18	27	.24
18	.16	28	.13
19	.15	29	.14
20	.16	30	.23
21	.69	31	.69

This shows that constant B in the equations representing the materials USV 747-5, USV CR 88, USV 55A, and USV 33, all essentially high strength low elongation constructions, is reasonably the same for each case. This is more striking in the case of the six inch span than the eight inch span. Undoubtedly as the span is increased, the effects of bearing failure and other parameters not accounted for in the form of the equations play a greater part. The value of constant B for the high elongation nylon board shows great departure from the other types.

In computing the constants B, above, the value of one-half the test span was taken as one-half the center to center spacing of the hat sections. Using the edge separation distances as the span length would not change the comparative value of the figures, although in more detailed work it is obvious that some study would be required to establish the effective span relationship for this type of test.

*Continued*

It was stated previously, that the linear deflection term of the equation was intended to account for the flexural resistance of the materials during deflection. As in the case of the cubical coefficients, these linear term coefficients follow a general pattern dependent upon the properties of the material. They are consistently highest for the equations describing materials with the greatest gross flexural strength, or stiffness, and lowest for the most flexible panels.

In many instances this linear deflection term coefficient of the equations has a negative sign. This is not physically explainable by reference to the equations, since it would mean that the flexural resistance of the bending at the supports was actually contributing to the deflection. This is obviously not physically true because the stiffness of the board has been shown to be important in reducing the deflection under load. This again is the result of forcing the data to fit an equation which does not take into account all the significant parameters.

In this connection, it should be noted that the effect of a slackness or looseness of the backing board across the supports at the start of a test, would result in a stress strain curve having a large amount of deflection under low pressurization at the outset. The subsequent tightening of the board would then produce a deflection pattern similar to that of a board of the same material which did not have this initial looseness. Fitting equations to these two trials would then present the following difficulty. The equation fitted to the stress strain curve with the large initial deflection would not physically represent the data, since no provision was made in the form of the equation to account for the initial tension conditions of the installation. This would result in a negative coefficient for the first deflection term to bring the value of the cubical term into conformance with the low pressures exerted in the initial portion of the deflection. The subsequent higher order of the cubical or membrane term, as the deflections become larger, would then reduce the effect of this negative term, resulting in an equation which would fit the limits with the desired accuracy.

In the same way, the equation resulting from fitting the data for the same type of board, without an initial looseness across the supports, would result in a form more nearly in agreement with the boundary conditions established for the general case. This equation would have a positive coefficient for the bending term and physical compatibility with the known effects. This situation in which the initial tension of the board across the supports greatly affects the analytical results, has obviously affected the equations on which this analysis was based. An initial looseness in the installation that resulted in a center deflection of as little as .050 inches at the center, under small loads, would be represented by approximately reducing the value of the linear deflection term coefficient by three. In the materials tested, two effects were additive in causing stress strain curves which required

*Conclusions*

negative coefficients for the deflection equations. First, the backing boards with the lowest gross flexural stiffness, were generally the most difficult to install on the test device in a uniform manner. This is to be contrasted with the equations for the USV 747-5 boards. Here, the physical structures of the board lends itself to a uniform installation because of its stiffness and flatness, and the deflection equations have positive values. In the more flexible, less uniformly flat boards, the negative deflection terms appear in the equations, becoming more predominant as the larger spans are used, where the difficulties of installation are increased.

Much information relating to the objectives of the work can be had by referring to the test results of the pressure deflection trials without resorting to specific property comparison.

It should be said, that the method of testing the support properties, produced results which illustrated the interaction of effects for which no specific cognizance was taken in the analysis. For example, testing was performed by recording the deflection at the center span, of a series of spans across the test piece. It was apparent in viewing the tests that much greater deflections were occurring in the hat section spacings on either side of the test area. In general, these were symmetrical amounts greater than at the central measuring position. However, since definite deflection measurements were taken only at the central hat section spacing, in the majority of tests, it can only be suggested that the decided differences in the stress strain curves obtained at various hat section spacings across the test panel, as illustrated by the three curves of Figure 18, would also exist in the general bulk of the data.

It is suggested that measurements of the kind illustrated in the stress strain curves of Figures 17 and 18, page 36 and 37, would be very useful in determining the elongation experienced by the fuel cell, in deflecting with the backing board during pressurization. It is obvious from Figure 17, that the measurements of deflection at the center of hat sections near the edge of the panel are greater than for center of the panel, where the additive resistance of fasteners on the hat sections on either side reduce the deflection. Measurement at the edges of the test panels is suggested for further work to establish the pressure conditions necessary to produce given elongations of the fuel cell supported by the backing board materials. The measurements taken at the center sections in the majority of this work, represent the minimum strain experienced by the panels. A more definite establishment of the relationship of this suspected action on either side of the center position should be examined in a more detailed study. Its effect in this work can only be mentioned as a possible parameter that was not considered in detail, except in trials 9 and 10. The stress strain curves of trials 9 and 10 show the increased resistance to

*Contrails*

deflection with additional fasteners, as compared to the regular test, trials 23 and 25.

Examination of the test panels, established that bearing failure actually did occur in the course of pressurization, permitting the original edge supports of the spans to slide toward each other. This would necessarily imply that the equations used to describe the pressure deflection data, patterned after Equation (1), would not be exact. However, in examining the results, it is obvious that the equations do describe and differentiate between various backing board constructions tested in a given manner. For example, the equations for trials 17, 18, 19, 20, and 21, show a descending value for the coefficients of the cubical terms in the order named. This same order with one exception exists for similar tests using the bladder type cell, rather than the self-sealing cell. See equations for trials 11, 12, 13, 14, and 15.

In comparable tests on the five materials using two types of fuel cells, it appears that the general mechanical properties of the boards influences the data sufficiently to permit identification of the material on the basis of its test performance. In these two sets of data the backing board with the greatest stiffness, highest resistance to bearing failure, and highest gross tensile strength gives a pressure deflection curve whose deflection term constants are highest in the group. This is true of the USV 747-5 backing board in all the pressure deflection trials. In comparison, the S 2N backing material with the lowest flexural rigidity, and lowest tensile strength, in the elongation ranges experienced by the deflecting panels, gives a pressure deflection history whose equation shows the lowest deflection term coefficients.

Unfortunately the interplay of properties over the range of spans used for testing does not result in a clear cut order of materials in between the extremes of the USV 747-5 and the S 2N boards. For example, the USV 55A material of trial 19 gives a pressure deflection history showing greater resistance to deflection than the USV CR 88 material of trial 18, with the self-sealing cell. Whereas the order of strength is reversed in the tests using the bladder type cells in examples 12 and 13. In examining the gross flexural, bearing, and tensile properties of the two materials, this action is difficult to explain. By virtue of its lower ultimate elongation, the USV 55A material would be expected to approach its maximum in all properties before the USV CR 88 material under similar conditions of strain. However, the greater deflection of the backing board and cell into the hat sections on either side of the central measuring position could conceivably bring about a firmer fastening condition at the center hat sections for the USV CR 88 material. This would result in a lesser deflection in this area, for a weaker material, because of less slippage at the supports.

*Conclusions*

The validity of such an explanation would require the measurement of the lateral displacement of the backing materials simultaneously with the deflections at the center of the span.

It is clear that the ultimate strength values generally obtained in mechanical properties tests contribute little to an evaluation of this type, where in general the strains occurring during the test, do not produce stresses exceeding the ultimate values of the materials. In general the discussions of this report make use of the ultimate elongation as an indication of the rate at which a material would approach its ultimate strength in tension, flexure, and bearing. This is the suggested explanation for the high deflections of the nylon construction which has tensile and bearing strengths very comparable to the constructions offering the most support.

Noticeable differences in the support offered by the test materials with self-sealing and bladder type fuel cells can be recognized throughout the test program. With some exceptions, the deflection of a given backing board material with a heavy self-sealing fuel cell backing is noticeably less under identical pressures than with the lighter bladder cell constructions. This is evidenced in the equations by higher values for the deflection coefficients in the trials where bladder cells were used, compared with trials using self-sealing cells. This is taken to mean that the higher tensile properties of the self-sealing cell, reinforces the resisting effects of the backing board to deflection.

Trials 53 through 60 show the variation that occurs in a series of tests representative of the methods used throughout the pressure deflection testing. By examining the equations for these tests in Table V, it appears that decided variations are inherent in the method, using the material most capable of repetitive installation.

The stress strain curves of these trials show that fastening failures appear at more uniform loads and strains, than the shape of the curve might suggest. In this series, the range of loads to cause failure is 6.50 to 9.00 pounds per square inch, while the range of deflections is from .520 to .570 inches. Fastening failure is indicated on the pressure deflection curves by sharp breaks in the curve with sudden deflections at the point of measurement. The greater uniformity of failure with elongation illustrated in these examples should be investigated in further work.

It would seem that two avenues are available in proceeding further with this work. First, it would be possible by proper design of test equipment to eliminate in great part the variation of tension across the supports. The mounted panels would then more nearly represent the boundary conditions for which analytical solutions to the problem of large deflections in plates is known, or good approximate solutions available. Second, it would seem more practicable in the end, to



analytically take this type of variation into account, in the design of the equations used to express the action of the backing board under test. Other factors of this same character, such as the deflection resulting from bearing failure, would naturally also have to be treated in the design of a proper equation.

The variations which have effected the results of this work, will also be present in actual service installations to some degree. For this reason, it might be argued that the analytical results would be reasonable without further refinement as a means of examining backing board support properties. This argument would apply of course, only to those variations such as drupe of the board between the hat section supports. The parameters which apply to the rate at which the strength properties of the materials, such as bearing strength, tensile strength, and flexural strength, approach their maximum values, and the interaction of these effects, would certainly need to be accounted for in a more rigorous analysis.

### CONCLUSIONS

#### GUNFIRE DAMAGE SIMULATION

#### INTERNAL EXPLOSION TEST

1. The internal explosion test at its present state of development, is capable of indicating variations in gunfire resistance of backing board materials, but to a lesser degree than gunfire tests. Greater concentration of the forces of the explosions should correct this deficiency.
2. The large test panel and jig used for internal explosion tests did not appear to add to the capability of the test sufficiently to warrant its use over a smaller test device. It served merely to show that the wide spread effects of the explosion, such as shearing at hat section supports and bearing failure at fastening points duplicated gunfire tests.
3. Complete simulation of gunfire damage to fuel cell backing boards was not achieved in this work. It is believed that further improvements in methods would result in a satisfactory test.
4. The internal explosion tests were not sensitive to the depth of the explosion in the fluid as the actual gunfire tests are known to be.
5. The use of actual air frame constructions for internal explosion testing in the form of aluminum hat sections and supports results in an expensive destructive type test method. It was established that the elasticity and resiliency of the test frame affects the results.

6. Shock absorbing pads such as U. S. Rubber Company "Ensolute", a unicellular, lightweight plastic foam material, placed between the fuel cell wall and the backing board test panel, was effective in reducing damage to the backing board in internal explosion tests.

It is recommended that a smaller test jig be used for the internal explosion method for simulating gunfire damage to backing board materials of fuel cells, similar to that described in WADC Technical Report 54-474 Part I. Further, that methods of concentrating the shock waves of the internal explosion technique be employed to localize damage in the simulated wound area. It is suggested that this may be accomplished by the use of reflection devices in the fluid, or shaped explosive charges.

Further work is recommended on the useful shape, size, and location of a simulated wound for internal explosion testing.

#### SUPPORT CHARACTERISTICS

#### PRESSURE DEFLECTION TESTING

1. The number and spacing of fasteners definitely affects the supporting ability of fuel cell backing board materials. In this regard, it is probable that frictional differences between support members, backing board, and fuel cell walls also have an appreciable effect on the deflection under load.

It is recommended that further work be done to ascertain the most suitable type and spacing of fasteners to provide maximum support consistent with optimum resistance to gunfire damage.

2. Heavy fuel cell constructions contribute appreciably to the supporting ability of the backing board with which they are used.
3. Stress strain curves of the type produced for evaluation of the support of backing board materials are useful in determining the deflections that may be expected in given installations and also the loads which are required to cause initial failure at fastening points.

It is recommended that the points of deflection measurement be increased to include all the hat sections in further work. This will permit evaluation of fuel cell elongations and other effects which were not maximum at the central sections of the test panels, by reference to the pressure deflection curves taken in areas of maximum deflections.

4. The general design of the pressure deflection test is quite adequate for producing stress strain curves.
5. The equations developed to represent the deflection of the backing material under fluid pressure loads, is useful in

*Continued*  
examining the support properties of various materials. These equations are also useful for extrapolating beyond the limits of pressure and deflection for which they were constructed.

6. The form of the equations used to describe the action of the test panels neglects the effects of the initial condition of the test panel across the supports and the effects ascribed to bearing failure.

It is recommended that a more exact solution for the equation representing the deflection of the test panels be devised which accounts for initial slackness of the material across the test supports and the increased elongations resulting from bearing failure of the material at the fastening points.

*Contrails*  
APPENDIX I

BACKING BOARD TEST MATERIALS

Six backing board test materials were chosen for evaluation by the test procedures of the report. These include; all Nylon constructions, all glasscloth with polyester resin impregnation, combination of glasscloth and cotton duck fabrics with polyester impregnation, and all Dacron construction.

This group included boards designed for Type I, Type II and Type III installation, as described in USAF Specification MIL-P-8045.

The all Dacron construction backing board was ordered from the Russel Reinforced Plastics Company. However, this material could not be delivered in time to be included in the evaluation. The description of the backing board materials included in the test program is given in Table VI below. It should be noted that the USV CR 88 materials consisted of laboratory and production types with some differences in properties. See Appendix VI, page 129, for details of this material.

TABLE VI

IDENTIFICATION OF BACKING BOARD TEST MATERIALS

<u>CODE</u>	<u>MANUFACTURER</u>	<u>FABRIC</u>	<u>RESIN</u>	<u>GAGE</u>	<u>WEIGHT</u>	<u>TYPE</u>
USV 747-5	U.S. Rubber	Fiber-glass & Duck	Polyester	.065"	0.47 #/FT. <sup>2</sup>	I
USV CR 88 Laboratory	U.S. Rubber	Glass-cloth rovings	Polyester	.065	0.44	III
USV CR 88 Production	U.S. Rubber	Glass-cloth rovings	Polyester	.035	0.31	III
USV 55A	U.S. Rubber	Glass-cloth	Polyester	.047	0.35	II
USV 33	U.S. Rubber	Glass-cloth	Polyester	.029	0.23	II
S 2N	Swedlow	Nylon	Nylon	.050	0.24	II
S 3N	Swedlow	Nylon	Nylon	.075	0.36	II

FUEL CELL BACKING BOARD INSTALLATION  
IN THE AIRFRAME INDUSTRY

Conferences were arranged with the aircraft engineering personnel of a representative group of aircraft manufacturers. The purpose of these conferences was to survey the problems of fuel cell backing board installation in aircraft and solicit suggestions regarding test procedures. The design of the work of this report was influenced in a great part by the many helpful suggestions offered by the aircraft industry.

The following conferences were held with the engineering representatives of the air frame manufacturers:

BOEING AIRCRAFT CO. 21, 22 June 1954	Wichita, Kansas
C. R. Strauss	Boeing Power Plant Engineering
D. Nordstrom	" " " "
J. Lynch	U. S. Rubber Co. Fuel Cell Engineering
C. C. Surland	U. S. Rubber Co. Divisional Development Laboratories
W. H. Smith	U. S. Rubber Co. Divisional Development Laboratories
NORTH AMERICAN AVIATION CO. 23 June 1954	Los Angeles, California
W. Kelso	Power Plant Engineering
W. Bratfish	" " "
J. Moran	" " "
T. Wise	U. S. Rubber Co. Fuel Cell Engineering
C. McElderry	" " " " " " "
C. C. Surland	U. S. Rubber Co. Divisional Development Laboratories
W. H. Smith	U. S. Rubber Co. Divisional Development Laboratories
DOUGLAS AVIATION CO. 24 June 1954	<sup>d</sup> El Segundo, California
C. Michel	Power Plant Engineering
G. McGhee	" " "
W. Judson	" " "

# Contrails

T. Wise	U. S. Rubber Co. Fuel Cell Engineering
C. McElderry	" " " " " " "
C. C. Surland	U. S. Rubber Co. Divisional Development Laboratories
W. H. Smith	U. S. Rubber Co. Divisional Development Laboratories

LOCKHEED AVIATION CO.  
24 June 1954

Los Angeles, California

J. Shannon	Power Plant Engineering
D. Sansel	" " "
R. Stobler	" " "
T. Wise	U. S. Rubber Co. Fuel Cell Engineering
C. McElderry	" " " " " " "
C. C. Surland	U. S. Rubber Co. Divisional Development Laboratories
W. H. Smith	U. S. Rubber Co. Divisional Development Laboratories

DOUGLAS AVIATION CO.

Long Beach, California

M. Curtis	Power Plant Engineering
I. Petrosky	" " "
T. Wise	U. S. Rubber Co. Fuel Cell Engineering
C. McElderry	" " " " " " "
C. C. Surland	U. S. Rubber Co. Divisional Development Laboratories
W. H. Smith	U. S. Rubber Co. Divisional Development Laboratories

The general problems of backing board installation were discussed in each of the conferences listed above. The engineering personnel of the companies visited, indicated that they would be willing to submit details of their fastening methods to WADC for use in this work:

In general, fastening devices consist of AN Standard Nut Plate with AN515 screw. Holes are drilled through the backing board into the structure, and the fastening made with screw and nut plate without torque control.

In one instance, a method was used that would seem to have merit in reducing deflection and fastener failure under load. In this system 7/16 inch holes are drilled in the backing board at the fastening points. 0.219 to 0.233 inch holes are drilled in the structure. The fastener then is comprised of a S-1114189-10R screw, an A3235-.020 inch washer, and an A8580-10-1 nut plate.

## *Contrails*

It was standard practice in the industry to use Bauer & Black 214 tape, or similar, to cover any sharp edges or projections in a structure before lining it with backing board.

In the matter of spacing and depth of stringers, little conformity could be found between the various aircraft investigated. In general, the bomber types utilized wider and deeper support sections than the lighter aircraft. In few instances, however, is the spacing between support members greater than 12 inches, or deeper than 6 inches.

## APPENDIX III

### INTERNAL EXPLOSION AND PRESSURE DEFLECTION TEST JIG

The essential construction of the test jig is shown in Figure 69, page 113. The fastenings that hold the backing board and support panel in contact with the fuel cell were damaged on the first explosion, and improved fastenings were added to the structure to overcome this deficiency. These are apparent in Figure 1, page 4.

The explosive charge, consisting of a fast burning catalyzed powder, was contained in standard 12 gauge shotgun cartridges. A cartridge was fitted into a breech, exposing the charge, and fitted with a firing pin to detonate the standard cap in the cartridge. The method of inserting the charge was simplified and improved by removing the threads from the breech that necessitated threading into the receiving plate in the threaded collar which screws onto the fuel cell fitting in such a manner that a rubber gasket on the threaded nipple protruding from the fitting is forced against the smooth outer wall of the breech to hold it in firing position. The breech can be mounted on the cell, with the charge immersed in the fluid inside the fuel cell as in Figure 1.

The panel that holds the supporting hat sections against the backing board, Figure 69, page 113, was constructed originally of 0.125 inch aluminum sheet, with the hat sections riveted to the sheet, and in subsequent trials the structure was modified to permit the use of a 0.500 inch aluminum plate. This structure was damaged in later explosion trials and a one-inch steel plate with one-inch steel hat sections four inches deep was constructed for further tests. See Figure 70. This test plate was able to withstand the explosions without damage. The hat section shape and spacing for all tests was 6 inches center to center as prescribed for cube gunfire tests in MIL-P-8045.

The fuel cell that contained the fluid in which the explosion was created can be seen in Figure 69. The protruding flange at the top of the cell caused buckling in the cell walls when it was placed in the cavity. An improved fuel cell for containing the fluid in the internal explosion jig was constructed and installed in the device. The cell was built to fit into the cavity in such a manner that, in an undistorted position, the cell bottom was in contact with the enclosure, and the top of the sealing flange met the upper inside surface of the jig. The remaining space on either side of the flange was filled with relatively incompressible plywood pieces cut to fill the cavity and prevent undue stresses from occurring on the cell walls during the explosion. See Figure 70.

The test panels were 30 inches high and 40 inches wide. The manner in which they were installed is illustrated in Figure 70, page 114. When Type I installations were tested the panels were attached to the test frame with adhesive tape to hold the panel in position until closure of



*Contrails*



FIGURE 69  
INTERNAL EXPLOSION JIG  
BACKING BOARD INSTALLATION

*Contrails*

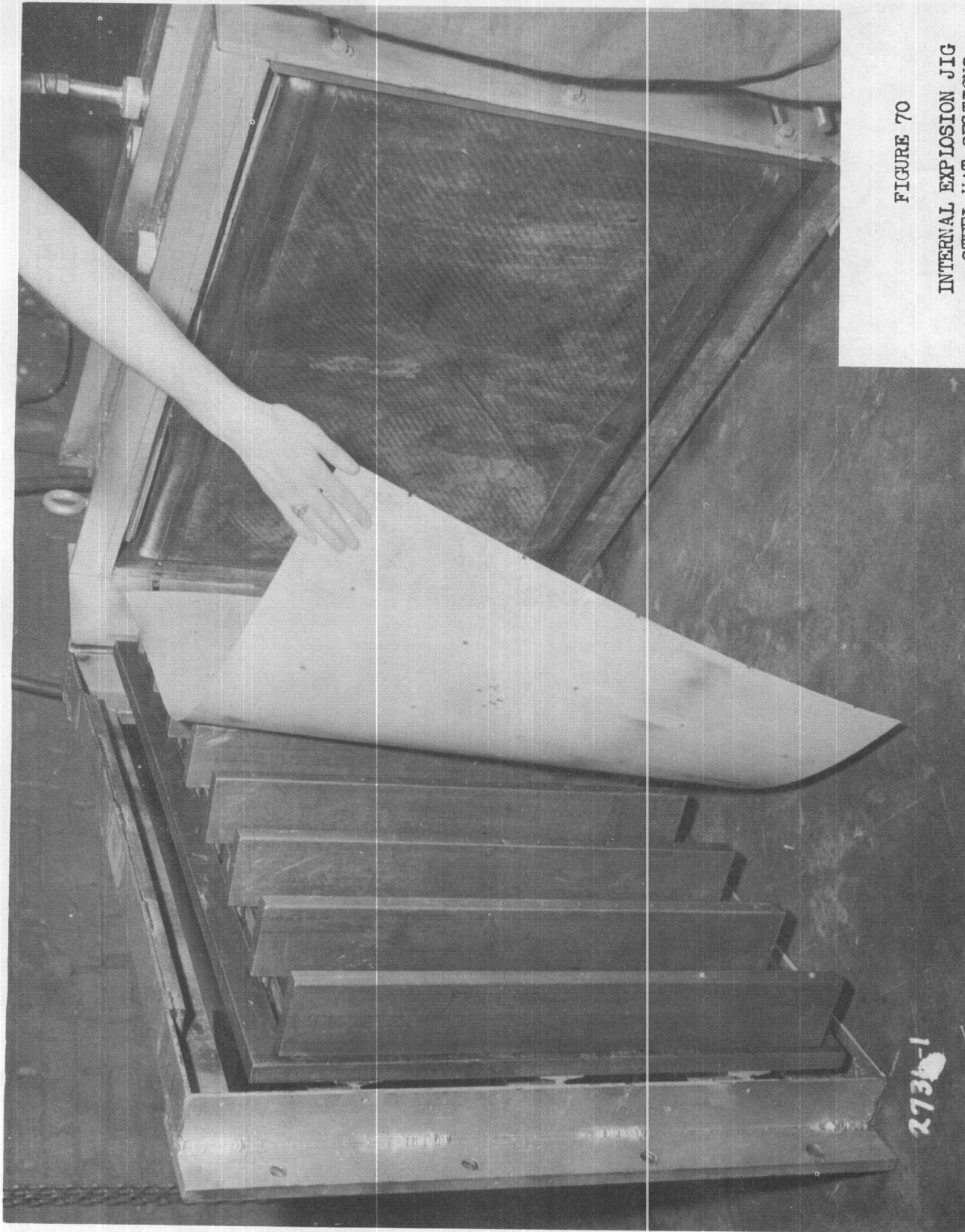


FIGURE 70

INTERNAL EXPLOSION JIG  
STEEL HAT SECTIONS  
AND  
SUPPORT PLATE

# Contrails

the test door and the pressure resulting from filling the fuel cell with water provided sufficient friction between the panel and the cell and hat section supports to maintain its position.

The simulated projectile wound in all trials consisted of two 3/8 inch holes in the center of the panel separated at their centers by two and one quarter inches, on a 45 degree angle with the vertical, connected by a saw cut. This wound was located midway between hat section supports, and centrally located on the test panels, except where noted in the Tables I, II and III.

The explosive charge was centered at the same elevation as the wounds, except as noted in Tables I, II, and III. The position of the hat sections on the test frame is shown in Figure 71, page 116. The first 14 panels were tested with the hat sections positioned as shown in the illustration, which located the horizontal position of the explosive charge directly behind the center hat section. On panel 15, the position of the hat sections was moved horizontally to bring the position of the test wound directly in front of the explosion. This arrangement was used in all subsequent testing.

All panels after panel 14 were installed as Type III backing boards. Panels 15 thru 18 were installed in the manner prescribed in MIL-P-8045 and MIL-T-5578A. Panels 19 thru 34 were mounted by frilling .1562 inch holes in the panel using a spacing jig and fastening the board with AN-515-8R10 screws into tapped holes in the steel hat sections.

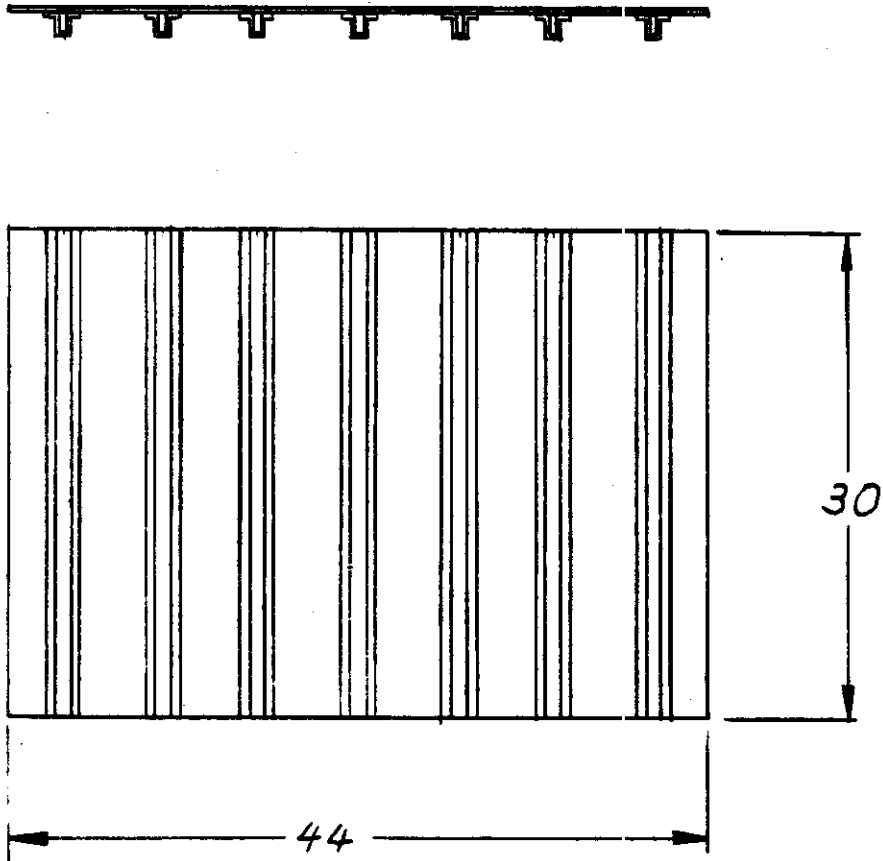


FIGURE 71  
TOP AND FRONT VIEW OF  
BACKING BOARD SUPPORT FRAME

FIGURE 72

HIGH SPEED PHOTOGRAPHY SETUP

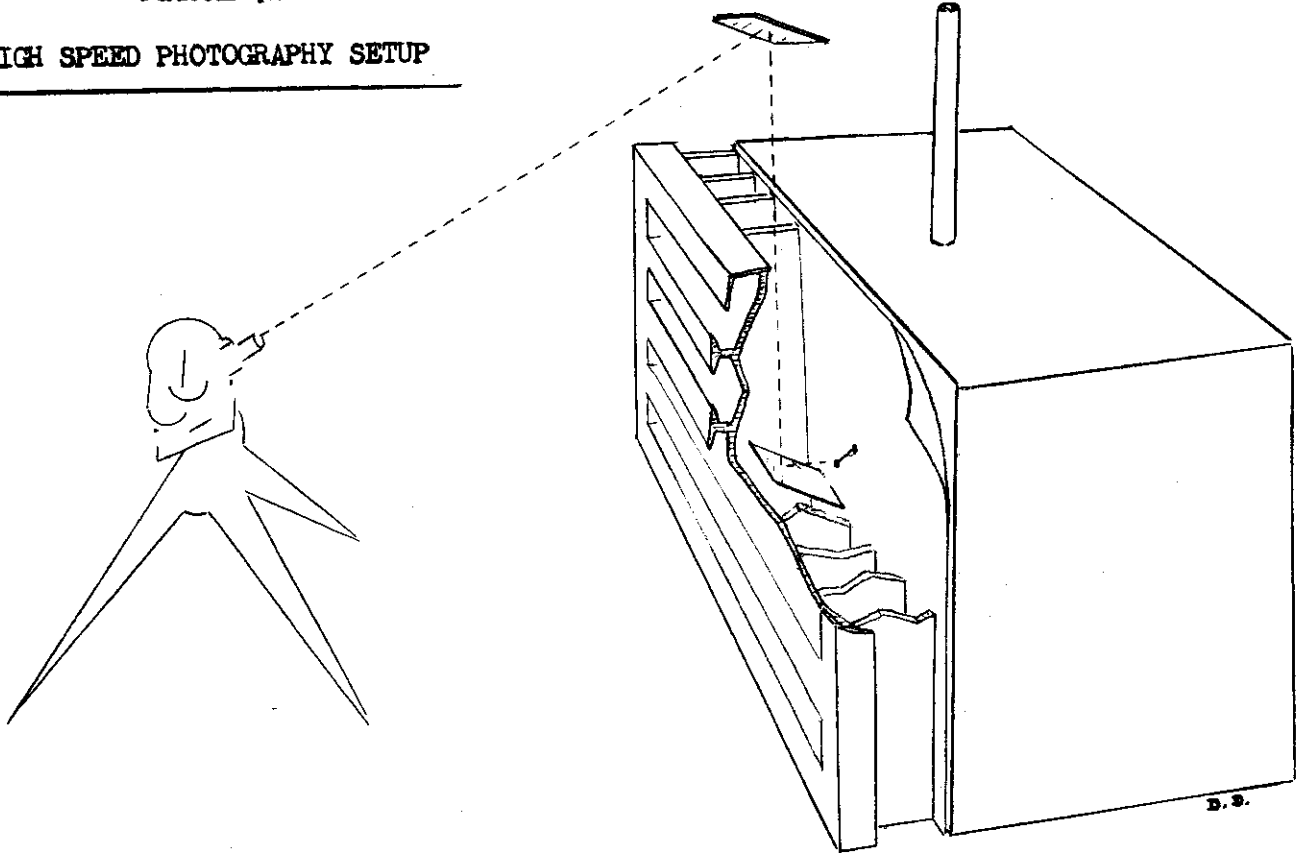
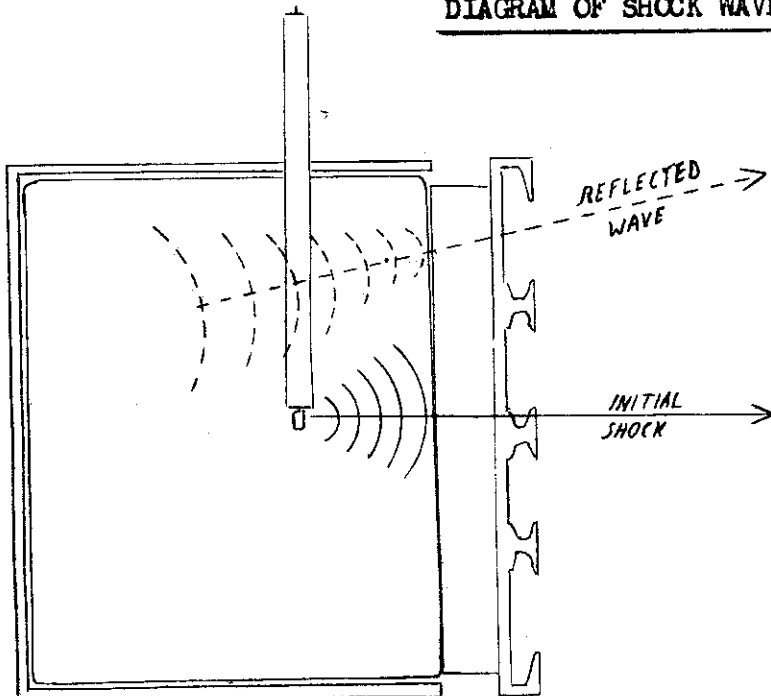


FIGURE 73

DIAGRAM OF SHOCK WAVE REFLECTION



MECHANICAL PROPERTIES  
OF BACKING BOARDS

The autographic strain recording equipment, described in Section II, Pressure Deflection Testing, under Test Methods and Equipment, page 23, was used to record elongations. The tensile strength and elongation of the backing boards was determined by Method 1011 of Federal Specification L-P-406b, 27 September 1951.

Elongations were recorded by attaching a clamping unit resembling a small "C" clamp to the sample such that a small spherical indenter, approximately 1/64" diameter is forced against the bench mark. The sensing arms of the transducer then rest against the screw on the end of which the indenter is fixed.

The extensometer and electronic recorder used for these measurements appear to have inherent reproducibility beyond the accuracy that is obtainable, due to variations in the samples and errors which result from slippage in the clamping units that are attached to the samples and activate the extensometer.

The data for the elongation of the backing board materials used in this work are listed in Table VII. In general, five samples were used, but in some instances ten samples were run. The standard deviation from the average and the limits of 95% confidence are given for each of the test materials.

TABLE VII

ELONGATION OF BACKING BOARD MATERIALS

<u>PANEL</u>	<u>ELONGATION (%)</u>	<u>STANDARD DEVIATION*</u>	<u>95% CONFIDENCE LIMIT</u>
<u>USV 747-5</u>			
WARP	3.35	0.28	± 0.35
FILLER	4.21	0.28	± 0.33
<u>USV CR 88</u>			
WARP	1.81	0.20	± 0.14
FILLER	4.00	1.14	± 0.78

\* From Average

TABLE VII (Cont.)

ELONGATION OF BACKING BOARD MATERIALS

<u>PANEL</u>	<u>ELONGATION (%)</u>	<u>STANDARD DEVIATION*</u>	<u>95% CONFIDENCE LIMIT</u>
<u>USV-55A</u>			
WARP	2.62	0.17	± 0.26
FILLER	2.71	0.17	± 0.21
<u>USV-33</u>			
WARP	1.74	0.18	± 0.22
FILLER	1.86	0.18	± 0.22
<u>S-2N</u>			
WARP	20.47	0.74	± 0.53
FILLER	29.02	1.27	± 0.91
<u>S-3N</u>			
WARP	20.62	0.64	± 0.46
FILLER	27.32	0.82	± 0.58

\* From Average.

The rather wide limits of the 95% confidence values probably represent the variability that exists in the properties of the materials and the variation introduced by the clamps used to activate the strain recorder. This is to be expected, since the difficulty in obtaining representative samples from woven materials is well known.

Table VIII, lists the mechanical properties of the materials described in Table VI. These data were obtained by test methods prescribed in Military Specification MIL-P-8045 (USAF), or equivalent.

It should be noted that data for the Modulus of Elasticity in Flexure is in some cases reported for two testing spans. This was included to show the dependence of the results on the test conditions.

MECHANICAL PROPERTIES OF TEST MATERIALS

USV 747 5

	<u>WARP</u>	<u>FILLER</u>
TENSILE (psi)	19,000	21,000
BREAKING STRENGTH (#/in.)	1,300	1,500
ELONGATION (%)	2.5	2.7
MODULUS OF ELASTICITY IN FLEXURE (psi) (16 to 18 times the gauge)	1,100,000	1,200,000
MODULUS OF RUPTURE (psi) (2" span)	21,500	22,600
MODULUS OF ELASTICITY IN TENSION (psi) (2" span)	1,040,000	1,080,000
SHEAR STRENGTH (psi)	13,800	15,700
BEARING STRENGTH (psi)	32,040	35,240
BEARING STRENGTH (#)*	336	369
TABOR STIFFNESS**	159	200
MODULUS OF ELASTICITY IN FLEXURE (psi) (2" span)	1,165,000	1,336,000
GAUGE	.063	
#/FT. <sup>2</sup>	.50	
IZOD IMPACT (ft.#/in.) (Notched)	23.1	35.7
HEAT DISTORTION (Deg. F. @ 264 psi.)	164	177

\* #/fastener.

\*\* Tabor Stiffness Gauge. Tabor Instrument Co.



*Contrails*  
TABLE VIII (Cont.)

MECHANICAL PROPERTIES OF TEST MATERIALS

USV CR 88

	GAUGE RANGE .050 - .060"		GAUGE RANGE .035 - .040"	
	<u>WARP</u>	<u>FILLER</u>	<u>WARP</u>	<u>FILLER</u>
TENSILE (psi)	33,200	18,300	48,000	27,800
BREAKING STRENGTH (#/in.)	1,770	960	1,700	1,000
ELONGATION (%)	1.8	4.0	2.8	3.1
MODULUS OF ELASTICITY IN FLEXURE (psi) (16 to 18 times the gauge)	1,053,000	555,000	933,000	700,000
MODULUS OF RUPTURE (psi) (2" span)	37,200	20,000	43,500	38,800
MODULUS OF ELASTICITY IN TENSION (psi) (2" span)	1,486,000	617,000	1,767,000	740,000
SHEAR STRENGTH (psi)	8,700	8,000		
BEARING STRENGTH (psi)			36,000	31,960
BEARING STRENGTH (#)*			211	190
TABOR STIFFNESS**			37	28
MODULUS OF ELASTICITY IN FLEXURE (psi) (2" span)	-----	680,000	1,000,000	-----
GAUGE	.050 - .060"		.035 - .040"	
#/FT. <sup>2</sup>	.44		.31	
IZOD IMPACT (ft.#/in.)	20.2	26.2		
IZOD IMPACT (ft.#/in.) (Unnotched)	35.3	32.3		
HEAT DISTORTION (Deg. F. @ 264 psi.)	160	157		

\* #/fastener.

\*\* Tabor Stiffness Gauge. Tabor Instrument Co.

*Continued*  
TABLE VIII (Cont.)

MECHANICAL PROPERTIES OF TEST MATERIALS

USV 55A

	<u>WARP</u>	<u>FILLER</u>
TENSILE (psi)	35,000	36,000
BREAKING STRENGTH (#/in.)	1,500	1,600
ELONGATION (%)	1.7	1.9
MODULUS OF ELASTICITY IN FLEXURE (psi) (16 to 18 times the gauge)	2,300,000	1,045,000
MODULUS OF RUPTURE (psi) (2" span)	50,200	21,500
MODULUS OF ELASTICITY IN TENSION (psi) (2" span)	1,640,000	1,430,000
SHEAR STRENGTH (psi)	16,300	19,800
BEARING STRENGTH (psi)	39,760	39,880
BEARING STRENGTH (#)*	255	253
TABOR STIFFNESS**	84	86
MODULUS OF ELASTICITY IN FLEXURE (psi) (2" span)	1,960,000	1,016,000
GAUGE	.048	
#/FT. <sup>2</sup>	.38	
IZOD IMPACT (ft.#/in.) (Notched)	24.1	28.5
HEAT DISTORTION (Deg. F. @ 264 psi.)	198	179

\* #/fastener.

\*\* Tabor Stiffness Gauge. Tabor Instrument Co.

*Control*

TABLE VIII (Cont.)

MECHANICAL PROPERTIES OF TEST MATERIALS

USV 33

	<u>WARP</u>	<u>FILLER</u>
TENSILE (psi)	35,900	33,600
BREAKING STRENGTH (#/in.)	1,078	1,000
ELONGATION (%)	1.74	1.86
MODULUS OF ELASTICITY IN FLEXURE (psi) (16 to 18 times the gauge)	1,300,000	1,032,000
MODULUS OF RUPTURE (psi) (2" span)	41,480	42,560
MODULUS OF ELASTICITY IN TENSION (psi) (2" span)	1,700,000	1,630,000
SHEAR STRENGTH (psi)	21,120	20,920
BEARING STRENGTH (psi)	32,800	35,050
BEARING STRENGTH (#)*	148	149
TABOR STIFFNESS**	29	30
GAUGE	.030	
#/FT. <sup>2</sup>	.25	

\* #/fastener.

\*\* Tabor Stiffness Gauge. Tabor Instrument Co.

*Contracts*  
TABLE VIII (Cont.)

MECHANICAL PROPERTIES OF TEST MATERIALS

S 2N

	<u>WARP</u>	<u>FILLER</u>
TENSILE (psi)	26,300	23,100
BREAKING STRENGTH (#/in.)	1,200	1,100
ELONGATION (%)	20.5	29.0
MODULUS OF ELASTICITY IN FLEXURE (psi) (16 to 18 times the gauge)	Not Applicable	Not Applicable
MODULUS OF RUPTURE (psi) (2" span)	Not Applicable	Not Applicable
MODULUS OF ELASTICITY IN TENSION (psi) (2" span)	159,000	99,200
SHEAR STRENGTH (psi)	14,500	14,300
BEARING STRENGTH (psi)	36,860	44,230
BEARING STRENGTH (#)*	260	311
TABOR STIFFNESS**	8.8	6.2
MODULUS OF ELASTICITY IN FLEXURE (psi) (2" span)	Not Applicable	Not Applicable
GAUGE	.043	
#/FT. <sup>2</sup>	.23	
IZOD IMPACT (ft.#/in.) (Notched)	27.6	25.2
IZOD IMPACT (ft.#/in.) (Unnotched)	21.6	24.5
HEAT DISTORTION (Deg. F. @ 264 psi.)	Too Flexible	Too Flexible

\* #/fastener.

\*\* Tabor Stiffness Gauge. Tabor Instrument Co.

MECHANICAL PROPERTIES OF TEST MATERIALS

S 3N

	<u>WARP</u>	<u>FILLER</u>
TENSILE (psi)	27,000	24,800
BREAKING STRENGTH (#/in.)	1,700	1,600
ELONGATION (%)	20.6	27.3
MODULUS OF ELASTICITY IN FLEXURE (psi) (16 to 18 times the gauge)	Not Applicable	Not Applicable
MODULUS OF RUPTURE (psi) (2" span)	Not Applicable	Not Applicable
MODULUS OF ELASTICITY IN TENSION (psi) (2" span)	145,000	140,000
SHEAR STRENGTH (psi)	14,200	17,600
MODULUS OF ELASTICITY IN FLEXURE (psi) (2" span)	Not Applicable	Not Applicable
GAUGE	.063	
#/FT. <sup>2</sup>	.34	
IZOD IMPACT (ft.#/in.) (Notched)	35.1	30.0
IZOD IMPACT (ft.#/in.) (Unnotched)	32.0	31.5
HEAT DISTORTION (Deg. F. @ 264 psi.)	Too Flexible	Too Flexible

*Contrails*  
APPENDIX V

CUBE GUNFIRE TESTS

Cube gunfire tests were completed on USV 747-5 and USV CR 88 backing boards on 15 December 1954 at the United States Rubber Company Gunfire Range. These tests were conducted and witnessed by R. D. Lemon and W. H. Smith.

The test panels were gunfired in accordance with MIL-P-8045 (USAF), item 4.3.2.7.1 with the exceptions noted.

Exceptions:

- a. Structure was at ambient temperature.
- b. AP ammunition was fired.

The materials were installed as Type III backing boards, in accordance with MIL-T-5578A.

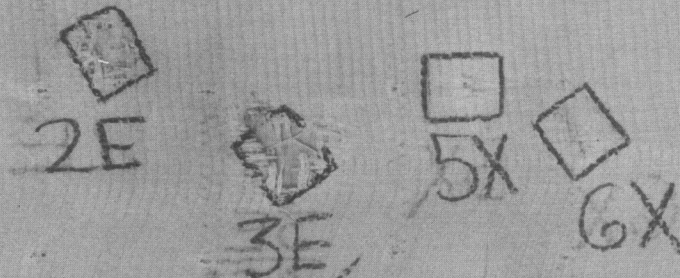
The number of the round fired entrance or exit shots were marked on the backing board panels. The 45 degree rounds are marked 45 degrees; all others are straight-in shots. See Figures 2 thru 5. "X" stands for exit, "E" for entry.

Following the firing, both panels remained fastened to the hat sections and had to be torn off for storage. All wounds in the fuel cell sealed without plugging.

Changes and improvements in the methods for continually producing a woven roving laminated backing board material, during the course of this work, resulted in a lighter construction of the USV CR 88 material than that used for the gunfire tests described above. This is described in Appendix VI, page 129. Additional cube gunfire tests on this lighter construction, 0.035 inches thick and weighing 0.31 pounds per square foot, are shown in Figures 74 and 75, pages 127 and 128. These tests were conducted at the United States Rubber Company shooting range on 28 March 1955, in the manner described above. Improved resistance to gunfire damage is apparent in the lighter construction by comparing Figures 4 and 5 with Figures 74 and 75. The damage shown around the gunfire wound for the lighter materials in Figures 74 and 75, in general, is of lesser extent and amount than that shown for the heavier construction of USV CR 88 of Figures 4 and 5.

*Contrails*

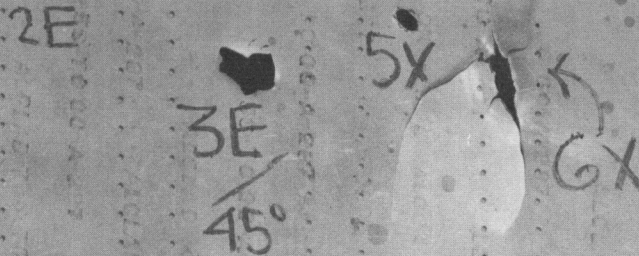
P-1509 DEPT. 181 4-28-55  
ROVING WEAVE AMB. TEMP.  
MIL-P-8045 TYPE III  
WARP ↔



2E - FULL TUMBLE  
3E - FULL TUMBLE  
5X - 1/4 TUMBLE

6X - FULL TUMBLE

P-1509 DEPT 181 4-28-55 •  
ROVING WEAVE AMB. TEMP. •  
MIL-P-8045 TYPE - III



2755-38

FIGURE 74

CUBE GUNFIRE TEST PANEL USV CR 88  
(IMPROVED CONSTRUCTION)

# Contrails

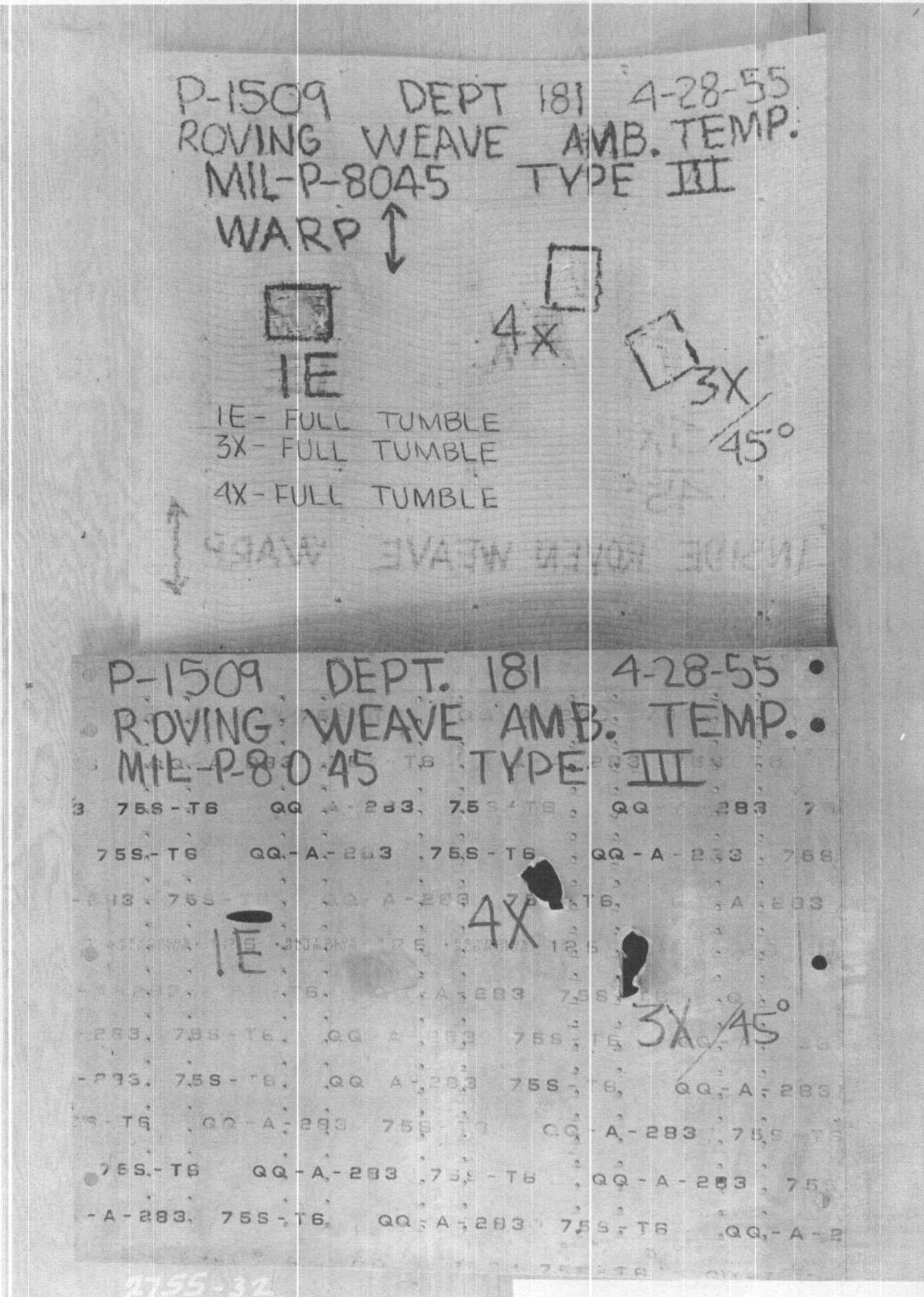


FIGURE 75

CUBE GUNFIRE TEST PANEL USV CR 88  
(IMPROVED CONSTRUCTION)



COMMERCIAL PRODUCTION OF USV CR 88  
BACKING BOARD

The development of a woven roving, polyester laminated backing material was originally accomplished with platen presses. This resulted in samples of small dimension adequate for the work of Part I of this report. The use of larger test panels for this part of the work required the development of methods for producing the backing board on continuous laminating equipment.

The USV CR 88 panels coded 3, 4, 16, and 17 in Tables I and II, pages 12 and 15, were representative of the material of the first successful production on commercial equipment. This resulted in a material with high percentage of resin. This is the material illustrated in Figures 4 and 5, cube gunfire tests on USV CR 88.

Later production changes and improvements in operation resulted in the production of a material of considerably lighter weight and gage. The test panels of Table III, coded Panels 19, 20, 22, 24, 25, 26, and 33 were of this lighter construction.

Gunfire tests of the lighter weight material reported in WADC Technical Report 54-474 Part I, compare very well with those of the heavier USV CR 88 material cited above. Subsequent cube gunfire tests on the construction typified by panels 19, 20, 22, etc., show better resistance to gunfire than that illustrated for the heavier cube gunfire panels of Figures 3 and 4. See Figure 74 and 75, pages 127 and 128, which illustrate cube gunfire data on USV CR 88 backing board 0.035 inches thick and weighing 0.31 pounds per square foot.

A description of the production and construction of the USV CR 88 materials of this report is given below:

Production of USV CR 88

Manufacturing

USV CR 88 was made on continuous laminating equipment. Gloss surface on one side, dull surface on reverse side. Commercial production of USV CR 88 was accomplished with the continuous press method.

Amount produced. 100 sq. ft.

# Contrails

## Materials:

Resins: Paraplex P-43  
Catalyst: Benzoyl Peroxide 2%  
Added Styrene: 8%  
Viscosity: 425 cps.  
Gel Time: 6 Min. at 180°F.  
Exotherm: 248°F., at 180°F. bath

## Fabric: Woven Roving

Oz. per sq. yd. 25.5  
Gauge in thickness .050  
Thread Count 5 x 5  
Breaking Strength Warp 900 lbs. per inch  
Fill 900 lbs. per inch

*Contrails*  
BIBLIOGRAPHY

1. Timoshenko, S.: Theory of Plates & Shells. McGraw-Hill Book Co., Inc., 1940.
2. Timoshenko, S., and Goodier, J.: Theory of Elasticity. McGraw-Hill Book Co., Inc., 1951.
3. Hoffman, Oscar, and Sachs, George: The Theory of Plasticity. McGraw-Hill Book Co., Inc., 1953.
4. Sechler, Ernest E.: Elasticity in Engineering. John Wiley & Sons, Inc., 1952.
5. Levy, Samuel: Square Plate with Clamped Edges Under Normal Pressure Producing Large Deflections. T. N. No. 740, NACA, 1942.
6. Levy, Samuel, and Greenman, Samuel: Bending with Large Deflection of a Clamped Rectangular Plate with Length-Width Ratio of 1.5 Under Normal Pressure. T. N. No. 853, NACA, 1942.
7. Ramberg, Walter, McPherson, Albert E., and Levy, Samuel: Normal-Pressure Tests of Rectangular Plates. T. N. No. 748, NACA, 1942.
8. Chi-Teh Wang: Nonlinear Large-Deflection Boundary-Value Problems of Rectangular Plates. T. N. No. 1425, NACA, 1948.
9. Chi-Teh Wang: Bending of Rectangular Plates with Large Deflections. T. N. No. 1462, NACA, 1948.
10. Den Hartog: Advanced Strength of Materials. McGraw-Hill Book Co., Inc., 1940.
11. Davis, D. S.: Empirical Equations and Nomography. McGraw-Hill Book Co., Inc., 1943.
12. Sokolinikoff, I. S. and E. S.: Higher Mathematics for Engineers and Physicists. McGraw-Hill Book Co., Inc., 1941.
13. Alfrey, T. Jr.: Mechanical Behavior of High Polymers. Interscience Publishers, Inc., 1948.
14. Cole, R. H.: Underwater Explosions. Princeton University Press, 1948.
15. Surland, Charles C., and Smith, W. H.: Evaluation and Development of Plastic Laminated Backing Board Materials. WADC Technical Report 54-474 Part I, March 1955.

# *Contrails*